



Universidade do Minho
Escola de Engenharia

Ricardo Jorge Paredes Sora

Development of a rapid surface temperature
heating system and its application to micro-
injection



Universidade do Minho
Escola de Engenharia

Ricardo Jorge Paredes Sora

Development of a rapid surface temperature
heating system and its application to micro-
injection

Master Thesis
Integrated Masters on Polymer Engineering

Work settled under supervision of:
Prof. Dr. António José Pontes
Prof. Dr. Felice de Santis
Prof. Dr. Roberto Pantani

DECLARAÇÃO

Nome: Ricardo Jorge Paredes Sora

Endereço eletrónico: rijo.2105@gmail.com

Telefone: 00351 911984139

Número do cartão do cidadão: 13965324

Título dissertação: **Development of a rapid surface temperature heating system and its application to micro-injection**

Orientador: Doutor António José Vilela Pontes

Ano de conclusão: 2014

Designação do Mestrado ou do Ramo de Conhecimento do Doutoramento:

Ciclo de Estudos Conducente ao Grau de Mestre em Engenharia de Polímeros

Declaro que concedo à Universidade do Minho e aos seus agentes uma licença não-exclusiva para arquivar e tornar acessível, nomeadamente através do seu repositório institucional, nas condições abaixo indicadas, a minha dissertação, no todo ou em parte, em suporte digital.

Declaro que autorizo a Universidade do Minho a arquivar mais de uma cópia da dissertação e a, sem alterar o seu conteúdo, converter a dissertação entregue, para qualquer formato de ficheiro, meio ou suporte, para efeitos de preservação e acesso.

Retenho todos os direitos de autor relativos à dissertação, e o direito de a usar em trabalhos futuros (como artigos ou livros).

Concordo que a minha tese ou dissertação seja colocada no repositório da Universidade do Minho com o seguinte estatuto:

- Disponibilização imediata do conjunto do trabalho para acesso mundial

Universidade do Minho, __ / __ / ____

Assinatura: _____

ACKNOWLEDGMENTS

This thesis was only possible thanks to the help provided by several people to whom I must give my gratitude.

First, I would like to thank my mentors, Dr. António Pontes, Dr. Roberto Pantani and Dr. Felice de Santis for the support and opportunity of developing this project, as well as the availability showed in order to solve the problems that occurred during this project.

A special thanks for all the people that helped me and contributed to this project, namely Antonio Iannaccone, Ricardo Campos, Henrique Pinto, Ângelo Rodrigues, João Paulo and Maurício Malheiro. Even the smallest aid had an important influence.

A huge thanks to my family for all the support, encouragement and comprehension. They were my lighthouse in trouble waters and without them, most likely I wouldn't accomplish so perfectly this project.

Finally yet importantly, I would like to thank DEP for the outstanding host in this past 5 years and to all my colleagues, with whom I developed a beautiful friendship and had such exceptional and amazing moments.

ABSTRACT

During filling stage, the constant mold temperature control strategy by circling coolant through cooling channels used in conventional injection molding causes an abrupt polymer solidification close to the mold surface and consequently resulting in a frozen layer. As the viscosity increases, the mobility of the polymer to fill the cavity is largely decreased influencing the frozen orientation. This phenomenon affects greatly the dimensional stability of the part and its optical properties, especially micro-injected parts in which high aspect ratios are precluded because of premature solidification.

Recently, several studies have been proposed in literature in an effort to obtain a fast and uniform heating and cooling through the mold surface during filling stage. Inspired in those studies, a new system for rapid surface heating was designed, built and applied to a cavity for micro-injection molding. To prove his feasibility as well as attempting to improve results, preliminary tests were conducted comparing theoretical and practical studies.

Furthermore, the system consists in a well-balanced electrical resistive thin component and an insulation layer and can increase the mold surface temperature of several tenths of celsius degrees in less than one second. Injection molding tests were then carried out comparing this and a conventional system using both amorphous and semi-crystalline materials as well as different surface temperature for two cavities with a thickness of 250 μm . Moreover, in order to check the effect of those surface heating test, specimens were characterized according to their optical (polarized light and bright-field microscopy), mechanical (tensile tests) and thermal properties (differential scanning calorimetry).

Keywords: Heat transfer; micro-injection molding; mold surface temperature; morphology; rapid heating; rapid cooling; thermoplastic materials;

ÍNDICE

INTRODUCTION.....	1
1.1. Introduction.....	2
1.2. Objectives	2
1.3. Content.....	3
STATE OF ART.....	5
2.1. Micro-injection.....	6
2.1.1. Applications.....	7
2.1.2. Materials	7
2.1.3. Conventional equipment	9
2.1.4. Molds.....	11
2.1.5. Processing Conditions.....	13
2.1.6. Design and geometry.....	13
2.2. Mold Surface Heating.....	14
2.2.1. Functional requirements and constituent elements	15
2.2.1.1. Stiff, strong and durable mold with a low thermal mass	15
2.2.1.2. Means for a rapid heat generation and removal in the mold surface portion ..	16
2.2.2. Research	26
PRELIMINARY STUDY	28
3.1. Preliminary Study.....	31
3.1.1. Selection of materials.....	31
3.1.1.1. Mold and Polymer Layer	31
3.1.1.2. Insulation Layer	32
3.1.1.3. Heating Generation Layer.....	35
3.1.2. Obtainment of a film	36
3.1.2.1. Experiment	37

3.1.2.2.	Experimental procedure	37
3.1.2.3.	Result	38
3.1.3.	Theoretical and Pratical Study	39
3.1.3.1.	FlexPDE	39
3.1.3.2.	LabVIEW	40
3.1.3.3.	Results	42
4.1.	Micro-specimen	51
4.2.	Micro-injection machine	52
4.3.	Mold	53
4.4.	Heating system	57
4.5.	Processing and injection conditions	58
CHARACTERIZATION		62
5.1.	Optical characterization	63
5.1.1.	Results	65
5.2.	Mechanical Properties	68
5.2.1.	Results	71
5.3.	Thermal Properties	73
5.3.1.	Results	74
CONCLUSION.....		76
6.1.	Conclusion	77
6.2.	Future Works.....	78
BIBLIOGRAPHY.....		80
ATTACHMENTS		86
Attachment 1.....		86
Attachment 2.....		88
Attachment 3.....		89

Attachment 4.....	91
Attachment 5.....	93
Attachment 6.....	95
Attachment 7.....	100
Attachment 8.....	101
Attachment 9.....	104
Attachment 10.....	105
Attachment 11.....	106

FIGURES INDEX

Figure 1 – Micro-injection molding steps.	6
Figure 2 – Examples of microinjection molding parts with one component (left) and two components (right)	7
Figure 3 – Example of an injection unit for a micro-injection molding machine.	9
Figure 4 – Comparison of feeding channels to mold micro-part with conventional molding machine (right) and with microinjection molding machine (left).	11
Figure 5 – Comparison between mold temperature in the classical and variotherm processes.	12
Figure 6 – Scheme and illustration of mold temperature changes during RHCM processes.	15
Figure 7 – Schematic of heat transfer process in injection molding showing three contributions in heat transfer: Q_1 , convected heat from the melt; Q_2 , heat conducted to the mold; and Q_3 , heat generation inside the thermoplastic.	17
Figure 8 – Rapid heating mechanisms and their divisions.	17
Figure 9 – Principle of the electrical resistance heating with low-frequency current.	18
Figure 10 – Illustrative image of the induction heating principle.	18
Figure 11 – Illustrative image of the proximity heating principle.	19
Figure 12 – Heating (a) or cooling (b) according to Peltier’s effect.	20
Figure 13 – Rapid cooling mechanisms and their divisions.	20
Figure 14 – Illustrative image of the layers that constitute the rapid surface temperature heating system.	29
Figure 15 – Scheme illustrating the heat flux and intensity through the protective coating layer when positioning the heat elements at the mold surface.	30
Figure 16 – Hot squeezer, i.e. Carver Laboratory Press, used in the experiment.	36
Figure 17 – Illustrative image of the pellets placed in the aluminium plates.	38
Figure 18 – Illustrative image of the polyethersulfone result at ideal parameters.	39
Figure 19 – Scheme illustrating the system elaborated for the practical study.	41
Figure 20 – Comparison between the rapid surface temperature heating system with and without an insulation layer.	42
Figure 21 – Influence of the thermal conductivity on rapid surface temperature heating system.	43
Figure 22 – Comparison of temperature distribution through the protective coating between two strain gages distanced by 5 mm (left image) and 0 mm (right image).	44

Figure 23 – Influence of the insulation layer thickness on rapid surface temperature heating system.	45
Figure 24 – Influence of the protective coating thickness on rapid surface temperature heating system.	46
Figure 25 – Comparison between theoretical and practical temperature profile achieved after 1 second.	47
Figure 26 – Comparison between theoretical and practical temperature profile achieved from 1 to 5 seconds.	48
Figure 27 – Comparison between theoretical and practical temperature profile achieved from 5 to 14 seconds.	49
Figure 28 – Scheme of the system idealized for a micro-injection molding machine.	51
Figure 29 – Generic dimensions of the micro-specimen (dimensions on millimeters).	52
Figure 30 – Comparison between the dimensions of the micro-specimen and an one cent coin.	52
Figure 31 – Boy 12A micro-injection machine.	53
Figure 32 – Scheme of the micro-injection mold (exploded view).	53
Figure 33 – Scheme of the extraction holes exploded to pass the copper wires from the strain gage.	54
Figure 34 – Back view of the cavity insert after (left) and before (right) manufacturing without “open-close compartment”	55
Figure 35 – Back view of the cavity insert after manufacturing and with closed compartment (left) and before manufacturing and with open compartment (right).	55
Figure 36 – Top view of the cavity insert after (left) and before (right) manufacturing.	56
Figure 37 – On top, the part achieved when the cold pit allows the material to flow through two impressions. On bellow, the part achieved when the cold pit allows the material to flow through one impression, which can pass to the impression that has one gate (right) or two gates (left).	56
Figure 38 – System of strain gages connect in parallel by copper wires.	57
Figure 39 – Rapid surface heating temperature system applied on a micro-injection molding machine (part 1).	58
Figure 40 – Rapid surface heating temperature system applied on a micro-injection molding machine (part 2).	58
Figure 41 – Zones of the specimen chosen to be optically chacterized.	64

Figure 42 – Equipments and accessories needed to optical characterization: a) polish machine; b) microtome; c) Olympus transmission microscope; d) plastic mold used; e) Resin and hardener (Epofix kit)	65
Figure 43 – Light polarized microscopy results for polypropylene conditions.	65
Figure 44 – Scheme explaining the division of zones for characterization.	66
Figure 45 – Bright-field microscopy (top) and polarized light microscopy (bottom) results of the same zone, which correspond to the weld line location.....	68
Figure 46 – Lengthen of a cylindrical specimen submitted to tensile load.	69
Figure 47 – Typical strain-stress graphic.	69
Figure 48 – Instron 4505 strength testing machine.....	70
Figure 49 – Stress results obtained for the one gate polypropylene specimens.....	71
Figure 50 – Stress results obtained for the two gates polypropylene specimens.	71
Figure 51 – Stress results obtained for the one gate polystyrene specimens.	72
Figure 52 – Stress results obtained for the two gates polystyrene specimens	72
Figure 53 – DSC 7 produced by Perkin Elmer.	73
Figure 54 – Degree of crystalline results obtained for the one gate polypropylene specimens. ...	74
Figure 55 – Degree of crystalline results obtained for the two gates polypropylene specimens..	75
Figure 56 – Datasheet of Edistir N1910 (part 1).....	86
Figure 57 – Datasheet of Edistir N1910 (part 2).....	87
Figure 58 – Datasheet of Moplen HP548R	88
Figure 59 – Datasheet of BASF Ultrason E 3010 (part 1).....	89
Figure 60 – Datasheet of BASF Ultrason E 3010 (part 2).....	90
Figure 61 – Datasheet of Mitsui AURUM 450 (part 1).....	91
Figure 62 – Datasheet of Mitsui AURUM 450 (part 2).....	92
Figure 63 – Variables of the FlexPDE script.	95
Figure 64 – Example of the material properties input on FlexPDE software.	95
Figure 65 – Example of the strain gage input on FlexPDE software.	96
Figure 66 – Equation implanted for the generation of heat.....	96
Figure 67 – Implementation of region 1 (all components) on FlexPDE.....	97
Figure 68 – On left, implementation of region 2 (insulation layer). On right, implementation of region 3 (heating generation layer).	97

Figure 69 – On left, implementation of region 4 (in the strain gage). On right, implementation of region 5 (in the strain gage, if used more than 1). 98

Figure 70 – Implementation of regions 6 and 7 (in the polymer layer)..... 98

Figure 71 – Code related to the temperatures reached between each layer..... 98

Figure 72 – Code related to the visualization and data save. 99

Figure 73 – Technical drawing of one open-close compartment. 101

Figure 74 – Technical drawing of the other open-close compartment. 102

Figure 75 – Technical drawing of the cavity insert without the open-close compartments. 103

Figure 76 – Characteristics of Boy 12A micro-injection machine. 104

TABLES INDEX

Table 1 – List of materials that fulfil a set of properties and specification for microinjection molding. [4].....	8
Table 2 – List of micro-molding machine commercially available and their characteristics. [16]..	9
Table 3 – Generic comparison between heating techniques.....	21
Table 4 – Comparison of different methods for mold rapid heating based on different performance criteria. [31].....	1
Table 5 – Material and relevant properties chosen for the mold and polymer layer.....	32
Table 6 – Materials chosen for injecting.....	32
Table 7 – Weighting table for the selection of the main property for the insulation material.....	33
Table 8 – Materials and their relevant properties selected for the insulation layer.....	34
Table 9 – Best materials for the insulation layer.....	34
Table 10 – Material and his relevant properties for the insulation layer.....	35
Table 11 – Material and his relevant properties for the heat production layer.....	36
Table 12 – Experiments made and ideal parameters (in italic) for the obtainment of the polyethersulfone film.....	39
Table 13 – Conditions performed for the micro-injection molding process.....	59
Table 14 – Processing conditions performed for the micro-injection molding process.....	60
Table 15 – Skin-core ratio results.....	67
Table 16 – Datasheet of OMEGA SGD-4/120-LY13.....	93
Table 17 – Data related to the tensile tests.....	105
Table 18 – Data related to the DSC tests.....	106

ABBREVIATIONS AND ACRONYMS LIST

3C – Computing, communication and consumer

CNC – Computer numerical control

EDM – Electrical discharge machining

IA – Information application

PES – Polyethersulfone

RHCM – Rapid heat cycle molding

RSHTS – Rapid surface heating temperature system

CHAPTER 1

INTRODUCTION

1.1. Introduction

As know, injection molding technology is the most widely used process for manufacturing plastic parts due essentially to geometric flexibility of parts, high productivity, among others. Between the factors that affect injection molding, such as material, geometry and mold, it is safe to affirm that one of the most critical parameters is the mold temperature control, as it influences not only the injection pressure but also the injection speed. The most common strategy of mold temperature used in industrial production is the continuous cooling method, mainly due to the yet relatively difficulty to heat and cool the cavity surfaces rapidly and uniformly within a short molding cycle time, so as to not only improve the part quality but also ensure high production efficiency.

[1]

Applying a correct dynamic mold temperature will allow to decrease the resistance of the flow along the cavity, reducing processing times and increasing process stability and optical properties of the final product. Ideally, temperature should be higher than solidification point during filling, in order to allow a complete filling without excessive pressure and stress on the material and after filling, the temperature should be quickly decreased bellow the solidification point to obtain a solid polymeric part in reasonable times. [2]

In the recent past years, market is increasing his demand for lower, lighter and thinner parts along with performance requirements of high mechanical strength, accuracy and surface appearance, especially with the booming development of the 3C and IA. [3] Therefore, controlling the mold temperature efficiently in micro-injection molding is a critical and relevant issue.

1.2. Objectives

The main aim of this work is testing and applying a controlled heating/cooling surface temperature system for manufacturing parts with better quality than those manufactured by a conventional method in micro-injection molding. Therefore and to achieve this, the following secondary objectives were performed:

- Bibliographical review of micro-injection molding and mold surface heating;
- Definition of a method to heat up the surface and the materials that constitute it;
- Theoretical and practical experiment of the method;
- Conception and production of a molding insert;
- Injection and characterization of samples;

- Thesis writing.

1.3. Content

In each chapter, a different matter is discussed and therefore, a brief synthesis is presented:

- Chapter 1, State of art: A bibliographical search was conducted in order for the reader fully integrate and perceive the basics of this work, as well as acquire knowledge needed about it. The main focus is addressed on the rapid surface temperature heating system. In addition, the search will be directed also to micro-injection molding process as it is an important factor too.
- Chapter 2, Preliminary Study: A rapid surface temperature heating system was thought (layout and materials) and, in an attempt to evaluate his feasibility, tests were conducted.
- Chapter 3, Application to micro-injection: Here it is possible to find the exclusive cavity developed to shelter the rapid surface temperature system tested, as well as the machine which will inject the parts plus the processing and injection conditions performed.
- Chapter 4, Characterization and discussion: The injected parts were mechanically, optically and thermally characterized and the results of that characterization were discussed in this chapter.
- Chapter 5, Conclusion: In this chapter, the final conclusions about the work are discussed taken into account the objectives proposed. Moreover, there will be recommended possible future works surrounding this theme.

CHAPTER 2

STATE OF ART

2.1. Micro-injection

Micro-injection molding is the process of transferring a thermoplastic material, in the form of granules, from a hopper into a heated barrel so that it becomes molten and soft. The material is then forced under pressure inside a mold cavity, where it is subjected to holding pressure for a specific time to compensate for material shrinkage. The material solidifies as the mold temperature decreases below the glass transition temperature of the polymer. After sufficient time, the material freezes into the mold shape and gets ejected, and the cycle is repeated. [4]

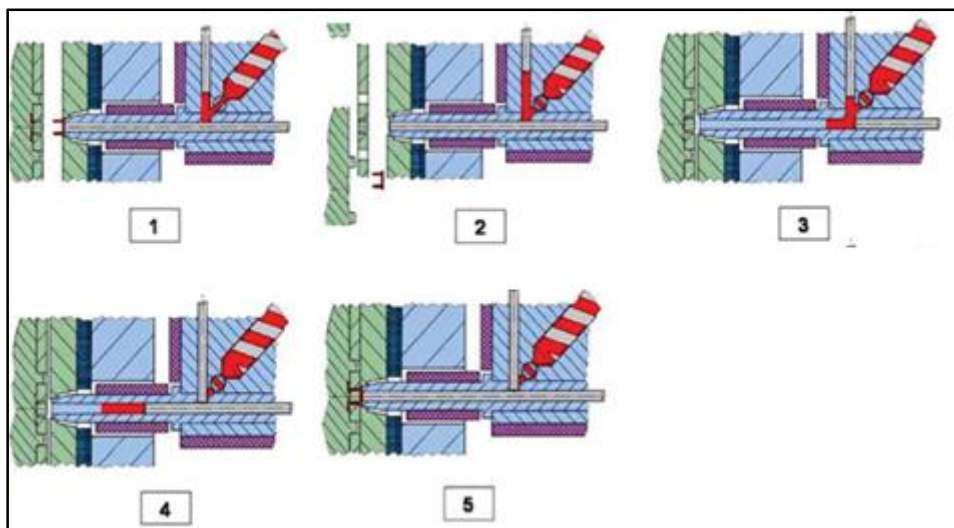


Figure 1 – Micro-injection molding steps. [5]

This technology is one of the most promising fabrication technologies for thermoplastic polymer micro-parts. Moreover, when it is referred as a promising fabrication technology, it means that it is predicted an annual growth rate of about 10%. [6, 7]

Moreover, micro-injection molding allows producing details or parts with very low dimensions at low price, as well as integrating functions during processing. Comparing with the conventional injection molding, this technique has the advantage of processing parts with a higher precision, reproducibility and quality, besides the very low dimensions referred previously. In fact, the concept of microinjection comes from the idea of transferring the high potential of injection molding to produce a thin part in an economic, efficient and detailed manner.

However, the term very low dimensions has many interpretations and therefore, there is not a concrete definition for it. According to one of those many interpretations, a micro-part must present the following three characteristics:

- Parts weighting only one fraction of a gram or a volume of one fraction of a pellet (usually the weight of the part injected is less than 0,1 g)
- Parts with details in micro scale.
- Parts with micro scale precision, i.e. tolerances in micro scale.

In addition, for all the topics above, the micro-molded part can have dimensions that are not in micro scale. [4, 8, 9, 10].

2.1.1. Applications

Nowadays, the parts molded by microinjection are used in many areas, namely microelectronics, micro-optics, micro-fluidics and micro-mechanics. However, the tendency is to bet in the medical and electrical areas, as well as other applications with high technical accuracy. [11]

The most widely sold micro molding product is the CD and DVD. However, there is a great variety of applications for this molding process, e.g. holograms, spectrometers, lenses, optical switches, optical fiber connectors, waveguides, anti-reflective surfaces, optical gratings, photonic structures, pumps, valves, nebulizers, ink jets, capillary analysis systems, device for investigation of living cells and flow sensors. [12]



Figure 2 – Examples of microinjection molding parts with one component (left) and two components (right). [13]

2.1.2. Materials

Selection of material is an important factor for micro-injection molding since it determinates the quality for the part molded. So, the material must have a high MFI (for correct filling of cavity by the material even with low pressures), stiffness and ductility (due to the low cavity area and for a safe part extraction) and mechanical behaviour (mainly to support the pressure

applied by the process and, therefore avoid rheological defects), as well as allowing the mixture with additives to improve the injection process. [14, 15]

The list of polymer materials that were processed with success, i.e. polymer materials that fulfil a set of properties and specifications are presented on table 1.

Table 1 – List of materials that fulfil a set of properties and specification for microinjection molding. [4]

Materials			
Amorphous		Semi-crystalline	
ABS	Acrylonitrile-butadiene-styrene	LCP	Liquid crystal polymer
COC	Cyclic olefin copolymer	PA 6	Polyamide 6
COP	Cyclic olefin polymer	PA 12	Polyamide 12
PAI	Polyamide imide	PBT	Polybutylene terephthalate
PEI	Polyetherimide	PE	Polyethylene
PC	Polycarbonate	PEEK	Polyetheretherketone
PMMA	Polymethylmethacrylate	PFA	Perfluoroalkoxy
PS	Polystyrene	PLA	Polylactic acid (polylactide)
PSU	Polysulfone	POM	Polyoxymethylene
MABS	Methylmethacrylate acrylonitrile-butadiene-styrene	PP	Polypropylene
SAN	Styrene acrylonitrile	PVDF	Polyvinylidene fluoride

SBS Styrene-butadiene-styrene

2.1.3. Conventional equipment

Micro-injection molding requires techniques and equipments that are different from the conventional way since the construction rules applied are not suitable to the micro-injection molding requirements. As example, the low precision of the machine hydraulic control, the difficulty on ensuring the right doses of material, the possibility of degradation for the injected material (melted material could be retained too long in the cylinder due to the unsuitable screws) and the difficulty on manipulating the components due to the low dimensions. Therefore, construction rules must be rethought and adapted to a micro scale. [16, 17]

Such adaptations involve the modification and development of the equipments by reducing the injection and closing units, changing the doses method (using a piston or a screw but with lower dimensions and different geometry) and changing its structure and auxiliary equipments. Those modifications and developments depend of the manufacturer solutions to decrease the material and energy consumption. [17]

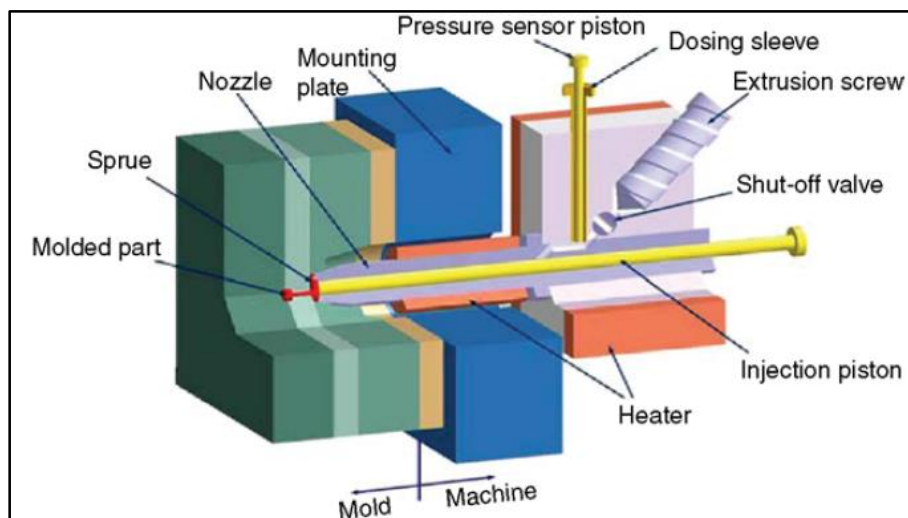


Figure 3 – Example of an injection unit for a micro-injection molding machine. [18]

Moreover, there is a series of manufacturers for micro-injection systems. Each manufacturer has his own characteristics, as seen in table 2.

Table 2 – List of micro-molding machine commercially available and their characteristics. [16]

Manufacturer	Model	Clamp force (kN)	Injection capacity (cm ³)	Injection pressure (bar)	Plasticization (screw or plunger)	Injection speed (mm/s)
APM	SM-5EJ	50	1	2450	14 mm screw	800
Babyplast	Babyplast 6/10	62.5	4	2650	10 mm plunger	-
Battenfeld	Microsystem 50	56	1.1	2500	14 mm screw	760
Boy	12/AM 129-11	129	4.5	2450	12 mm screw	-
Fanuc	Roboshot S200-I 5A	50	6	2000	14 mm screw	300
Lawton	Sesame Nanomolder	13.6	0.082	3500	10 mm plunger	1200
MCP	12/90 HSE	90	7	1728	16 mm screw	100
Milacron	Si-B17 A	147	6.2	2452	14 mm screw	-
Nissei	AU3	30	3.1	-	14 mm screw	-
Nissei	EP5 Real Mini	49	8	1960	16 mm screw	250
Rondol	High Force 5	50	4.5	1600	20 mm screw	-
Toshiba	EC5-01.A	50	6	2000	14 mm screw	150

Toshiba	NP7	69	10	2270	16 mm screw	180
Sodick	TR05EH	49	4.5	1970	14 mm screw	300
Sumimoto	SE7M	69	6.2	1960	14 mm screw	300

2.1.4. Molds

The mold development and manufacturing represents a challenge to micro-injection molding due to some differences with the conventional molding, namely dimensions, details and tolerances. Therefore, starting from the techniques used until the constitution of the mold, the rules applied to conventional injection molding are not the same.

The mold should be projected so the injection nozzle can touch the partition plane. In this way and, due mainly to the low thickness of the parts molded, the injection could be made directly in the part or in feeding channels. If it is chosen the second option, the feeding channels must be as short as possible to minimize thermal losses due to the low weight of parts. [16]

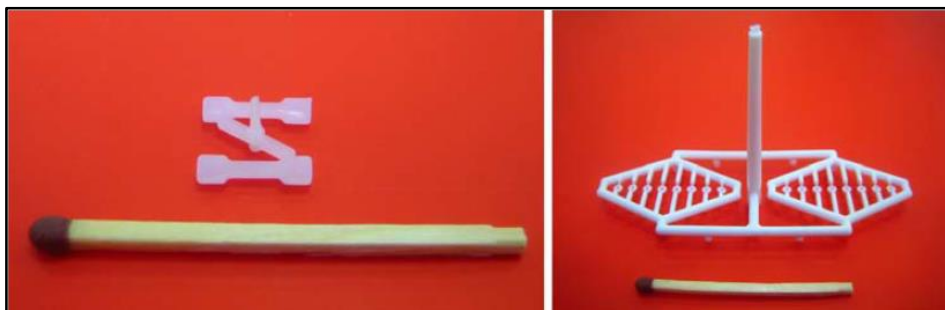


Figure 4 – Comparison of feeding channels to mold micro-part with conventional molding machine (right) and with microinjection molding machine (left). [18]

Also, due to the low thickness of micro-parts, the material injected reach all the cavity with a temperature very close to the cylinder temperature and, therefore, the risk of solidification and incomplete parts decreases. [16]

Because of the micro-part low dimensions, the exhaust gas system must be rethink in order to avoid defects. As a result, vacuum must be applied after the mold closes and before the injection of material in an effort to remove the air from the cavity. However, that technique implies

the application of O-rings to stanch completely the cavity and the use of a vacuum pump to render efficiently the air extraction. [19]

The clamping plates are very similar to the conventional injection molding except for the mold, which should be fixed to the machine to guarantee a perfect alignment and present a lower tonnage.

The material that constitutes the mold must have a very low thermal expansion coefficient to obey the strict tolerances imposed. In addition, any small displacement of dimensions could affect the precision and reproducibility of the process. Any strain gages or resistors and insulating plates used should be focused in compensate the heating loses as best as possible.

The injection temperatures in micro-injection are usually high due to the fast freezing of polymer melt in the cavity. So, as the cycle times are low, it is needed to use a Variotherm type system which allows a rapid and effective control of the mold temperature, extending the frozen period of polymer melt during filling stage, as presented in figure 5. Usually, resistors are installed in the mold along with conventional cooling channels. Therefore, it is possible then to assure a rapid heating of the plates in the injection phase by the resistors and a rapid cooling in the cooling phase by the conventional cooling channels. [20, 21]

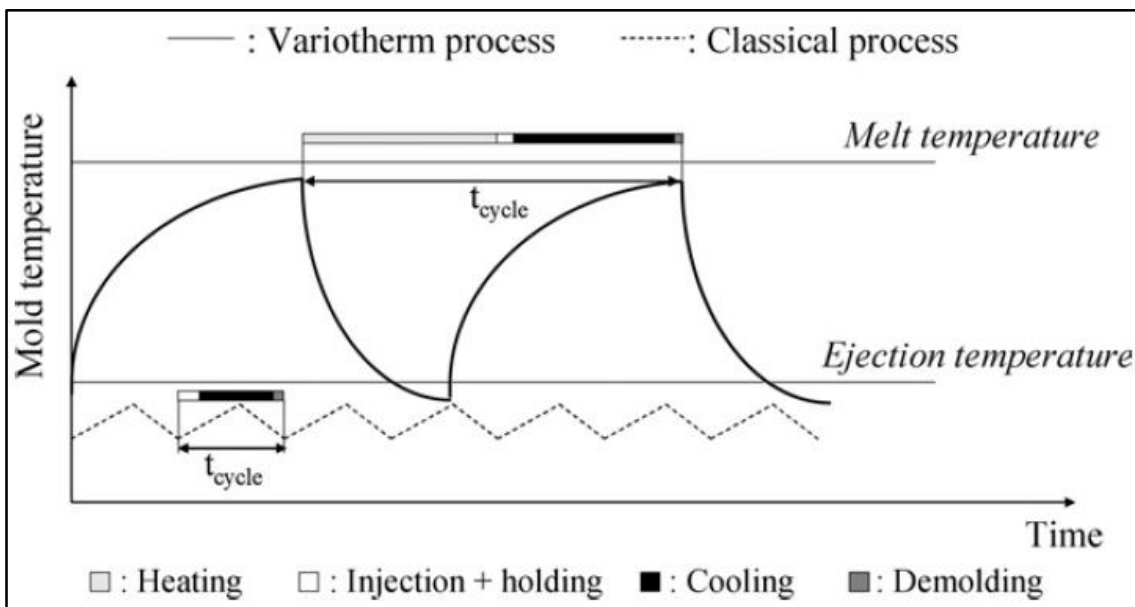


Figure 5 – Comparison between mold temperature in the classical and variotherm processes. [22]

Regarding to the extraction system, the conventional system used is not suitable for this type of injection since the extractors affect the surface quality upon contact and could provoke deformation to the micro-part. In addition, when the extractors move, they promote static electricity

and, as a consequence, adhesion to the mould. However, this problem is solved by introducing ionized air into the cavity or use a robot with vacuum suction.

In addition, to ensure dimension precision for a mold and therefore, strict tolerances, the molds can be manufactured either by CNC machining or by using EDM processes.

2.1.5. Processing Conditions

Every thermoplastic molding process has some parameters that are more important than others, in order to obtain the better molded part as possible. In microinjection, these processing parameters are: Injection temperature, mold temperature and dosage. These three parameters affect highly the quality and replication of a micro-part. There are also other variables, but their contributions to the results of a micro-part are not as important as the three one's spoken before. Those variables are: Injection speed, injection pressure, post-pressure and post-pressure time.

The ideal molding is to have a hot mold during filling stage and a cold mold during the cooling stage. Therefore, it must be used temperatures close to the glass transition temperature and melting temperature, depending of the polymer morphology, to allow a better injection and cooling phase and therefore, to make sure that the process has the best quality and replication as possible. [23]

2.1.6. Design and geometry

As microinjection is still a recent technology, there isn't a standardised approach related to design and geometry, only literature that provide approximations and specific problems solving, e.g. sink marks, frozen-layer, among many others.

Consequently, some general and special design recommendations used in conventional injection molding can be useful in microinjection molding, such as uniform part thicknesses, gate and runner positioning, cooling system distribution and ejection points for general recommendations and minimum channel dimensions, maximum aspect ratios, spacing between channels, surface roughness, flow direction and position of the ejection points for special recommendations. In addition, also, for the first recommendation, the effect of shrinkage on part demolding and shape stability becomes significant with higher aspect ratios. [4]

2.2. Mold Surface Heating

As known, the reduction of the cycle time is one of the key issues for economic success of micro-structured products. However, maintaining mold temperature at the correct processing conditions is difficult without increasing cycle time and thereby, production costs. [19, 24]

Besides the factors of material, part and mold designs, mold temperature is the most critical parameter since the other parameters, such as pressure and injection velocity, are all affected by it. [25]

Conventional injection molding generally uses a constant mold temperature control strategy. However, a new method using a dynamic mold temperature control strategy is enhancing the surface appearance of the molded parts, which is called RHCM. In addition, the control must be performed locally in the key features or the mold surface due to the large heat mass of the mold. [26, 27]

According to mold temperature variation, the RHCM process is divided into four stages including rapid heating, high-temperature holding, rapid cooling and low-temperature holding. At the beginning of the process, the mold cavity surfaces will be rapidly heated to a relatively tight temperature. At the following high-temperature holding stage, the polymer is injected out through the nozzle and runner system to fill mold cavity. After the mold cavity has been completely filled, the injection mold will be rapidly cooled to solidify the shaped polymer in the mold cavity. After that, at the following low-temperature holding stage, the injection mold is opened to take out the molded part. [28]

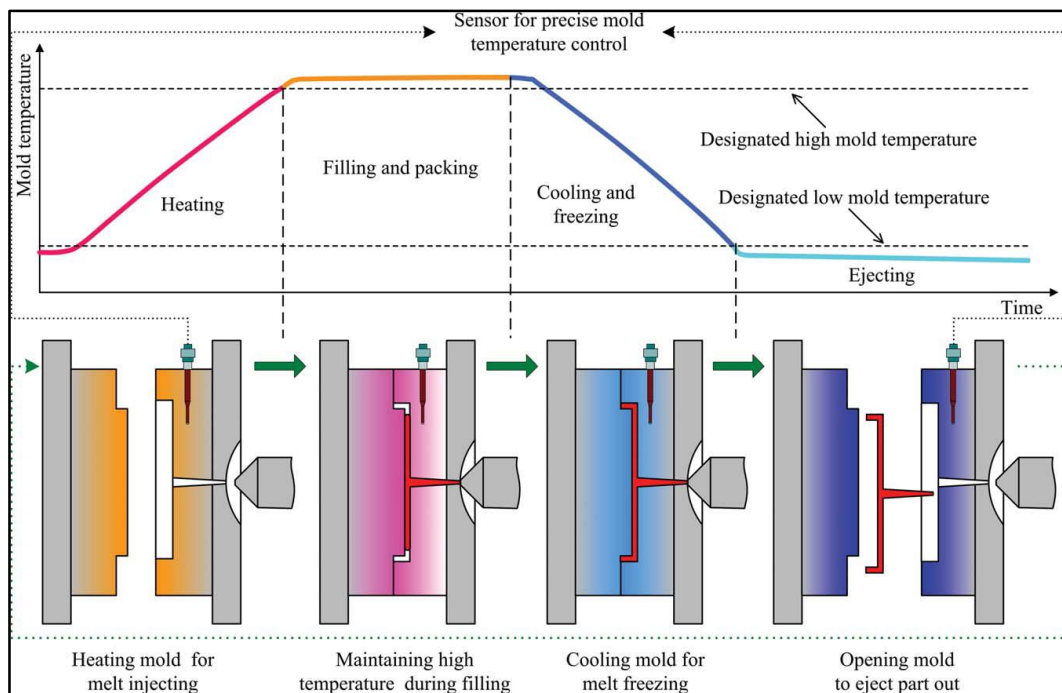


Figure 6 – Scheme and illustration of mold temperature changes during RHCM processes. [29]

The mold should be heated and cooled alternatively according to the requirements of the polymer to melt in the cavity surface temperature so as to achieve an ideal mold temperature control. By doing this, the premature solidification of the polymer melt and the resulting frozen layer, the mobility of the polymer melt especially the melt close to the cavity and the filling resistance can be reduced. Additionally, it also can be used to reduce the residual stress of the molded part and increase the flow length of the polymer melt so as to mold thin wall part or the part with micro-features. [28, 30]

2.2.1. Functional requirements and constituent elements

For a functional rapidly heatable and coolable mold, there are three requirements elements that must be followed due to their influence: a stiff, strong and durable mold with a low thermal mass; means for rapid heat generation in the mold surface portion; and means for rapid heat removal in the mold surface portion. [31]

2.2.1.1. Stiff, strong and durable mold with a low thermal mass

The thermal mass describes how the mass of an object provides inertia against temperature fluctuations and it can be defined by the following equation:

$$M=m \cdot C_p = \rho \cdot V \cdot C_p \quad (1)$$

Where m is the mass, C_p is the specific heat, ρ is density of the mass and V is the volume of the mass. The equation above indicates that, in order to have a low thermal mass, a low density, a low specific heat, a small volume or even a combination between these three aspects are the most relevant factors. However, the low density and the low specific heat are intrinsic material properties that can't be modified, only when designing a new mold through material selection. This means that only the volume of material being heated has a practical relevance, but it is limited due to mold design constraints, particularly the size of the cavity and the required structural stiffness. As a consequence, other mechanisms, e.g. use of porous mass or insulated mass, could be used to reduce the actual volume of material involved in heating. [31]

2.2.1.2. Means for a rapid heat generation and removal in the mold surface portion

The mold surface heating can be derived from the same equation that is used for describing the heating transfer process in thermoplastic injection molding:

$$\rho \cdot C_p \cdot \left(\frac{\partial T}{\partial t} + v \cdot \nabla T \right) = \nabla \cdot (k \cdot \nabla T) + (\alpha \cdot \sigma : \dot{\gamma} \cdot \dot{s}) \quad (2)$$

Where ρ is density, C_p is specific heat, T is temperature, t is time, v is velocity vector, k is thermal conductivity, α is the fraction of deformation energy converted into heat, σ is a total stress tensor, $\dot{\gamma}$ is a strain rate tensor and \dot{s} is a heat generation source from a nondeformation field. The first contribution, i.e. $\rho \cdot C_p \cdot \left(\frac{\partial T}{\partial t} + v \cdot \nabla T \right)$, represents the convected heat from the melt, the second contribution, i.e. $\nabla \cdot (k \cdot \nabla T)$, represents the heat conducted to the mold and the third and last contribution, i.e. $(\alpha \cdot \sigma : \dot{\gamma} \cdot \dot{s})$, represents the heat generation inside the thermoplastic. With this equation it is possible to predict one of main problems of injection molding, i.e. the premature solidification of the melted polymer in the cavity.

In addition, also the boundary conditions are considered for mold surface heating, depending if the surface heating is made by convection, conduction or radiation.

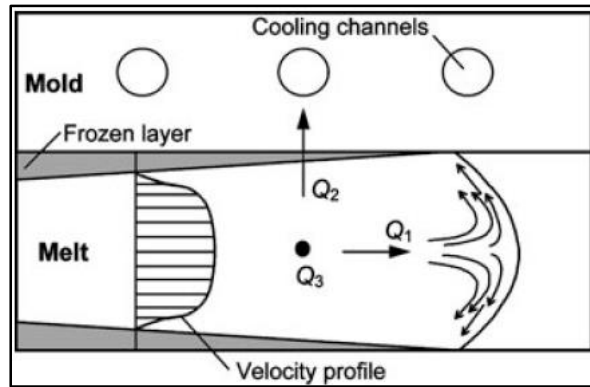


Figure 7 – Schematic of heat transfer process in injection molding showing three contributions in heat transfer: Q_1 , convected heat from the melt; Q_2 , heat conducted to the mold; and Q_3 , heat generation inside the thermoplastic. [31]

Furthermore, since there is no convection inside a solid mold material, the only two mechanisms relevant to mold rapid heating are heat generation and heat conduction. The difference between them is that heat generation is a source and heat conduction occurs through the application of boundary conditions. Typically, due to the low conductivity of polymers, heat generation is more used than heat conduction. The heating mechanisms and their divisions can be seen below.

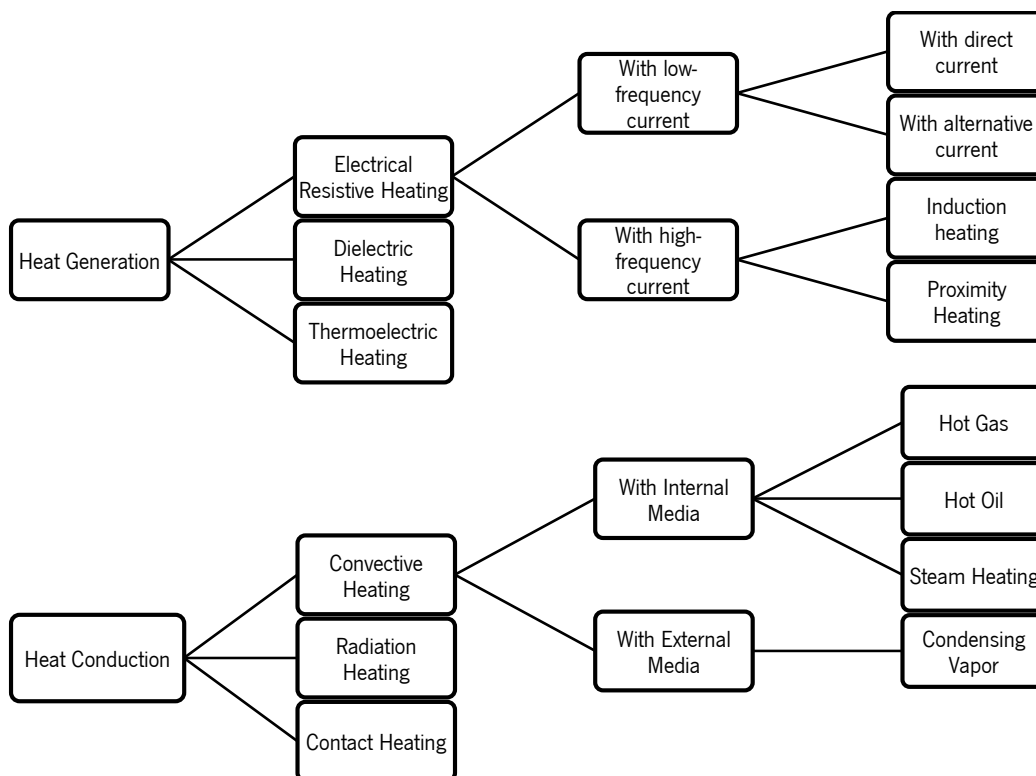


Figure 8 – Rapid heating mechanisms and their divisions.

The key feature for mold surface temperature control is the heating phase and therefore, knowing briefly about the types of heating is crucial.

Consequently, electrical resistive heating transforms electrical energy in heat energy. This type of heating can be a low or high-frequency. If is the first one, generally this method is composed by two layers: a heating and an insulation layer, as it is possible to observe in figure 9. Electrical current, which can be direct or alternative, is provided to a heater and this heater directs the heat towards the desired surface and the insulation layer. However, due to the difficulty to insulate efficiently (mechanically and thermally) the heat, this technique requires more studies to make it feasible.

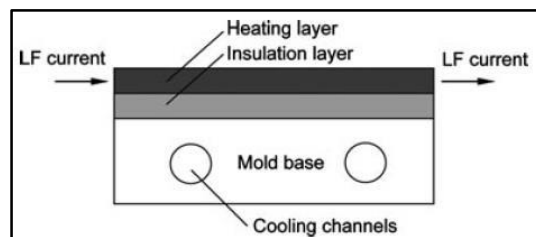


Figure 9 – Principle of the electrical resistance heating with low-frequency current. [31]

If on the other hand it is the second one, the heating can be provided by induction or proximity. In the induction heating, the part is introduced in a magnetic field generated by a coil where alternative current will be developed and when the magnetic field changes his value, heating will be created. The closer the coil is from the part, the greater heating is generated. [32]

In the figure 10 it is possible to observe the principle of this type of heating.

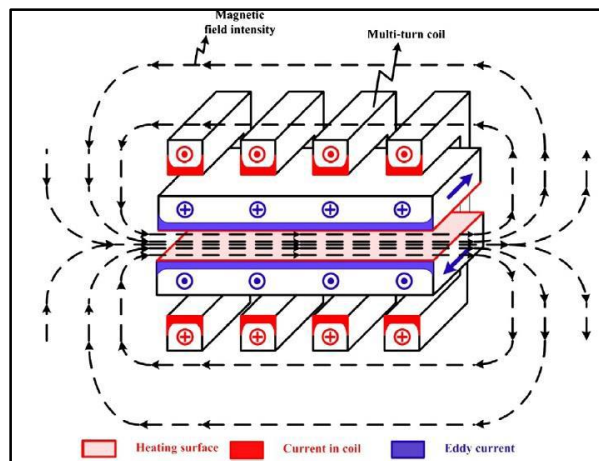


Figure 10 – Illustrative image of the induction heating principle. [32]

In the proximity heating, two mold plates close to each other form a small gap in which electrical current passes. Due to the proximity effect, that electrical current flows in opposite directions, tending posteriorly to flow into interior zones and consequently generating heat. This principle can be observed in figure 11. [33]

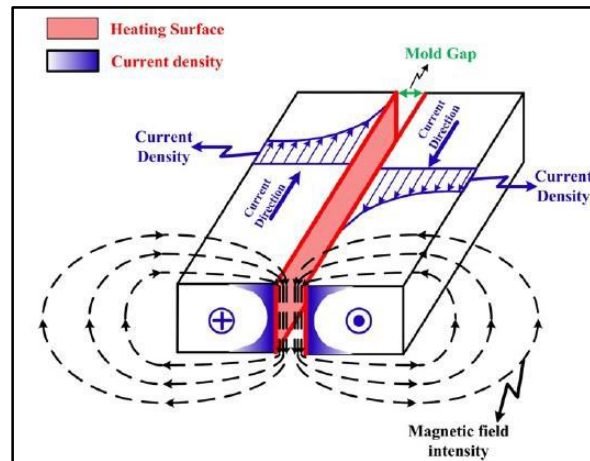


Figure 11 – Illustrative image of the proximity heating principle. [33]

As a note, all techniques derived by electrical resistance heating obey to the first law of Joule:

$$P=V*I=R*I^2 \quad (3)$$

Where P is the power (energy per unit time) converted from electrical energy to thermal energy, I is the current, V is the voltage and R is the resistance.

Other type of heating is dielectric heating. In order to promote the mold heating, using a dielectric material and an electric insulation is required. The dielectric material can be heat up by electromagnetic radiation of high-frequency using dipolar rotation. However, due to his limitations, this technique is often used to promote polymer heating instead and therefore, is commonly not used as a mold heater but as an auxiliary heating. [31]

Thermoelectric heating or Peltier effect indicates that a metallic joint of two different materials can produce heat or cold by absorbing or releasing thermal energy, depending on the direction and intensity of the electric current that circulates on that joint, as it is possible to verify in figure 12. Therefore, the thermal energy is proportional to the current, i.e., as the current increases his current intensity, the absorption or release of energy increases too.

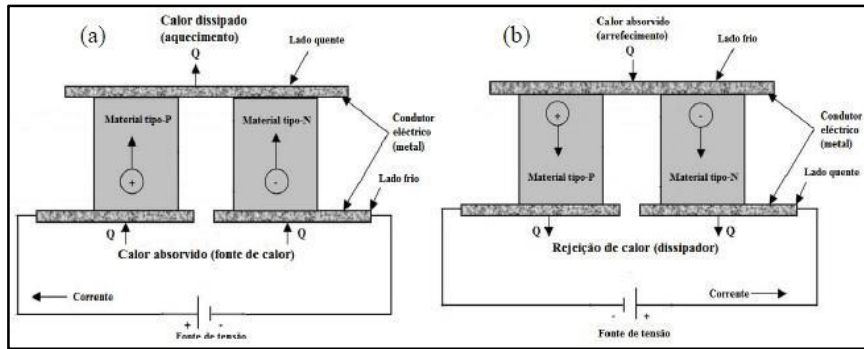


Figure 12 – Heating (a) or cooling (b) according to Peltier's effect. [34]

As the name says, convective heating transfers heat by convection between a fluid (water, steam, oil or gas) and a solid (mold steel), promoting externally or internally the mold heating. On the other hand, radiation heating transfers heat by radiation between an infrared system and a solid (mold steel). This system is similar to the induction heating since the difference is that halogen lamps are used instead of a coil.

Regarding to the cooling and in comparison with heating, it can be performed at considerably lower rate because, during cooling, the injection molding machine needs additional time for plasticising. Moreover, as the polymer in the cavity has a low thermal diffusivity and is cooled slowly, particularly for relatively thick parts, the thermal gradient developed in the cooling stage is much lower than that in heating stage. All the cooling mechanisms and their divisions can be seen in figure 13.

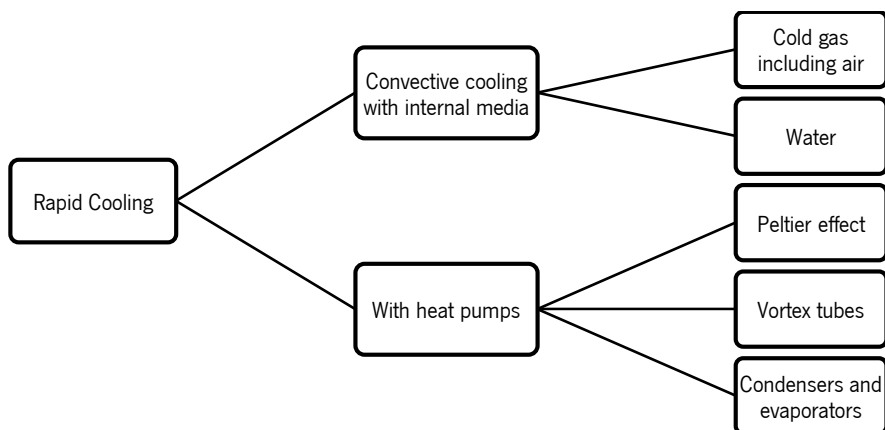


Figure 13 – Rapid cooling mechanisms and their divisions.

Finally and in order to understand and compare the influence of these techniques, two tables are presented containing information about the performance and general features of them:

Table 3 – Generic comparison between heating techniques.

Heating equipment	Cooling equipment	Cycle time	Tool surface (mm)
Gas flame	No	AT to 400 °C in 10 s	100 x 100 x 30
Rapid thermal response mould	No	AT to 250 °C to 50 °C in 11 s	72 x 25.4 x 12.7
Proximity heating	Air pockets	AT to 220 °C to 90 °C in 14 s	24.3 x 51
Electrical system	Water circulation	25 °C to 150 °C in 20 s AT to 205 °C to 32 °C in 30 s	n/a
Infrared halogen lamp	No	AT to 208 °C in 20 s	180 x 180
Water heating system	Cold water circulating system	30 °C to 160 °C in 40 s	n/a
Oil heating system	Cold oil circulating system	30 °C to 130 °C in 40 s	n/a
Special surface coating	Coolant circuit	n/a	n/a
Peltier device	Peltier device	Temperature control difficult due to power and response time	n/a

Table 4 – Comparison of different methods for mold rapid heating based on different performance criteria. [31]

TABLE III
Comparison of Different Methods for Mold Rapid heating Based on Different Performance Criteria

	Heating Uniformity	Maximum Energy	Heating Efficiency	Capability for Heating Complex Mold Shape	Capability for Heating Large Surface Area	Ability of Using Single Metallic Mold	Thermal Stresses	Ability for Active Heating	Complexity in Mold Design and Fabrication	Difficulty for Thermal Measurement
Low-frequency resistive heating	M ^a	H	H	M	M	Nearly impossible	Extremely high	Possible	H	M
Induction heating	M	H	M	M	M	Possible	M/H	Difficult	M/H	H
Proximity heating	L	H	M	L	L	Possible	M/H	Possible	M	H
Infrared radiation heating	M	H	L/M	M	M	Possible	M	Need a transparent mold	M/H	M
Internal oil heating	H	L	M	H	H	Possible	L	Possible	L/M	L
Internal steam heating	H	L	M	H	H	Possible	L	Possible	L/M	L
External hot air heating	M/H	M/H	L/M	M	L/M	Possible	M	Not possible	M	M
Flame heating	M/H	H	L/M	M	M	Possible	M/H	Possible	M/H	M
Passive heating	H	L	H	H	H	Possible	L	Not possible	L	H
Contact conduction heating	L/M	M/H	H	L	M	Possible	L	Difficult	M	M
Thermoelectric heating	M	L	L/M	M	L	Nearly impossible	H	Possible	M	M
Dielectric heating	M	Dependent on molding polymer	Dependent on molding polymer	M	L/M	Possible	L	Possible	L/M	H

^aH, high; M, medium; L, low.

2.2.2. Research

There are a lot different terminologies for mold rapid heating and cooling in literature but still it is relatively difficult to heat and cool the cavity surfaces rapidly and uniformly within a relatively short molding cycle time, so as to not only improve the part quality but also to ensure high production efficiency. [28] The authors intended to differentiate a particular technology from others but generally, the techniques obey to the same principles as the ones described in figures 9 and 13. Development of capable techniques for rapidly heating and cooling the mold surface portion is a difficult task because of the constraints set by the heat transfer process and the endurance limits set by the thermal, mechanical, and sometimes electrical properties of the materials used for the mold. The most successful area of applications for mold rapid heating and cooling is most likely in micro-injection molding. [31]

Regarding to the many types of surface rapid heating and cooling systems developed for injection mold temperature control, as the mold cavity surfaces are all directly heated and hence they all have relatively high heating efficiency, still there are technical problems or shortcoming and, for that reason, they aren't widely used in actual production at present. [28]

Even so, *Kim et al.* [35] developed a momentary mold surface heating process in which the gas flame was used to heat the mold cavity surfaces. Despite of the heat generate in a very short time, the temperature control was far from being precise.

Chen et al. [36] used electromagnetic induction heating and coolant cooling to rapidly heat and cool the mold cavity surfaces. However, due to embedding an induction heating inside the mold and an external drive, the control is not so precise.

Chang and Hwang [37] developed a rapid heating system to make use of infrared heating method to directly heat the mold cavity surfaces. Nevertheless, due to low design flexibility of the infrared heating device, achieving an uniform heating of the cavity surface is a difficult task.

Chen et al. [38] designed a gas-assisted heating system in which hot gas heated directly the cavity surfaces. However, the design of the hot gas channels are a limitation in order to achieve uniform heating of the cavity surface.

Jansen and Flaman [39] developed a multilayer resistive heating mold (insulator layer coated on the mold base and a heating layer coated on the insulator layer as the cavity surface) of which was able to change the surface temperature by 70°C in 0,2 s.

The progress about the effect of mold surface heating is still slow. Notwithstanding, *Kim et al.* [35] found that a high cavity surface temperature can significantly improve part gloss and brightness (for a 30% glass fiber reinforced polycarbonate).

Yao and Kim [40] stated that a hot cavity surface temperature before filling can significantly increase the flow length of the polymer melt and, as a consequence, low-pressure and low-speed can be used in filling extremely thin cavities.

Kim et al. [41, 42] and *Chen et al.* [36] reported that a high cavity surface temperature before filling does improve the replication accuracy of micro-feature parts.

Huang and Tai [43] found that the plastic glass transition temperature is the optimal cavity surface temperature before filling for improving the replication ability of part micro-structure.

Yoon et al. [44] and *Chen et al.* [45] testified that raising the cavity surface temperature before filling can significantly decrease surface roughness and increase surface gloss of microcellular injection molded parts.

Wang et al. [46] and *Chen et al.* [47] reported that the high cavity surface temperature before filling can visually eliminate weld line on part surface.

CHAPTER 3

PRELIMINARY STUDY

As referred on the objectives, the main aim of this work is testing a controlled heating/cooling system for the rapid manufacturing of parts with better quality than those manufactured by a conventional method in micro-injection molding. Therefore, it was necessary to search and design a system to heat up the mold surface thus enabling reduction of frozen-in orientation and stresses. The one that will be presented on this work is mainly inspired on Jansen and Flaman [39] which according to them, the requirements corresponding to heat surface in common injection molding conditions are:

- A temperature rise of 50 to 100 K during 1 or 2 s;
- A limited increase in cycle time after heating of 20%;
- A homogeneous plane heating source;
- Proof against large shearing forces and pressures up to 1000 MPa;
- A smooth, wear resistant, upper surface which shows little interaction with the injected polymer.

Therefore, a heating element satisfying all the requirements must consist of a steel mold wall, an insulation layer, a heat producing layer and a protective coating. [39] The same analogy is used in our system as can be seen in the image 15. However, this project is different regarding to the materials chosen and has unique features concerning the design for a cavity where the system is introduced, as will be seen posteriorly.

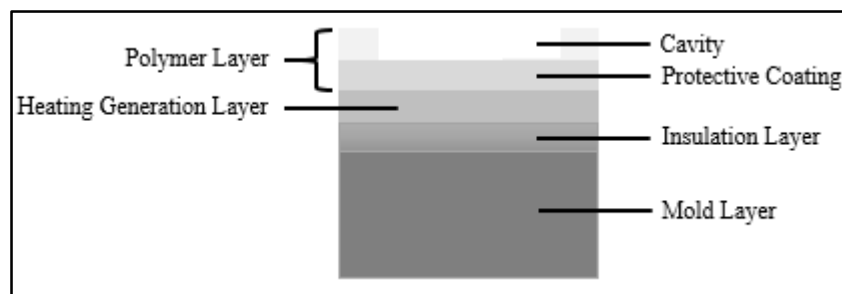


Figure 14 – Illustrative image of the layers that constitute the rapid surface temperature heating system.

Moreover, some initial considerations concerning the layers that constitute our system should be explained in order to understand their importance and influence on the rapid surface temperature heating system:

- Mold layer: must provide mechanical stiffness, strength and durability to endure the molding process.

- Insulation layer: main concern is addressed in electrical and thermal insulation. Therefore, material characteristics such as service temperature, thermal conductivity and volumetric heat capacity are crucial for a good performance of this layer.
- Heat generation layer: focused obviously in producing heat to the cavity through conduction. However, some restrictions should be taken into account such as: mold heated until a constant temperature before filling stage in order to allow an easier flow of the melt towards the cavity; heating power and duration should be regulated according to the heater specifications; positioning of the heating elements at mold surface to increase the response to temperature changes, as can be seen in figure 15; and homogeneous distribution of the heating elements to obtain an uniform orientation.
- Polymer layer is divided in two sections for a simpler comprehension: a protective coating and a cavity.
 - Protective coating's only function is to avoid direct contact between the heat produced by the heating generation layer from the melted polymer. In addition, the protective coating also provides a flat surface in order to help acquiring the geometry of the molded part.
 - Cavity function is to receive the melted polymer and acquire the desired geometry for the molded part.

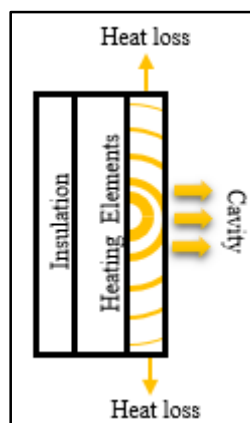


Figure 15 – Scheme illustrating the heat flux and intensity through the protective coating layer when positioning the heat elements at the mold surface.

3.1. Preliminary Study

After definition of the layers and their functions for the rapid surface temperature heating system, a preliminary study was made in order to evaluate the feasibility of it. This preliminary study was divided in three phases:

- Selection of materials for each layer: based on the characteristics required for the functions previously listed. In addition, since one of the requirements for the insulating layer is having a film form, an experiment transforming pellets into a film was also performed, as it will be explained later.
- Theoretical study: mainly focused in achieving the temperature profile on the mold surface, but also understand and maximize it. Therefore, the following studies were made: contribution of the insulation to the system; effect of the insulation thermal conductivity; response of two strain gages distanced between them in one axis on the temperature profile along the protective coating; and influence of both insulating and protective coating thicknesses.
- Practical study: has the same focus of the theoretical study, i.e. temperature profile on the mold surface, but its purpose is only to compare theory and practice and so, prove the veracity of the theoretical results.

3.1.1. Selection of materials

3.1.1.1. Mold and Polymer Layer

First of all, the mold and polymer layer are in the same topic since while doing the research, there was resemblances between the characteristics for both layers. So, the relevant characteristics when selecting material for both mold and polymer layer are the following ones:

- Durability, in order to be capable of resisting to thermal cycles caused by successive heating and cooling.
- Mechanical stiffness, in an effort to be sure that the molded part doesn't have marks and its reproduction is precise;
- Strength, in an attempt to support any possible structure variation caused by the molding process;

Briefly, those requirements are thought to ensure that the molding process occurs without any flaw for a long period of time. And also since those requirements are similar to the ones normally thought in the common mold industry, steel is the choice. Therefore, the kind of steel chosen and some relevant properties to the rapid surface temperature heating system can be seen on table 5.

Table 5 – Material and relevant properties chosen for the mold and polymer layer.

Mold and Polymer Layer					
Material	λ ($W * m^{-1} * K^{-1}$)	ρ (kg/m^3)	C_p ($J/kg * K$)	Thickness (mm)	Layer
				1	Mold
Stainless Steel	21.6	7760	2865	0.25	Protective Coating
				0.3	Cavity

Regarding only to the polymer layer, also the materials which will be injected into the cavity were submitted to a selection. The kind of polymers selected are a crystalline plastic and an amorphous plastic and they were chosen not only according to characterization which will be posteriorly displayed but also because I will take advantage of data given by [48].

Table 6 – Materials chosen for injecting.

Kind of polymer	Generic Name	Grade Name	Datasheet
Amorphous	PS	Edistir N1910	Attachment 1
Crystalline	PP	Moplen HP548R	Attachment 2

3.1.1.2. Insulation Layer

As previously said before, the selection of material for the insulator layer is mainly dependent of three characteristics:

- Service temperature: Describes the maximum recommended temperature at which a material can be used without compromising its performance. As the insulation is next to the heater and it is planned to not use a surface temperature higher than 150°C, a safe value selected for this characteristic is defined as being equal or higher than 170°C;

- Thermal conductivity: Quantifies the material ability to conduct thermal energy, i.e. provide heat. It is clear that materials who have a high thermal conductivity conduct thermal energy faster and effective than material with a low thermal conductivity. Therefore, as the objective of this layer is to provide both electrical and thermal insulation, the search must focus on a low value of the thermal conductivity. After research, that value is set to be equal or lower than $0,25 \text{ W}\cdot\text{m}^{-1}\cdot\text{K}^{-1}$.
- Volumetric heat capacity: For a material point of view, this characteristic defines a given volume material ability to store internal energy while undergoing a given temperature change, but without undergoing a phase transition. Thus, it is also known as the product between density and specific heat capacity of a material. For our purposes, the more ability a material has to store internal energy, the less heat is conducted. So, the search must focus on high values for density and specific heat capacity. After research, the value for density and specific heat capacity should be equal or higher than $1000 \text{ kg}\cdot\text{m}^{-3}$ and $1000 \text{ J}\cdot\text{kg}^{-1}\cdot\text{K}^{-1}$, respectively.

In addition, another requirement is that the polymer should present a film form and should the lowest thickness as possible. After identifying all the main requirements for the insulation layer, understanding which of those characteristics has a higher relevance than the other is a critical step for the selection of insulation material. Therefore, through a weighting table, represented in table 7, ordering the requirements by their importance is possible.

Table 7 – Weighting table for the selection of the main property for the insulation material

Weighting Table						
	A	B	C	D	Total	Pf
A	-	0.5	1	1	2.5	5
B	0.5	-	0.5	0.5	1.5	5
C	0	0.5	-	0.5	1	4
D	0	0.5	0.5	-	1	4

Legend:

0 – less important; 0.5 – equally important; 1 – more important

A = Thermal Conductivity; B = Service Temperature; C = Density; D = Specific Heat

As shown above, thermal conductivity is the most relevant characteristic for this material selection, followed by service temperature and density and heat capacity. As a rule, next step is searching in generic databases by the predetermined order which materials fit in the requirements, as it is possible to see in table 8. In addition, it is crucial to mention that due to some issues, namely the lack of film suppliers for the desired kind of polymers and the very expensive prices, the search was focused on pellets that posteriorly were transformed in a film.

Table 8 – Materials and their relevant properties selected for the insulation layer.

Material	λ (W * m⁻¹ * K⁻¹)	Service Temperature (°C)	ρ (kg/m³)	C_p (J/kg * K)
Polytetrafluorethylene (PTFE)	0.24	260-290	2100-2200	1200-1400
Polyetheretherketone (PEEK)	0.25	154-260	1260-1320	1340
Polyethersulfone (PES)	0.13-0.18	175-220	1370-1460	1100
Polyimide (PI)	0.1-0.35	260-360	1310-1430	1090
Polyetherimide (PEI)	0.22-0.25	170	1270-1300	2000

Source: [49, 50]

On table 8, among the five materials presented and respecting the importance order, polyethersulfone and polyimide stand out for being the best ones mainly because of the low narrow for the thermal conductivity values (polyethersulfone) and the possibility of finding a very low thermal conductivity value (polyimide). So, in order to choose the material, a search for a grade was conducted, having the following results:

Table 9 – Best materials for the insulation layer.

Material	Grade Name	Datasheet
Polyethersulfone (PES)	BASF Ultrason E 3010 PES	Attachment 3
Polyimide (PI)	Mitsui AURUM 450	Attachment 4

According to the databases, both materials could be perfectly chosen for this purpose but since polyethersulfone has a slightly lower thermal conductivity (difference of approximately $0.2 \text{ W} \cdot \text{m}^{-1} \cdot \text{K}^{-1}$) and also it is easier to acquire, the material chosen is polyethersulfone which has the following relevant properties for the insulating layer:

Table 10 – Material and his relevant properties for the insulation layer.

Insulator Layer				
Material	λ $(\text{W} \cdot \text{m}^{-1} \cdot \text{K}^{-1})$	ρ (g/m^3)	C_p $(\text{J}/\text{kg} \cdot \text{K})$	Thickness (mm)
Polyethersulfone (PES)	0,15	1370	1000	0,25

3.1.1.3. Heating Generation Layer

There are an unlimited number of heaters that could be chosen for this project. However, for the heating generation layer, strain gages were the material selected as heater mainly because of the the topics presented bellow:

- very low thickness;
- achieve relatively high temperatures, i.e. until a maximum of 200°C ;
- large thermal conductivity;
- commercially available with the lowest cost possible;

Generally, strain gages are considered as physically simple device which can be easily applied in a straightforward manner for elementary measurements of surface strains. [51] However, when the strain gages perform that measurement, they change in size by thermal expansion, changing also the electrical resistance of the gauge which connected with wires allows the production of heat. The objective is availing this fact in order to heat the mold surface.

Concerning the types of strain gages available, the most common ones are the bonded type which are made into a metallic grid form with a zig-zag pattern and cemented between two pieces of thin paper, depending on the nature of the carrier and the encapsulation characteristics. In the next table, the strain gages properties are presented:

Table 11 – Material and his relevant properties for the heat production layer.

Heating Layer				
Material	Nominal Resistance (Ω)	Dimensions (mm)		Max V (Vrms)
		Grid	Carrier	
OMEGA SGD-4/120-LY13	120	5,70*3,80	7,90*7,10	12

Source: Attachment 5

3.1.2. Obtainment of a film

According to what was said before, in order to achieve a film form for the insulation layer, a hot squeezer was used, as seen in figure 16. Briefly, the experiment consists in putting pellets between two plates of aluminium and afterwards, carefully introduced them into and in contact with a hot squeezer, where they will melt. After a certain period of time, pressure is applied in order to achieve the desired thickness and then, with the contribution of cold water, it is possible to remove the film. The expected result is a film a thickness of approximately 200 μm without any visible defect, which could compromise his performance.

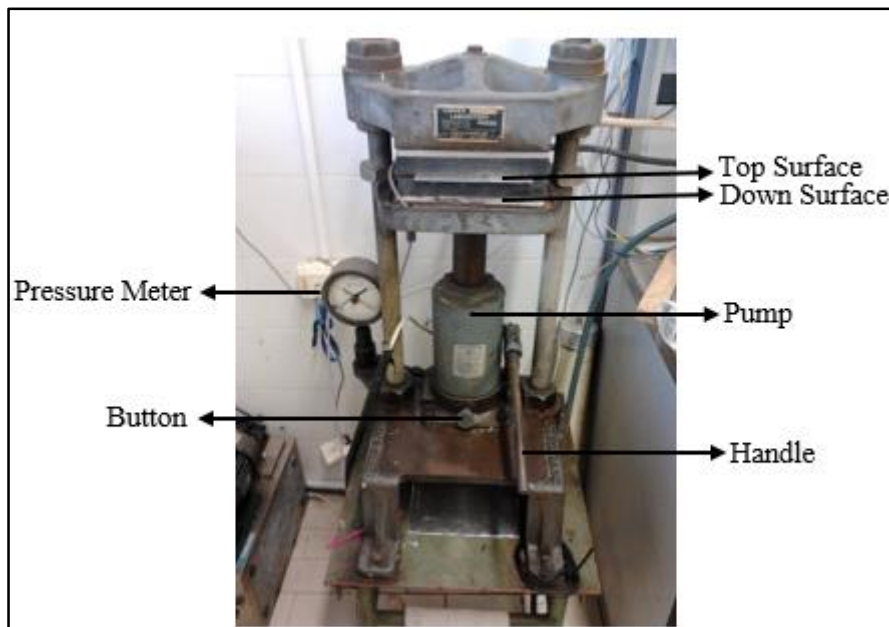


Figure 16 – Hot squeezer, i.e. Carver Laboratory Press, used in the experiment.

3.1.2.1. Experiment

Before starting the experimental procedure, pre-treatment of the pellets was required in order to decrease the probability of obtaining defects and consequently, improve the performance of the film. This pre-treatment is related to the removal of the water present on the PES pellets by using a stove with the following parameters:

- Temperature: Between 100°C and 110°C;
- Existence of gas and vacuum inside the stove;
- Residence time: 12 hours.

In addition, temperature calibration of the hot squeezer was also performed. The temperature chosen needed to be higher than the glass transition temperature of the polymer in order to enable the melting of the material. So, as polyethersulfone has a glass transition temperature between 210 to 230°C, the temperature of the machine should be higher than 230°C.

3.1.2.2. Experimental procedure

When the two aspects explained in the experiment topic are dealt with, then it is possible to begin the experimental procedure which has the following steps:

- 1) Place the pellets on a plate of aluminium and set them as close as possible, as it is on figure 17, with the help of a spoon or a tweezer;
- 2) Put the second plate of aluminium on top of the pellets;
- 3) Carefully, put the pellets and plates between the top and down surface of the Carver Laboratory Press;
- 4) Use the handle until the plates are in perfect contact with the pellets. Note that in this step, the pressure meter should show 0 bar as the objective is only to melt the pellets;
- 5) Use again the handle, but apply pressure in an effort to obtain the desired thickness;
- 6) Remove the plates from the surfaces with the aid of gloves and put the plates immediately in a container with cold water;
- 7) Separate the two plates and remove the film.
- 8) Clean the plates with acetone and repeat the experiment if another film is desired.

As a note, thickness was measured by a micrometer.

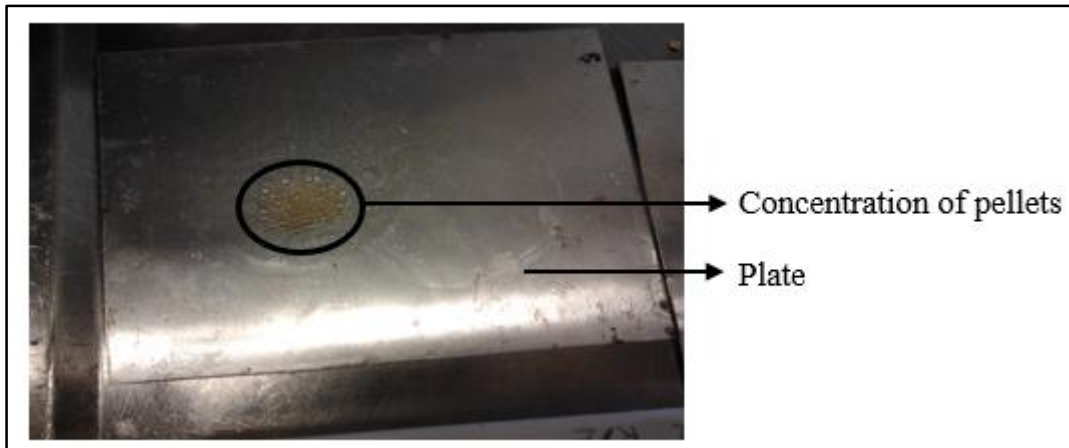


Figure 17 – Illustrative image of the pellets placed in the aluminium plates.

The parameters of this experiment were: heating time, where a longer heating time promotes a better melting of the pellets; heating temperature, where the temperature can't be too high because the pellets could degrade but can't be too low because the pellets need to be melted; pressure, which affects the thickness of the film; pressure time, which influences the thickness distribution along the film, i.e. a longer pressure time means a better distribution of the melted pellets.

However, this procedure has some disadvantages that can affect the film quality, such as: continuous use of the plates where due to the constant heating and cooling that the plates suffer, after a determined number of cycles, they begin to degrade and release substances which could interfere with the film; disposal of the pellets in the plate (as close as possible), where the closer pellets are from each other, the uniform distribution of thicknesses along the film will be; removal of the film from the plates that for some unknown reason, in some experiments, the use of the anti-adhesive in order to easily remove the film from the plates affected the results by increasing greatly the appearance of voids. And, for that reason, most of the films were difficult to remove from the plates. The solution found for that removal was carefully bending the plates in different positions which inevitably changed the flatness of the plates; and finally, stability where due to a potential compromise of the disposal of the pellets spoken before, the introduction of the plates and pellets in the machine require steady hands and patience.

3.1.2.3. Result

After experiments consisting on changing just one and maintain the other parameters and, afterwards observe the result, the ideal values and result obtained were the following ones:

Table 12 – Experiments made and ideal parameters (in italic) for the obtainment of the polyethersulfone film.

Processing parameters	Unit	Values		
Heating Temperature	°C	260	280	300
Heating Time	min	16	18	20
Pressure	bar	6,5	8	9,5
Pressure Time	min	3	4	5

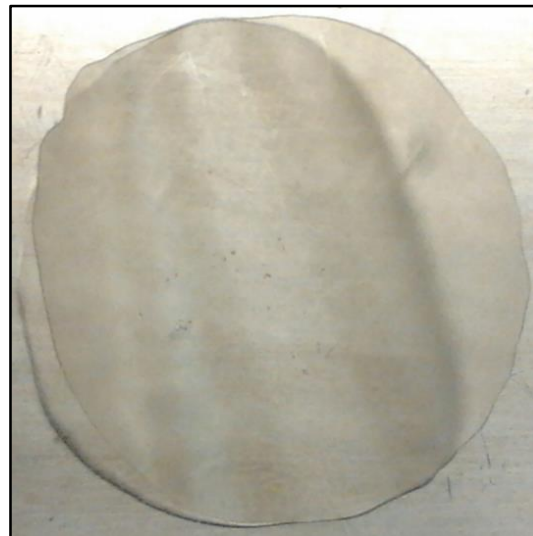


Figure 18 – Illustrative image of the polyethersulfone result at ideal parameters.

As shown in figure 18, the existence of visible voids is practically zero and the thickness, after measurement, is approximately 200 μm which indicates that the objective initially proposed is reached. Next step is using the film acquired as the insulator layer for the rapid surface temperature heating system by testing it in a practical way.

3.1.3. Theoretical and Pratical Study

3.1.3.1. FlexPDE

FlexPDE is a software labeled as a “scripted finite element model builder and numerical solver”. In other words, from a script written by the user, FlexPDE performs the operations necessary to turn a description of a partial differential equations system into a finite element model, solve the system, and present graphical and tabular output of the results. [52]

FlexPDE's contribution on this work was achieving theoretical results related to the rapid surface temperature heating system. However, a script had to be written and so, the crucial conditions in order to obtain results were the following ones:

- Partial differential equations used to describe the temperature profile through the layers, i.e., equations 1 and 2;
- Material characteristics of each layer;
- Placement of a thermocouple between both protective coating and cavity layer and parallel to the heater;
- Use of one heater providing an electrical power of 7.5 W during 1 second;
- Injected material selected was a generic polypropylene homopolymer unfilled with a processing temperature of 200°C.

Plus, the script used with the components spoken above can be seen on attachment 6.

3.1.3.2. LabVIEW

LabVIEW is a software tagged as a system-design platform and productive development environment for creating custom applications that interact with real-world data or signals through the use of a visual programming language called “G”. This allows to tie together data acquisition, analysis, and logical operations and understand how data is being modified.

For this particular work and since the objective is comparing with FlexPDE results, this software was mainly focused to acquire the temperature profile provided by the strain gages for a period of time, as it will be possible to see posteriorly in the practical results. Therefore, a source code using “G” programming language and a system which can efficiently acquire and reproduce the rapid surface temperature heating system was required, which can be seen on attachment 7 and figure 19 respectively.

Regarding to the source code, three conditions are different from the script wrote on FlexPDE: first, a block of polymer represented in figure 19 was used and consequently, the injection temperature isn't represented. However, since heating is provided before filling stage, the injection temperature can be considered as negligent.; second, the time of heat generation will be longer, i.e., 5 seconds, in order to evaluate more precisely the evolution of the temperature curve along the time. Plus, the time defined is 5 seconds because the curve starts to present a steady behaviour above that time; third and last, the thickness of the insulator film is 180 μm for both studies.

Concerning the system which acquires the temperature profile and reproduces the rapid surface temperature heating system, a lithium-based battery is connected to a plug, in order to receive and regulate current, to a switch for interrupting the current or, when clicked diverting the current to the strain gage and to one wire cable of the strain gage for closing the circuit. So, when the switch opens the circuit, strain gage will provide heat and a thermocouple will measure that heat. The data of that measurement is obtained by passing, as a signal, to an electronic amplifier which increases the power of the signal and, through a device called NI USB-6210, the data is delivered to a computer which displays the results according to the source code elaborated.

In addition, the practical results showed are an average result based on the temperature profile of five tests performed in an attempt to increase the precision of the comparison. As a note and a relevant factor is the main element which can affect that comparison: the positioning of the thermocouple and strain gage.

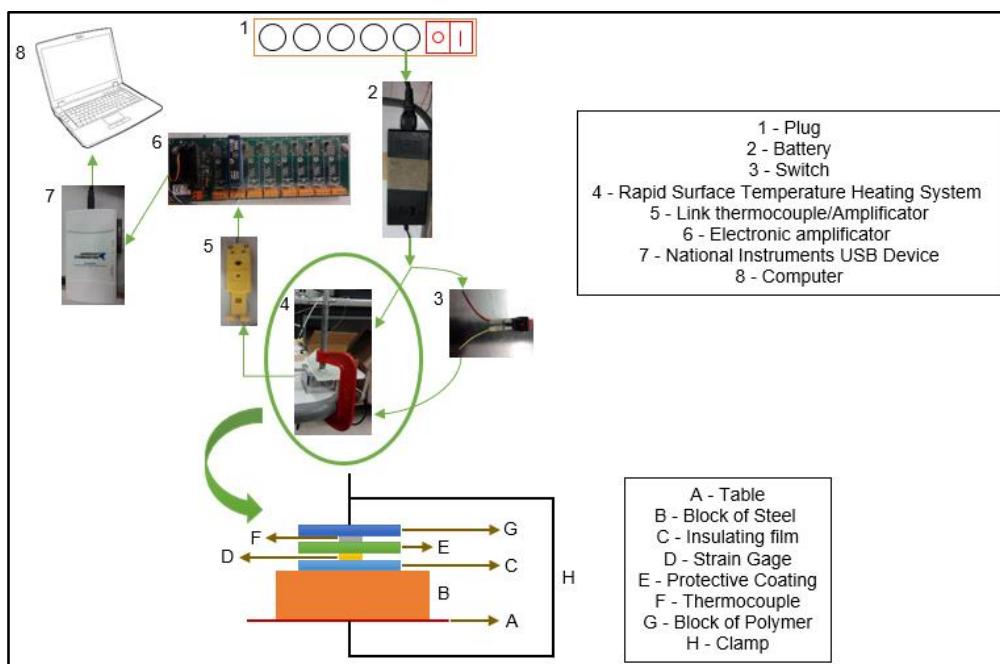


Figure 19 – Scheme illustrating the system elaborated for the practical study.

3.1.3.3. Results

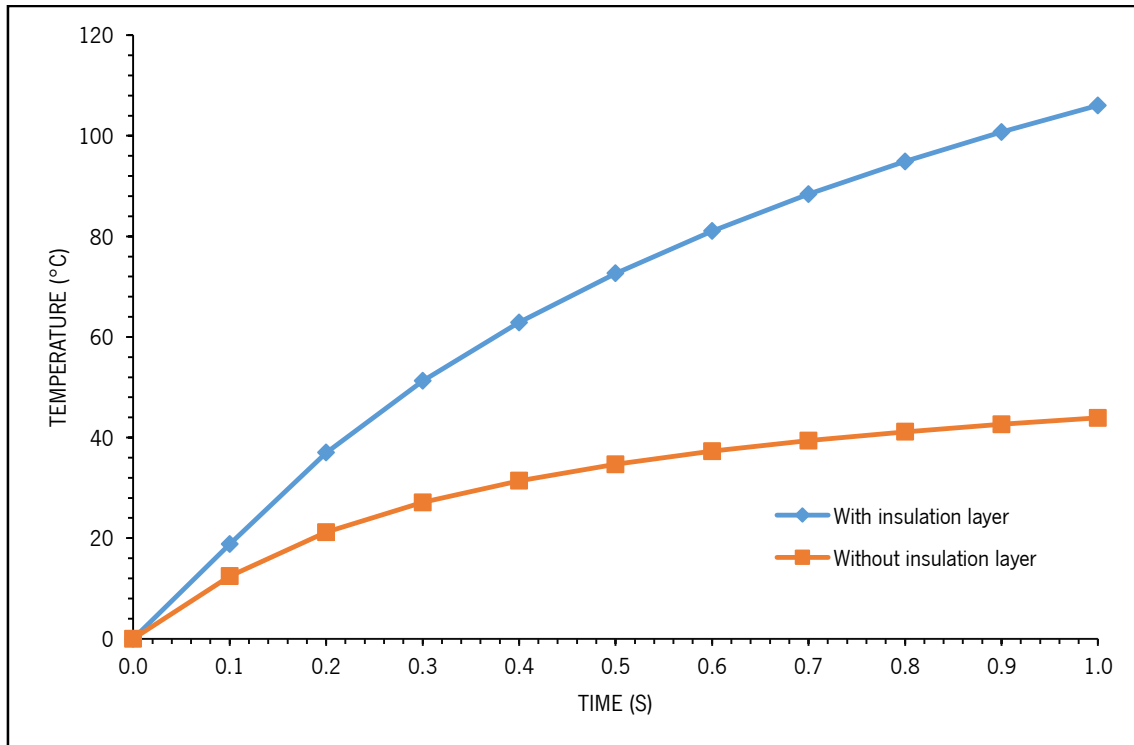


Figure 20 – Comparison between the rapid surface temperature heating system with and without an insulation layer.

In case of not existing an insulation between the mold layer and the heat production layer means that approximately half of the heat produced would dissipate through the mold layer. Whereas, having an insulator will focus that heat towards the cavity, increasing not just the efficiency of the heating but also the temperature at the surface. This can be confirmed by the result in figure 20 in which, after 1 second of heat generation, the temperature arrived with and without insulation layer is 106.0°C and 43.9°C, respectively.

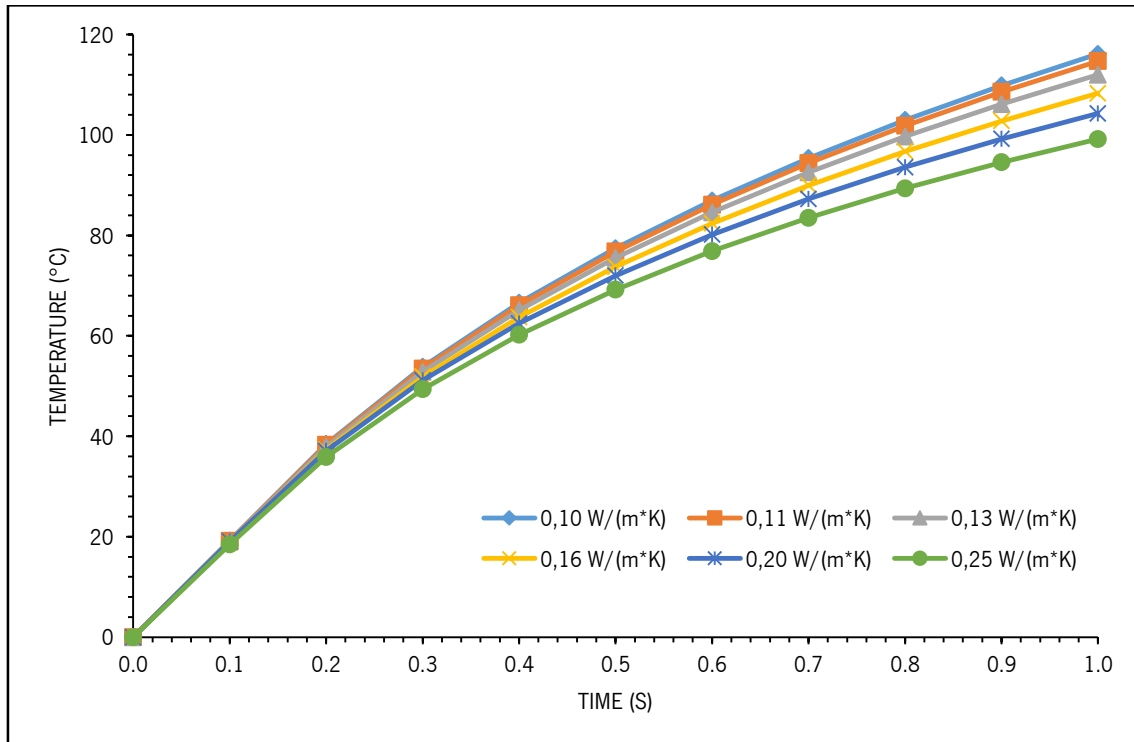


Figure 21 – Influence of the thermal conductivity on rapid surface temperature heating system.

As said before, a lower value of the thermal conductivity means less heat conducted by a material. Since there is a conductive surface on the other side, i.e. protective coating, that heat not conducted will be “directed” to it and therefore, it is expected an increase of the temperature at the surface. This is supported by the result in figure 21 in which, after 1 second of heat generation, the temperatures arrived for 0.10, 0.11, 0.13, 0.16, 0.20 and 0.25 W/(m*K) are 116.2, 114.7, 112.0, 108.3, 104.3 and 99.2°C respectively.

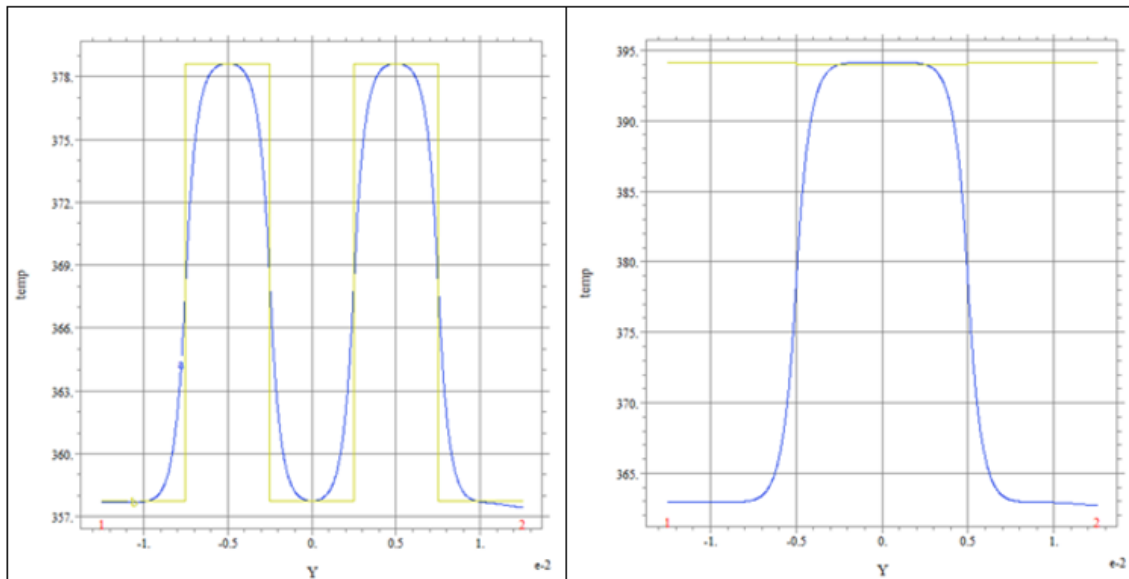


Figure 22 – Comparison of temperature distribution through the protective coating between two strain gages distanced by 5 mm (left image) and 0 mm (right image).

First of all, in figure 22, the blue color represents the heat distribution and the yellow color represents the temperature achieved. With this in mind, the figure 22 shows that putting two strain gages distanced by 0 mm instead of 5 mm, with the same conditions, will not just increase temperature at the surface (difference of approximately 14°C), but also distribute heat in an efficient way towards the cavity. Therefore, it is important that strain gages are as closest as possible from each other.

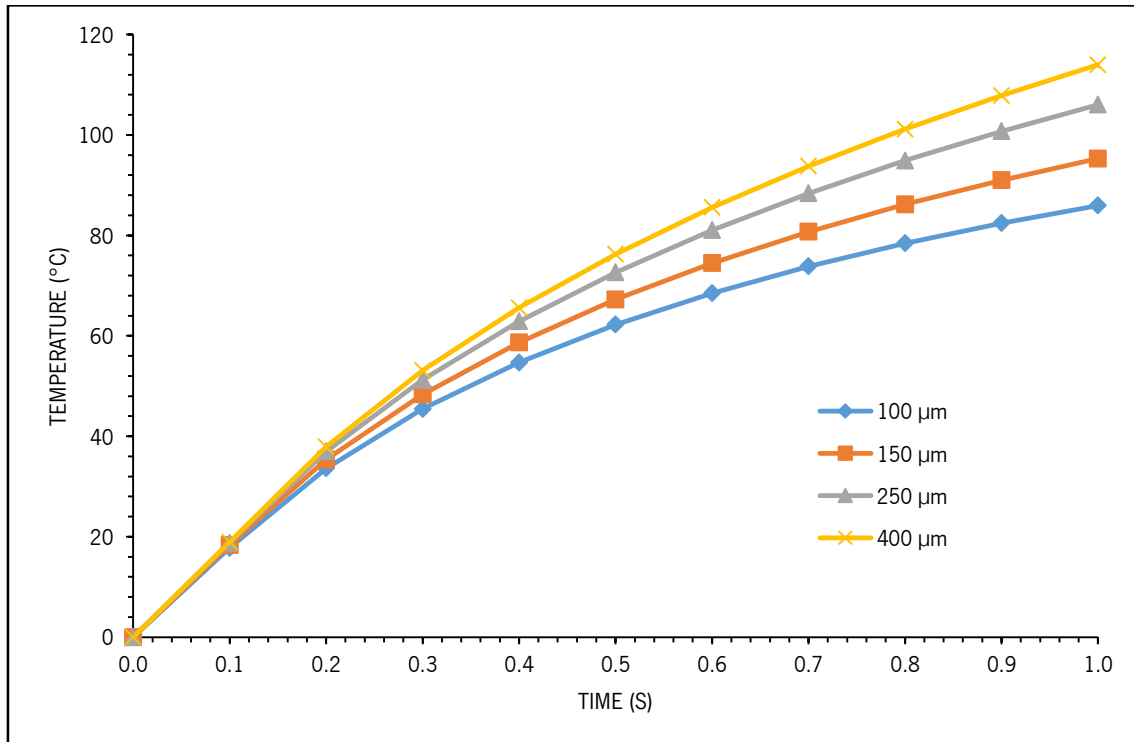


Figure 23 – Influence of the insulation layer thickness on rapid surface temperature heating system.

Another important parameter studied was the thickness of the insulation layer since if it is too thick, then increases the cooling time too much, otherwise, if it is too thin, then the surface temperatures will stay too low. Achieving a middle ground between those two factors is essential so the temperature desired is reached and the cycle time is the smallest as possible. The results of figure 23 shows that for a thickness of 100, 150, 250 and 400 μm , the temperatures achieved are 86.0, 95.3, 106.0 and 114.0°C respectively.

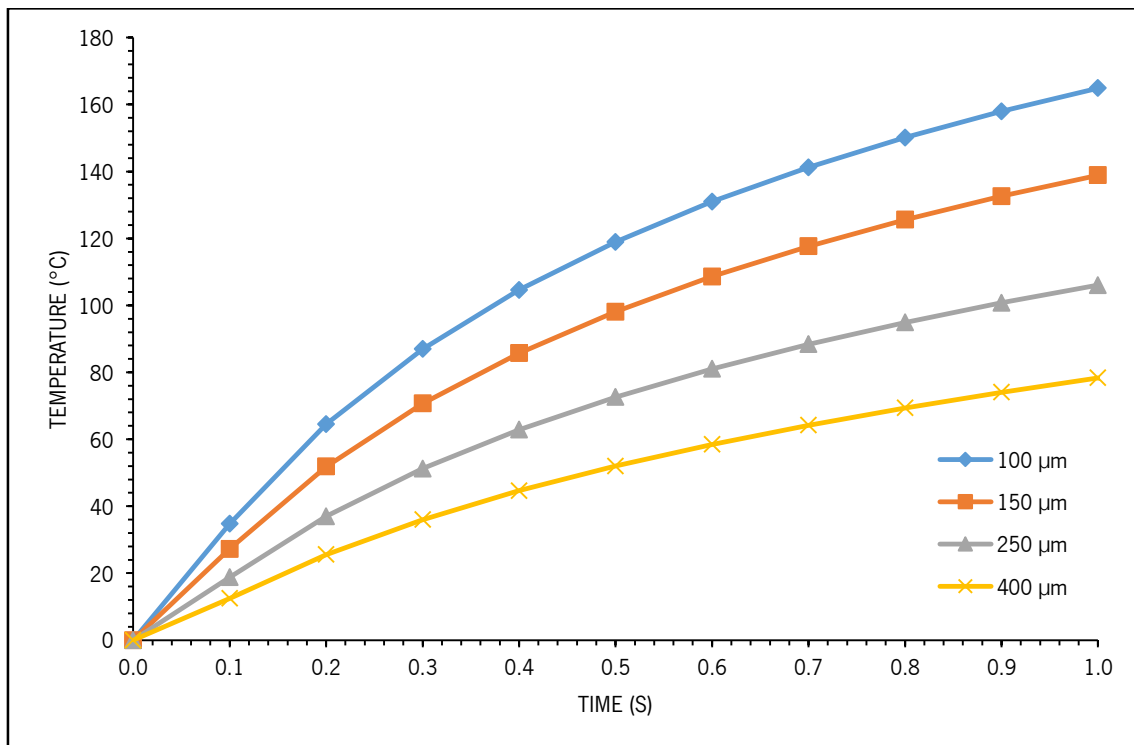


Figure 24 – Influence of the protective coating thickness on rapid surface temperature heating system.

As the thickness of the protective coating increases, the temperature at the surface decreases because there is simply more path for the heat to cross until reaches the surface and consequently, heat would be more dissipated through the protective coating. However, that thickness can't be too thick or too thin due to the same reason as the one enunciated in the insulator layer thickness. Nonetheless, results achieved are represented in figure 24 which for a protective coating thickness of 100, 150, 250 and 400 μm , the temperatures arrived are 164.9, 138.9, 106.0 and 78.3°C respectively.

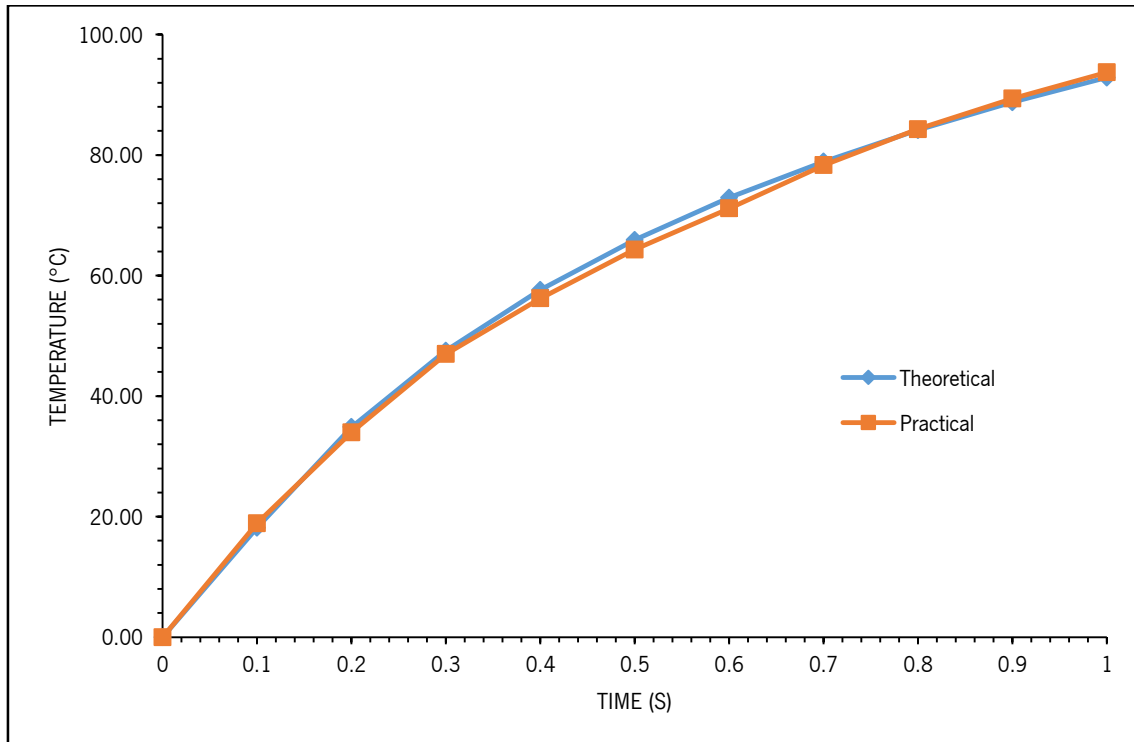


Figure 25 – Comparison between theoretical and practical temperature profile achieved after 1 second.

As can be seen on figure 25, the profile of the curve and temperatures reached are very similar which indicates that the theoretical tests are valid and feasible until 1 second of heating generation. As a note, the biggest temperature difference between this two curves is approximately 3°C which enhances the similarity between results.

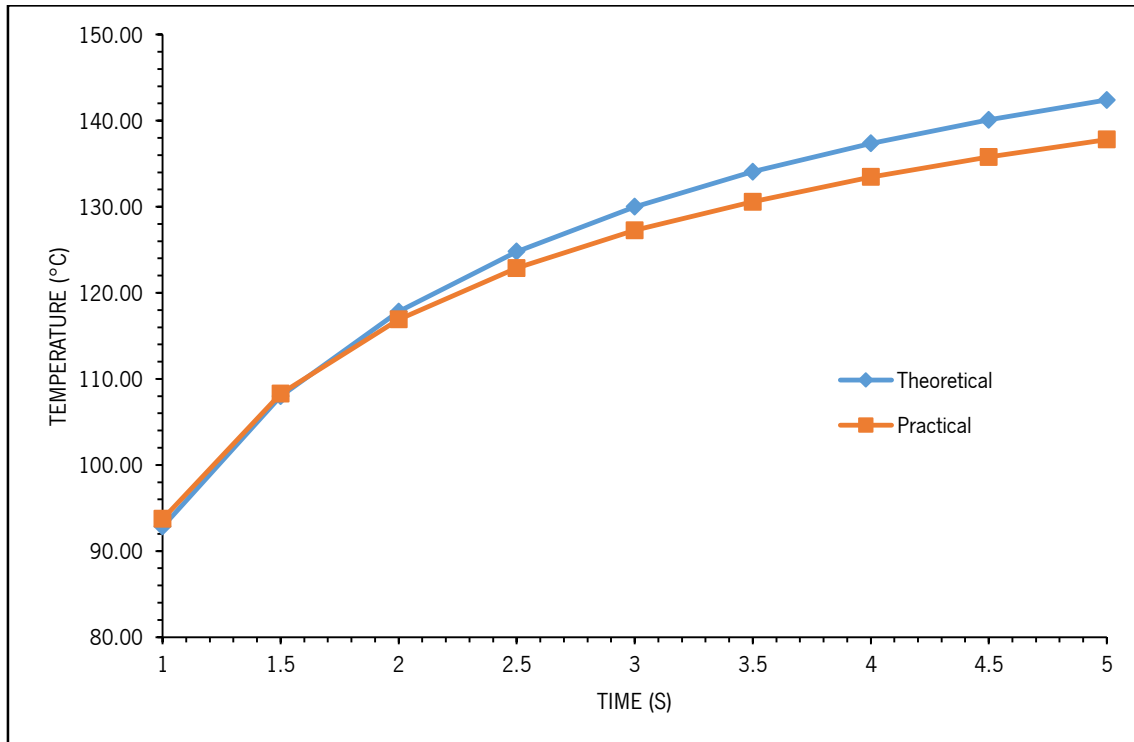


Figure 26 – Comparison between theoretical and practical temperature profile achieved from 1 to 5 seconds.

As enunciated before, to evaluate more precisely the evolution of the temperature curve along the time until it reaches the steady state, the study has prolonged until 5 seconds. In the figure above, it is possible to observe that the difference between the curve and temperature increases comparing to figure 25, namely a maximum of 7°C at 5 seconds. However, the curve behaviour is similar and the temperatures reached are satisfactory for a strain gage heating.

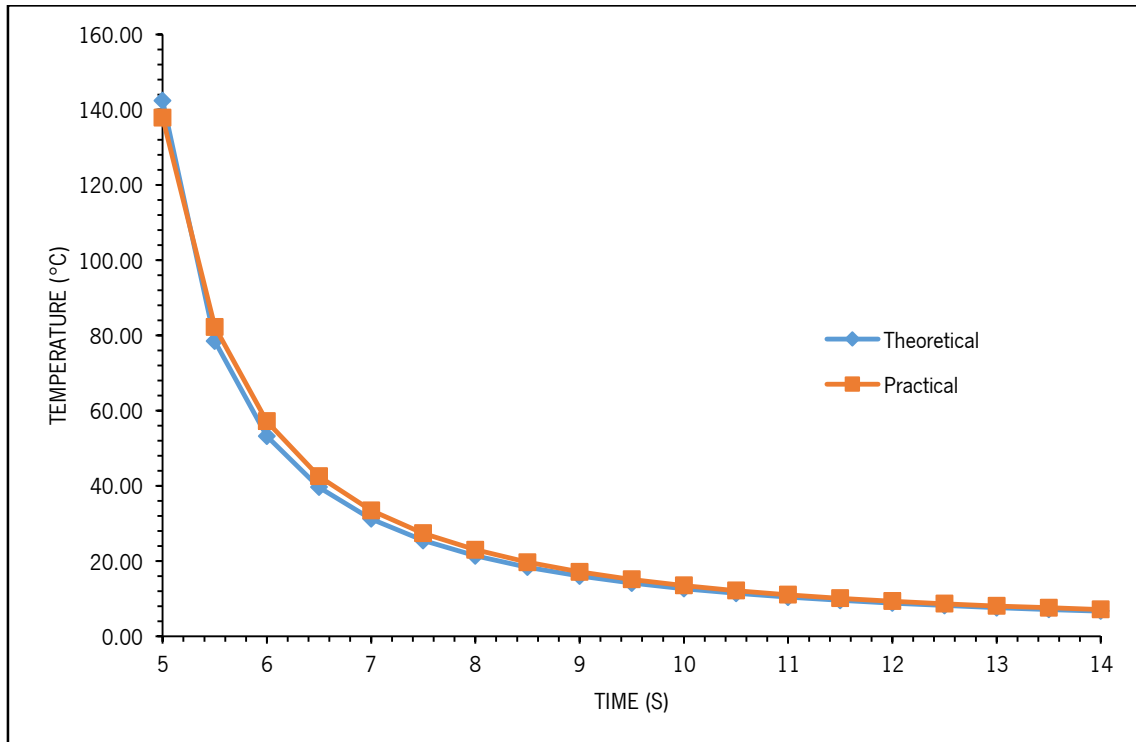


Figure 27 – Comparison between theoretical and practical temperature profile achieved from 5 to 14 seconds.

In addition, the cooling temperature profile was also evaluated and from figure 27, it is possible to observe the biggest temperature difference is positioned on 5 seconds (7°C) and, most importantly, the time that is needed to cool down the system until a determined temperature without any type of circling coolant.

CHAPTER 4

APPLICATION TO MICRO-INJECTION

Applying the system as similar as the one used on the preliminary practical tests, i.e. figure 19, and inject micro-parts using it is the objective of this chapter. However, that system had to suffer some changes since the micro-injection machine used demanded it. Nonetheless, the basic idea remains the same:

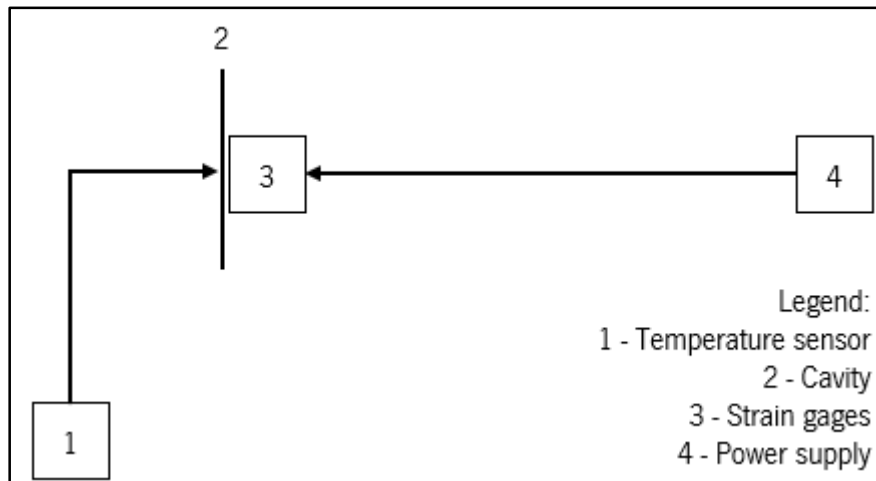


Figure 28 – Scheme of the system idealized for a micro-injection molding machine.

A temperature sensor is connected to the cavity and its function is just reading the temperature at the surface before filling stage. On the other hand, a power supply is connected to the strain gages by copper wires properly isolated so the power supply can provide the voltage needed to achieve the desired temperature at the surface. Inside the cavity, the following components must be presented to reproduce faithfully the work done on preliminary study: strain gages (heating generation layer), a polyethersulfone film (insulation layer) and a steel rectangular plate (mold layer). In an effort to simplify, the assembly of those components will be called RSHTS (rapid surface heating temperature system).

4.1. Micro-specimen

The specimen produced for this work is presented on figure 29. The geometry chosen for the specimen has into consideration the posterior characterization performed.

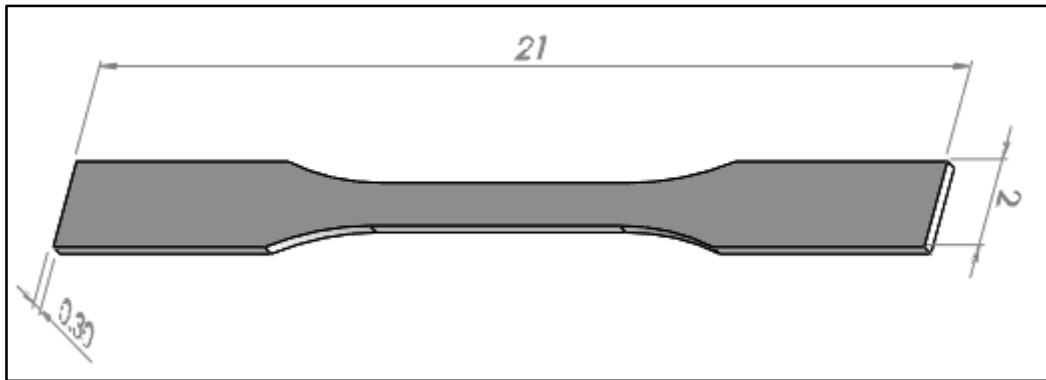


Figure 29 – Generic dimensions of the micro-specimen (dimensions on millimeters).

As an effort to the reader have a notion of the micro-specimen dimensions, the following figure compares it to an one cent coin.

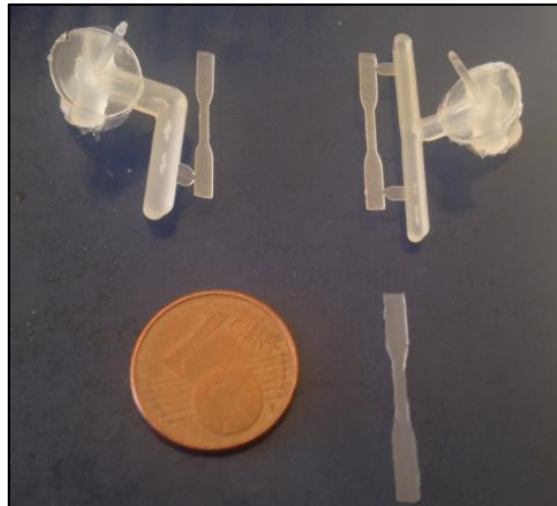


Figure 30 – Comparison between the dimensions of the micro-specimen and an one cent coin.

4.2. Micro-injection machine

The micro-specimens were produced in a Boy 12A machine, as seen in figure 31, that exists in the polymer engineering department of Minho's University. This equipment was specially developed to produce micro-parts of high precision allowing a correct dosage of the material to inject. In attachment 9 are shown the characteristics of this machine.



Figure 31 – Boy 12A micro-injection machine.

4.3. Mold

The mold used for producing the micro-specimen mentioned previously is located in the micro-injection laboratory of the polymer engineering department of Minho's University and can be visualized in figure 32. This type of mold possesses an important feature, which led to its choice for this project: possibility of changing the cavity insert, the flat insert or both. Plus, this feature will also make easier the assembly of RSHTS in the mold.

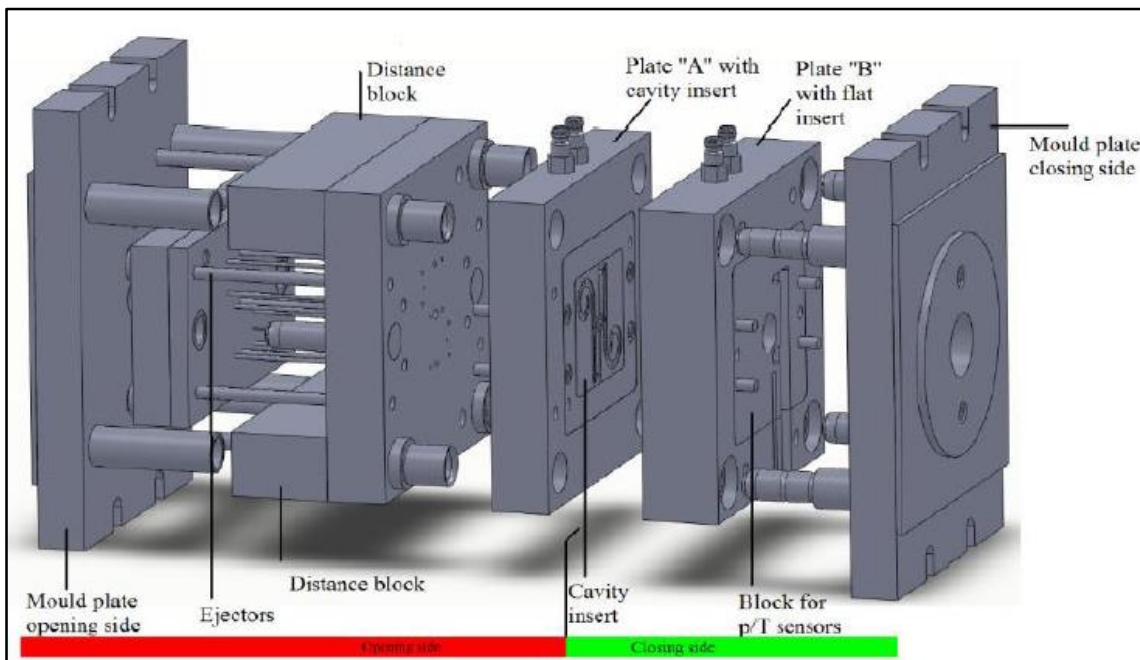


Figure 32 – Scheme of the micro-injection mold (exploded view).

For this particular work, all the components of figure 32 will remain the same except for two: cavity insert and ejectors.

Regarding the ejectors, they were removed from the mold. The idea is to use the holes from the extraction system to pass the wires that connect the strain gages to the power supply, as seen in figure 33. Consequently, the extraction of the micro-specimen is made manually and so, draft angles were a concern taken into account (smallest draft angle is 2° , which can be seen on attachments). Moreover and as a note, an antiadherent spray was used before the injection of a condition in order to make the extraction easier.

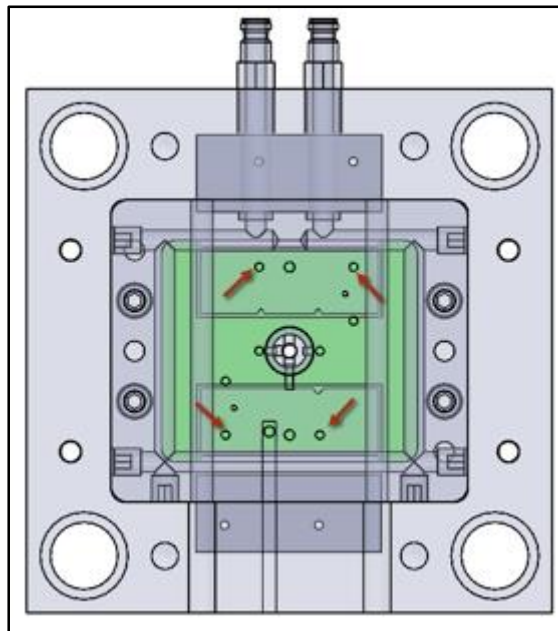


Figure 33 – Scheme of the extraction holes exploited to pass the copper wires from the strain gage.

Other aspect changed was the cavity insert mainly due to the assembly of RSHTS in it. Therefore, a new insert was designed. The back view of that new insert, figure 34, shows two gaps and those gaps are the place where the components are introduced. This gaps are an unique feature which will be called: two “open-close compartments”. The function of the compartments can be described by figure 35 which tries to show that before introducing RSHTS, the compartment is open and once it is introduced, the compartment is closed so the cavity insert can be placed in the mold. Another and an important concern was the mechanical resistance of the polymer layer since the pressure and speed injection could provoke a displacement on that part and therefore, change the flatness of the cavity insert. However, according to [2], injection tests were performed with thicknesses of the polymer layer equal to the one desired in this work without any problem related to that.

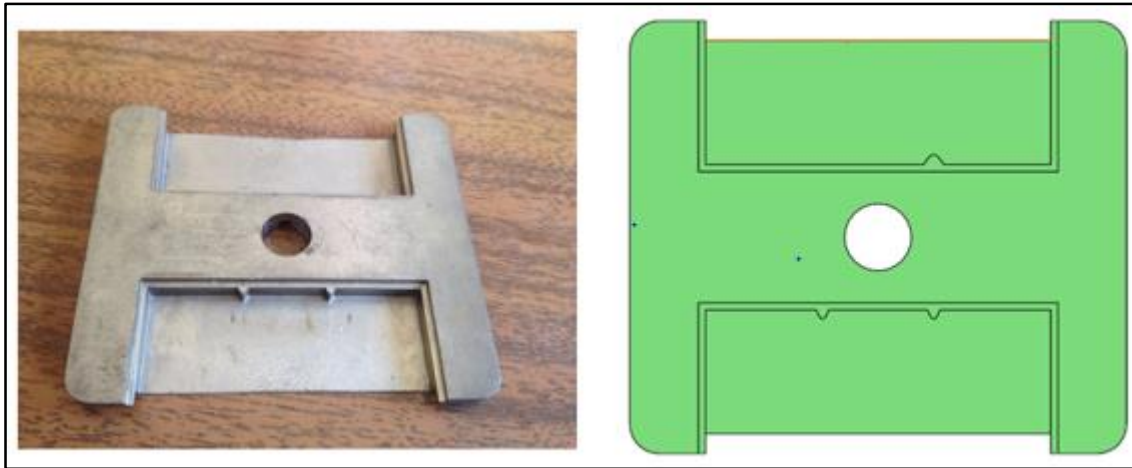


Figure 34 – Back view of the cavity insert after (left) and before (right) manufacturing without “open-close compartment”



Figure 35 – Back view of the cavity insert after manufacturing and with closed compartment (left) and before manufacturing and with open compartment (right).

Also the front view of the cavity insert was designed (figure 36-left) so a weld line can be formed on one side and compared later with the exact same moldation on the other side but without a weld line (figure 36-right). The runner cross-section and gate chosen was a modified trapezoidal and side ones, respectively, due mainly to the small sizes involved. Feeding channels were designed according to have a balanced flow of the polymer melt through them, so the two cavities could finishing filling stage at approximately the same time. This feeding channels balancing was tested with a trial-error method by Moldflow software. Dimensions of the cavity insert can be found on attachment 8.

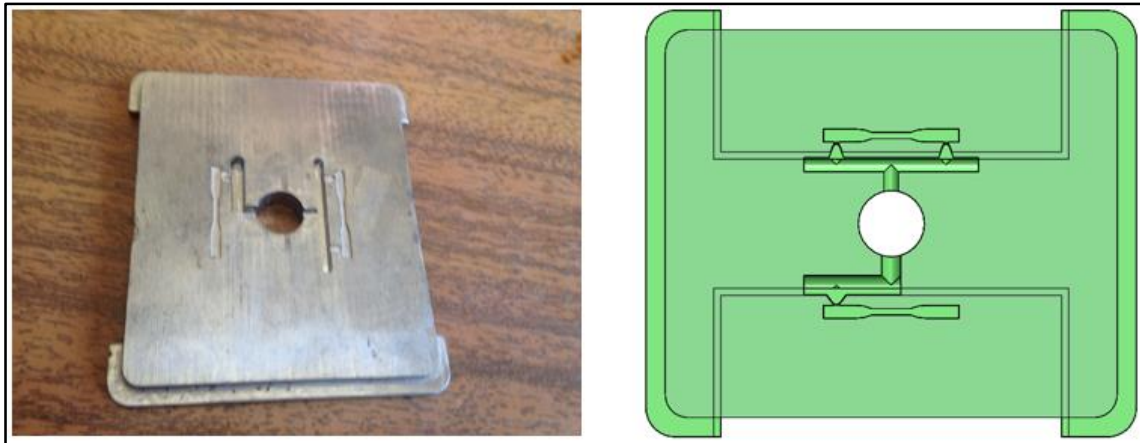


Figure 36 – Top view of the cavity insert after (left) and before (right) manufacturing.

Finally, there is one last feature, a cold pit, which allows to the material to flow through the two impressions or just one impression, as seen in figure 37.

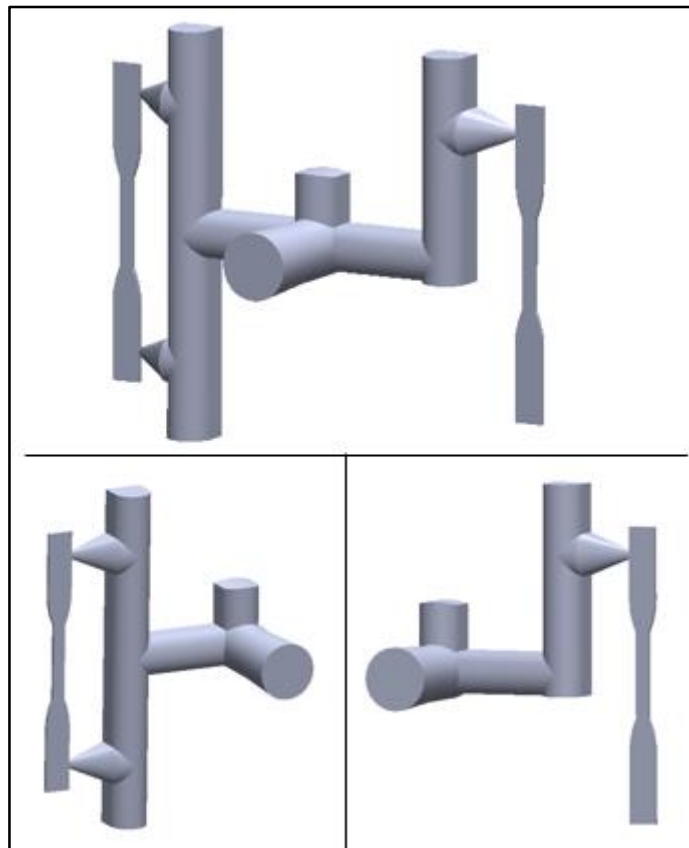


Figure 37 – On top, the part achieved when the cold pit allows the material to flow through two impressions. On below, the part achieved when the cold pit allows the material to flow through one impression, which can pass to the impression that has one gate (right) or two gates (left).

4.4. Heating system

As explained previously, strain gages were used to heat up the mold surface and the closer they are from each other, the more intense and uniform was the temperature distributed along the cavity. Therefore, when creating the heating system, strain gages were positioned as close as possible. The number of strain gages used was six in an effort to cover all the cavity surface and, those strain gages were connected in parallel for mainly two reasons: first, for a fast replacement of one or more strain gage in case of not working or other issue. The one not functional could be easily detected by measuring the resistance from a multimeter; second and the most important one, the voltage applied by the power supply to achieve the desired temperature is lower comparing to a connection in series. The creating of the heating system followed the bellow steps:

1. Place the strain gages as close as possible from each other and find a weight to keep the strain gages steady;
2. Cut the isolation of a cooper wires and place that cutted zone in contact with just one of each strain gage wires;
3. Once in contact, weld them and place tape between them in order to isolate only the wires.
4. Repeat steps 2 and 3;
5. Measure the resistance of the system on the edge of the two copper wires with the support of a multimeter in order to check if all strain gages are properly connected.



Figure 38 – System of strain gages connect in parallel by copper wires.

After creating the heating system, the polyethersulfone film and the steel rectangular plate were cut in an effort to have the same length and width as the heating system. Posteriorly, they were fixed above the heating system and placed in the cavity insert compartment where, after putting the copper wires passing through the holes, the compartment was closed. Later, the cavity insert with all the components assembled was placed on the mold, the wires were connected to the power supply and a thermocouple was placed on the mold surface to measure the temperature provided by the heating system, as it is possible to see on figures 39 and 40.

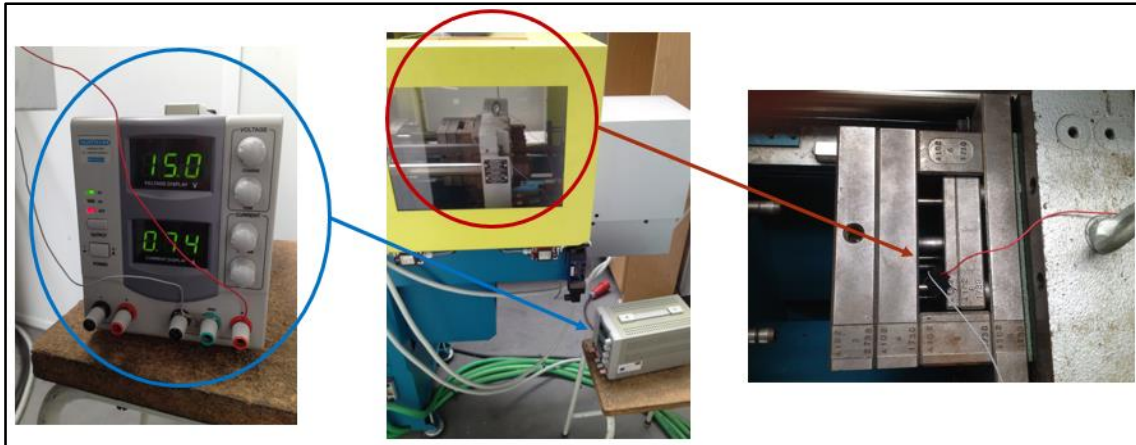


Figure 39 – Rapid surface heating temperature system applied on a micro-injection molding machine (part 1).

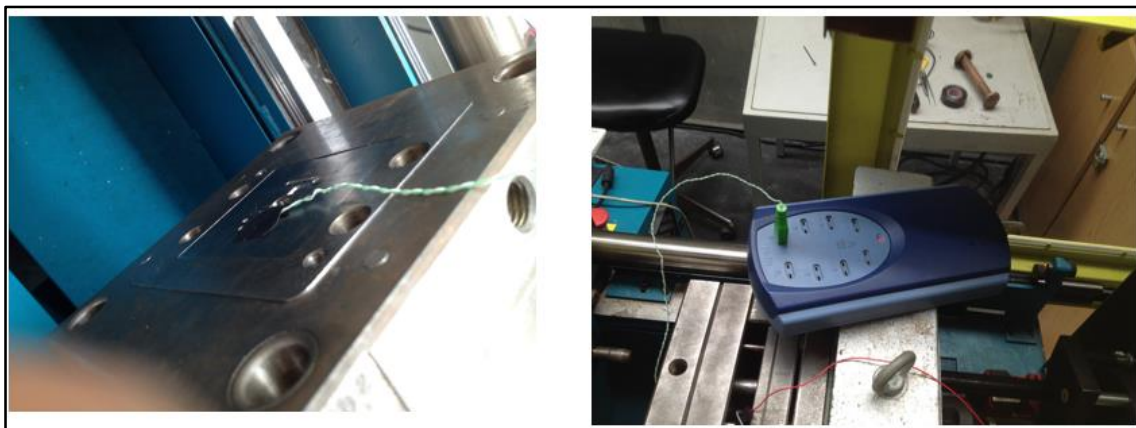


Figure 40 – Rapid surface heating temperature system applied on a micro-injection molding machine (part 2).

4.5. Processing and injection conditions

As the objective of this work is to compare the rapid surface heating temperature system with a conventional one, the conditions executed for that purpose can be seen in table 13. To simplify the analysis and discussion of the results, the one gate impression and the two gates impression were injected separately by manipulation of the cold pit. Also the temperatures chosen to heat up the mold surface were 40, 80 and 120°C and the voltage needed to reach those

temperatures was 13, 17.5 and 23 V respectively. Those temperatures were chosen according to a study [27] which tested the influence of the cavity surface temperature just before filling on part surface appearance and texture in RHCM and found out that there is a critical cavity surface temperature for each plastic material. The idea is to compare a temperature close to the critical one (120°C) with other temperatures (so it can be evaluate the evolution of the cavity surface temperature on the specimens, e.g., 40 and 80°C) plus the conventional way.

As a note, the temperature of the mold surface without heating system is approximately 21°C, measured by the thermocouple after stabilization of the molding process. The resistance of the heating system was always measured before performing each condition in an attempt to confirm the functionality of all the strain gages. Futhermore, for every condition performed, the processing conditions are presented on table 14. The values of pressure, speed and cooling time were determined after trial and error.

Table 13 – Conditions performed for the micro-injection molding process.

Conditions performed				
Material	Number of gates	System	Temperature (°C)	Designation
PP (Moplen H548R)	1	Conventional	21	C1.PP23
		RSHT	40	R1.PP40
			80	R1.PP80
			120	R1.PP120
	2	Conventional	21	C2.PP23
		RSHT	40	R2.PP40
			80	R2.PP80
			120	R2.PP120
PS (EDISTIR N1910)	1	Conventional	21	C1.PS23
		RSHT	40	R1.PS40
			80	R1.PS80
			120	R1.PS120
	2	Conventional	21	C2.PS23

		40	R2.PS40
	RSHT	80	R2.PS80
		120	R2.PS120

Table 14 – Processing conditions performed for the micro-injection molding process.

Processing Conditions			
	Zone 1	240°C	
	Zone 2	240°C	
Injection temperature	Zone 3	230°C	PS e PP
	Zone 4	220°C	
	Zone 5	210°C	
		35 bar	PP
Injection pressure		50 bar	PS
		30 mm/s	PP
Injection speed		40 mm/s	PS
		10 s	PP and PS
Cooling time			

CHAPTER 5

CHARACTERIZATION

At the end of injecting all the conditions performed, the characterization was the last step of this work. The experiments made were tensile test (mechanical characterization), polarized light microscopy and bright-field microscopy (optical characterization) and differential scanning calorimetry (thermal characterization).

5.1. Optical characterization

When light interacts with polymer materials, several phenomena can occur such as light refraction, absorption or diffusion. The behaviour of those materials when light is present is determinant in particular applications. The optical properties of a plastic product depend essentially of the material composition and the processing conditions. Controlling those factors is essential to obtain the desired properties.

The microscopy of polarized light is similar to the common microscope of bright-field but with special optical and mechanical accessories, namely two polarized filters given by the name of polarizer and analyser. In the transmission microscope, the polarizer is positioned in front of the condenser whereas the analyzer is installed between the objective and the ocular. Both of them are dichroic filters which decompose the electric vector of the luminous waves into two perpendicular vectors (absorbed and transmitted). Thus, when the analyzer and the polarizer are positioned 90° between each other, there is extinguishment of the light above the analyzer. The quality of a polarized light microscope is determined by the perfection of extinguishment between crossed polarizers. [53]

In the bright-field microscopy, the transmission microscope was also used. In this technique, the contrast is generated by changes on the absorption or diffusion of light in the different zones of the specimen. The absorption produces reduction of the intensity or total elimination of certain wave lengths of the light. [53]

In this characterization, the bright-field microscopy was used in an effort to help finding the weld lines of the specimens by characterizing the dispersion degree. On the other hand, the polarized light microscopy was used in an attempt to identify the crystalline structure of semi-crystalline materials.

In order to proceed to their characterization, it is needed to prepare the specimens, as can be seen below in the experimental procedure. The specimens were cutted longitudinally with a thickness of $15\ \mu\text{m}$ by a glass knife which is positioned in a Leitz 1401 microtome, figure 42. The

visualization of the cutted specimens was made by an Olympus transmission microscope and a Leica digital machine. The objective used was a 1.66 with different ampliations.

The zones studied of the specimen can be seen in figure 41 and they were chosen because it is the last zone where the polymer melt completely finish filling the specimens.

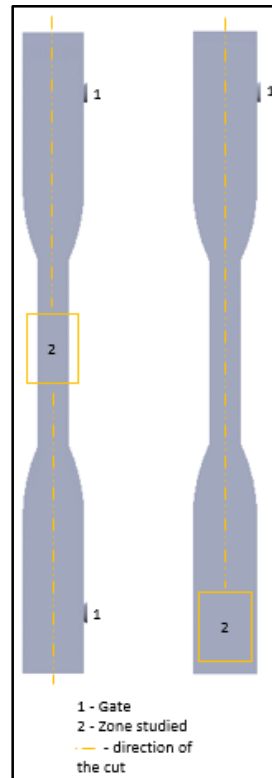


Figure 41 – Zones of the specimen chosen to be optically characterized.

The experimental procedure performed was:

1. Place the sample perpendicularly to a plastic mold with the help of glue;
2. Put 15 ml of resin and 5 ml of hardener in two cups separately and posteriorly, mix them in a third cup;
3. Place the mix of resin and hardener (Epofix kit, figure 42) on the mold and wait 8-10 hours until it becomes solid.
4. Remove the plastic mold and saw the resin that surrounds the sample;
5. Polish the surfaces and make a chamfer on it;
6. Place it on a microtome and remove the sample;
7. Cover one lamella and glass slide with Canada's balsam and place the sample between them;
8. Put a weight on top and wait 24 hours;

9. Observe sample by a microscope.



Figure 42 – Equipments and accessories needed to optical characterization: a) polish machine; b) microtome; c) Olympus transmission microscope; d) plastic mold used; e) Resin and hardener (Epofix kit).

5.1.1. Results

The results achieved for each polypropylene condition can be seen in the following image:

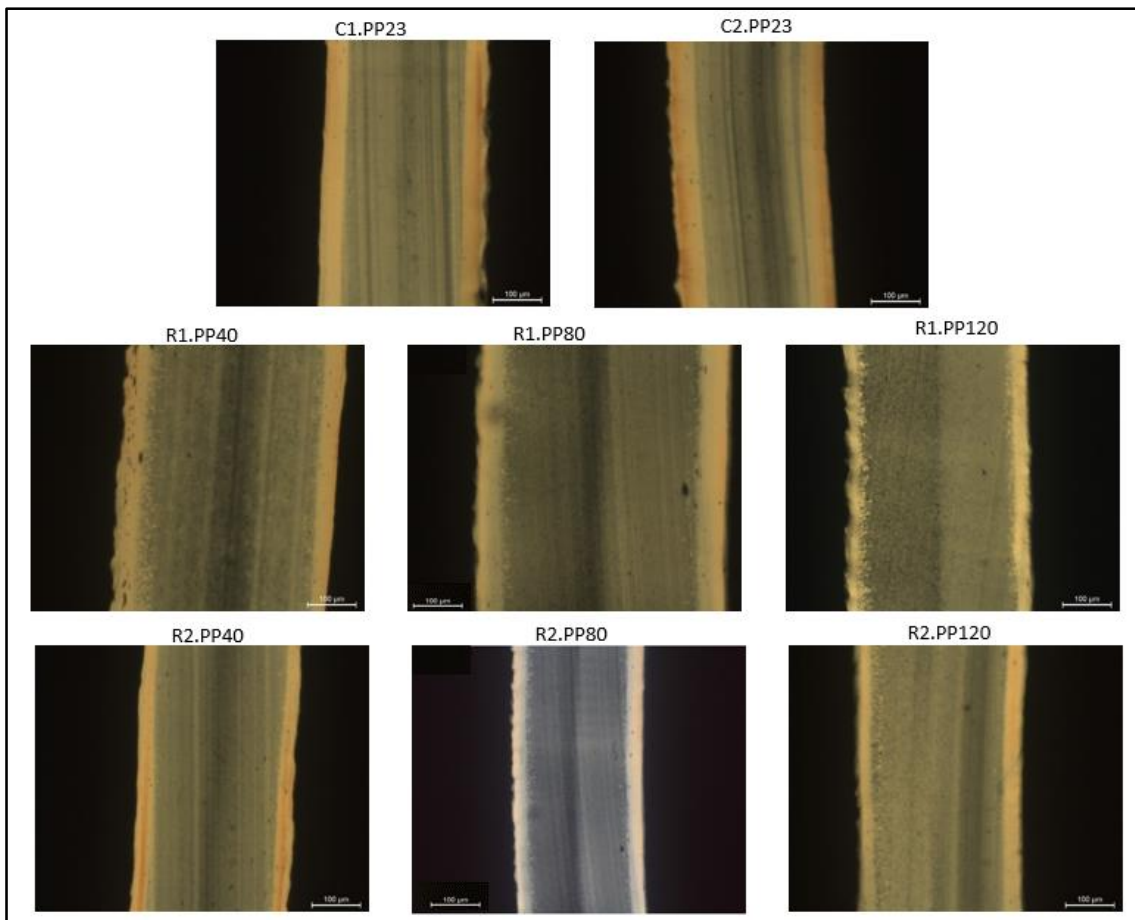


Figure 43 – Light polarized microscopy results for polypropylene conditions.

First of all, before explaining the results it is needed to refer that during cooling stage, one side of the specimen will in contact with steel (where heat is generated) and the other with the flat insert, and because the flat insert is at different temperature comparing with the steel side, both side of the specimen will produce different results, as seen figure 44 (left),. In order to make the explanation simpler, the zones will be called AA (heating side) and BB (contact with flat insert) and they are already organized in figure 43 according to figure 44 (right).

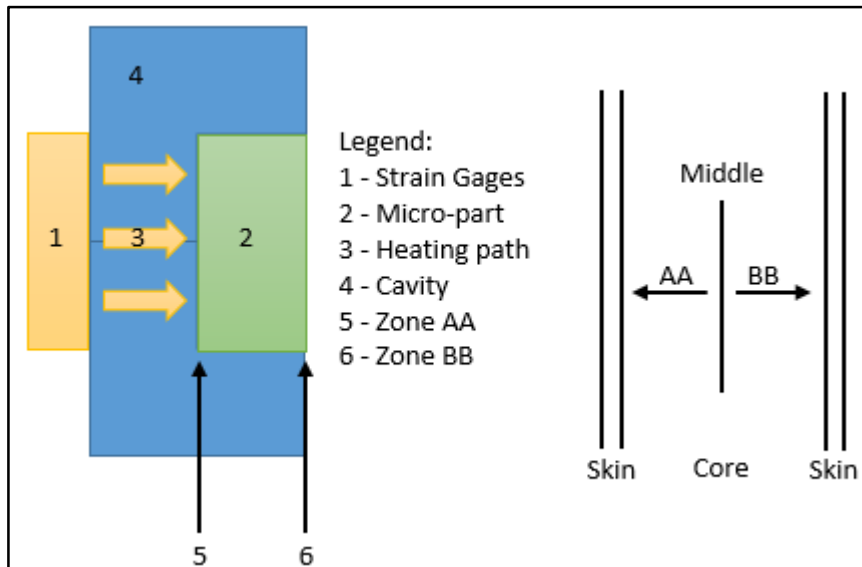


Figure 44 – Scheme explaining the division of zones for characterization.

Conventionally, as the mold surface temperature increases, the internal stress decreases and the melt flows better through the cavity but, the cycle time increases due to the solidification of the final part. Therefore, the polymer melt has more time to crystallize and so, the spherulites formed have higher dimensions and can orientate better through the part. With this in mind, it is possible to see in figure 43 that with the increase of the mold surface temperature, the zone AA tends to have a more defined and oriented crystalline structure than zone BB since it is closer from the generation of heat. Especially studying the evolution of one gate results (R1.PP40, R1.PP80 and R1.PP120) where it is clear to see that tendency difference between zones AA and BB. However, in the two gates results, the AA zone is less defined and oriented than the one gate ones possibly due to the path taken by polymer melt during filling stage (comparison of the zone area of R2.PP80 and R2.PP120). Nonetheless, the same effect occurred on both one and two gates.

In addition, comparing the results obtained with and without surface heating, especially at higher temperatures, both zones AA and BB present an obvious better crystalline structure.

Moreover, the skin-core ratio was determined, as seen in table 15.

Table 15 – Skin-core ratio results.

Condition	Skin-core ratio
C1.PP23	0.27
R1.PP40	0.22
R1.PP80	0.21
R1.PP120	0.18
C2.PP23	0.28
R2.PP40	0.2
R2.PP80	0.2
R2.PP120	0.18

Since the dimensions of the parts are on a micro scale, the difference between conditions in the skin-core ratio can be considered high, as it is possible to see on table 15. Plus, it is obvious to observe that with the increase of the surface temperature, the ratio skin-core decreases, especially when comparing the conventional with the surface heating system. In addition, there is no significant difference in the ratio between having one and two gates with the same surface temperature (maximum of 0.01).

On another subject and as known, when two fronts meet, the orientation changes. However, finding a weld line was impossible using polarized light microscopy since in zone 2 (figure 45), it was not possible to observe such change. Therefore, in an attempt to characterize it, bright-field microscopy was performed (figure 45, bellow) and the idea was to observe the dispersion variation of any existing particles. And, as seen, it is possible to determine the weld line (green) according to the dispersion variation of the particles (red). Nonetheless, the result makes possible to determinate only that there is a weld line. Even knowing that the parts were processed with micro-injection molding, it was expected that with two gates, a weld line could be formed in an attempt to be analysed and quantified (as did with skin-core ratio) by polarized light microscopy according to the surface temperature.

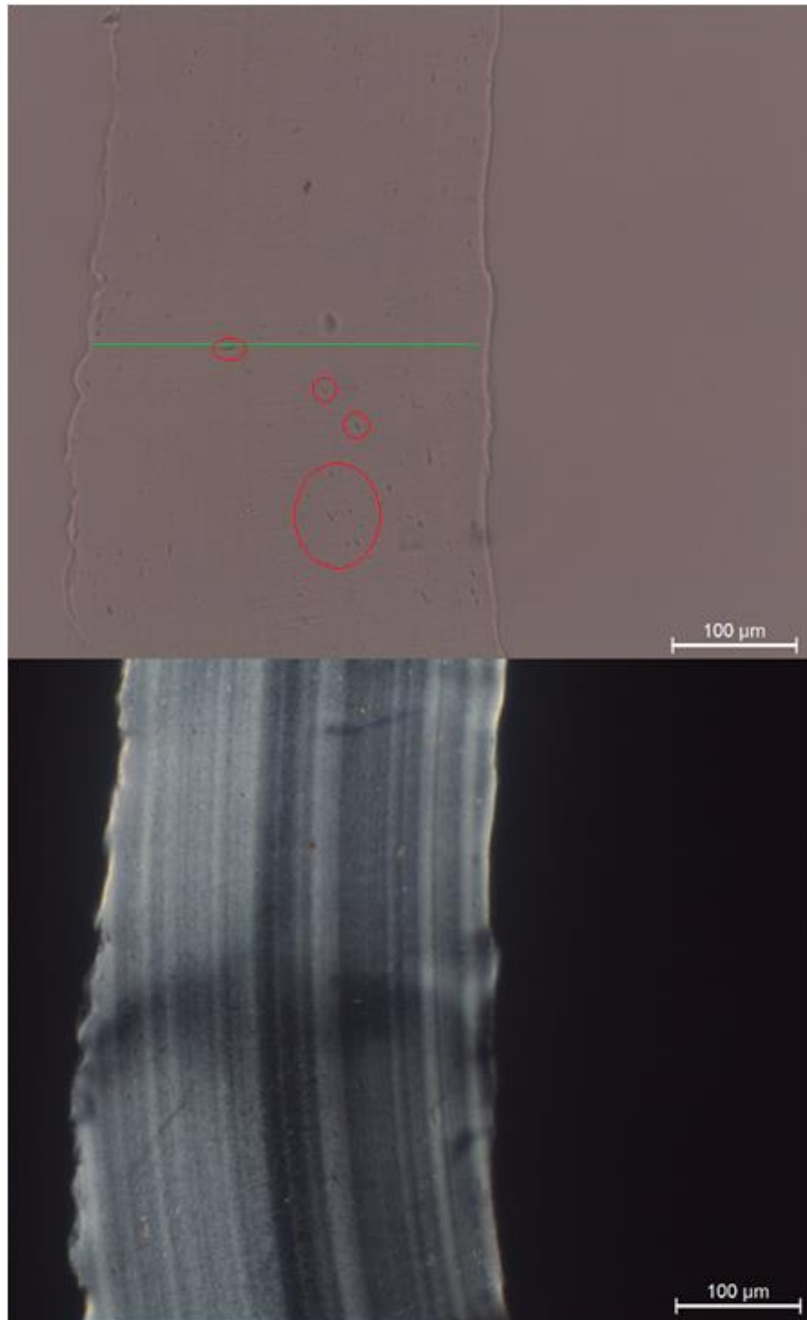


Figure 45 – Bright-field microscopy (top) and polarized light microscopy (bottom) results of the same zone, which correspond to the weld line location.

5.2. Mechanical Properties

The mechanical properties constitute an important role in the characterization since they describe the reaction of a material to physical forces. Consequently, it is possible then to study the mechanical influence of the mold surface heating in the final part.

The tensile tests consist in the application of an uniaxial tensile load on the ends of a specimen at constant speed which tends to lengthen until rupture. The following figure shows, schematically, how the test is done:

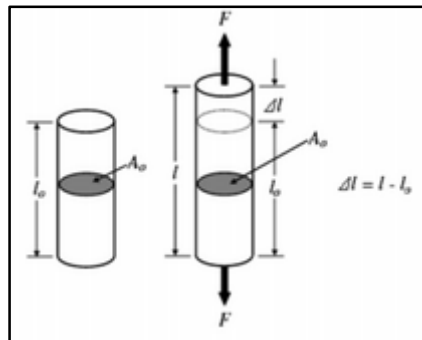


Figure 46 – Lengthen of a cylindrical specimen submitted to tensile load.

In this test, the variation of the initial length (L) is measured in function of the load applied. Posteriorly, a graphic of force-displacement is obtained and converted into a graphic of strain-stress. The stress is determined by the ratio between the force (P) applied and the section area (A_0):

$$\sigma = \frac{P}{A_0} \quad (4)$$

The strain is defined by the following expression:

$$\epsilon = \frac{\delta}{L} \quad (5)$$

Where δ represents the length variation in a certain instant. The following shows a typical curve of a strain-stress graphic:

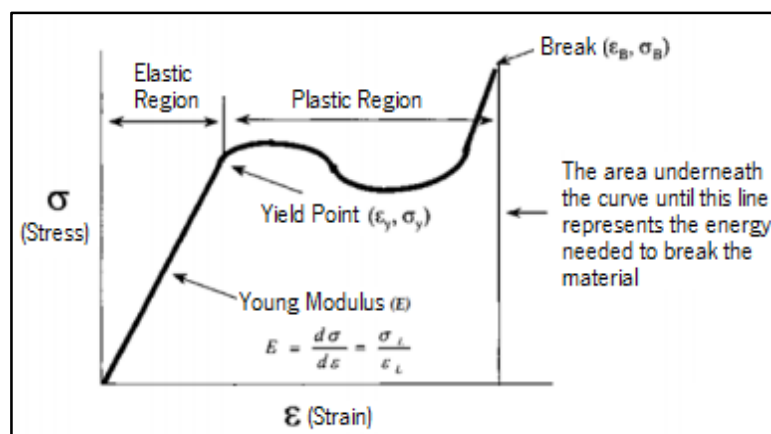


Figure 47 – Typical strain-stress graphic. [54]

The plastic region, when the yield starts to begin, represents the permanent strain region of the material. Consequently, the material can't return to its initial dimensions once it reaches this region. The end of this region is characterized by the break of the material. The area underneath the curve usually characterizes the behaviour of the material, generally depending on the chemical nature and processing conditions of the material. [55]

In the study of the mechanical properties, tensile tests were performed in an effort to characterize the behaviour of the injected material with and without RSHT. The machine used for these tests was an Instron 4505, figure 48, in which 8 tests were made for each condition with a speed of 1 mm/s, a distance between the moorings of 8 mm and at room temperature. All the tests followed the standard ASTM D1708. Strain and elastic modulus were not calculated mainly due to the micro dimensions of the specimen which impeded the measure of a precise length variation and therefore, results are not displayed.



Figure 48 – Instron 4505 strength testing machine.

5.2.1. Results

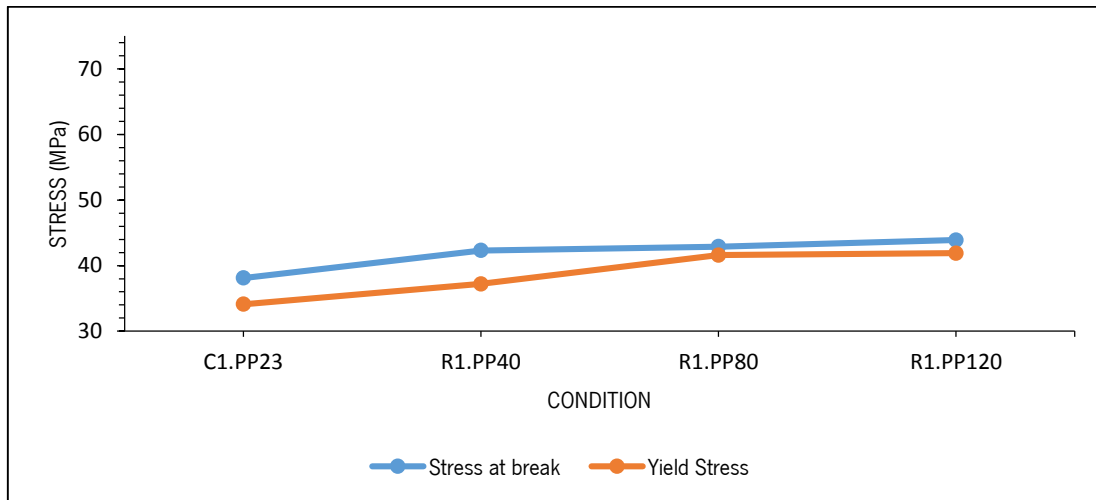


Figure 49 – Stress results obtained for the one gate polypropylene specimens.

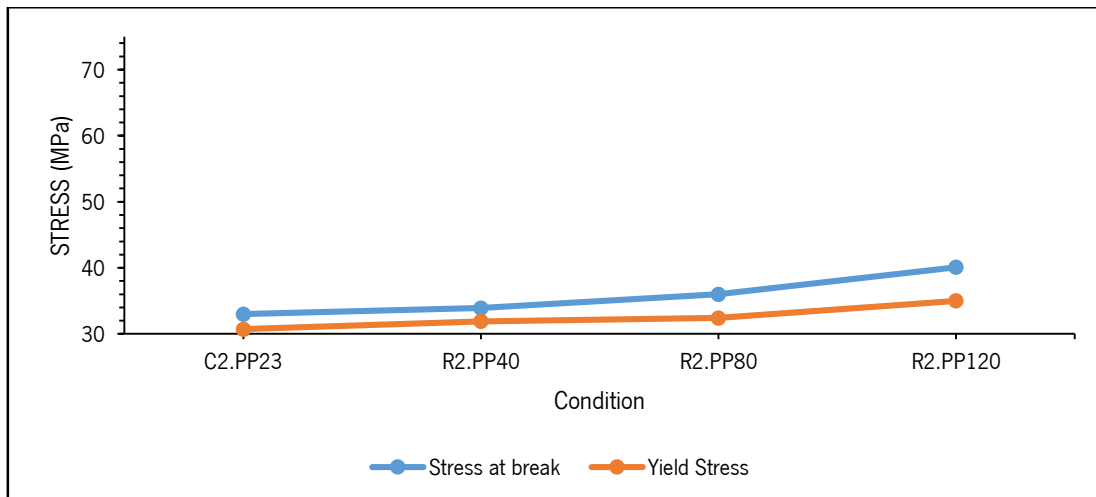


Figure 50 – Stress results obtained for the two gates polypropylene specimens.

As seen in figures 49 and 50, as the surface temperature is increased, both values of yield stress and stress at break are increased for the polypropylene specimens. Regarding the yield stress results, comparing the conventional with the best tensile test. i.e., 120°C, there is an increase of 7.8 MPa and 4.3 MPa, for one and two gates respectively. On the other hand, doing the same comparison but with the stress at break, the increase is 5.8 MPa and 7.1 MPa for also one and two gates respectively. The degree of the polymer chain orientation can explain the results obtained since the orientation of the polymer chains are closely related to the tensile strength. Consequently, as the surface temperature increases, the polymer chains get more time to arrange themselves since the cooling rate is decreased. Accordingly, with that increase of time, more crystalline zones will be caused and so, the tensile strength results are improved.

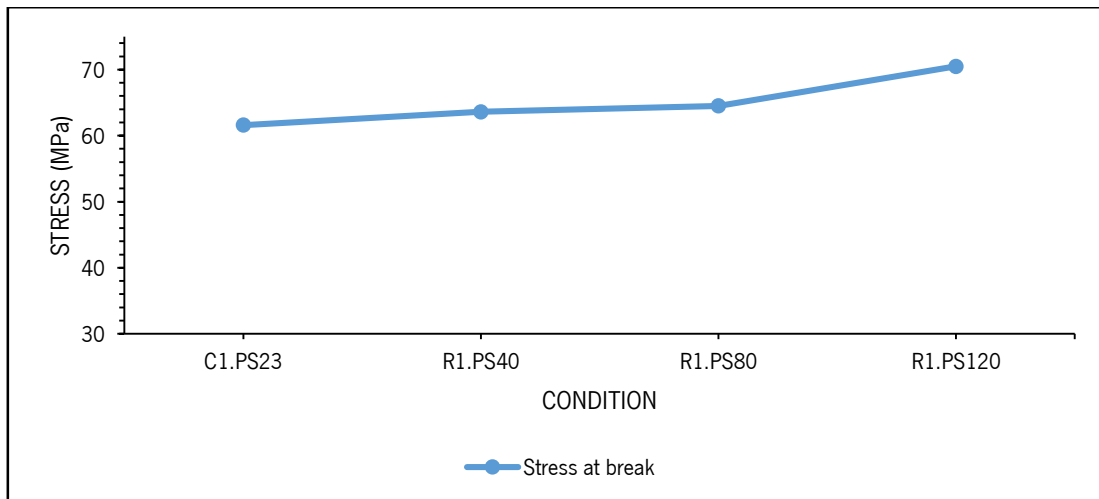


Figure 51 – Stress results obtained for the one gate polystyrene specimens.

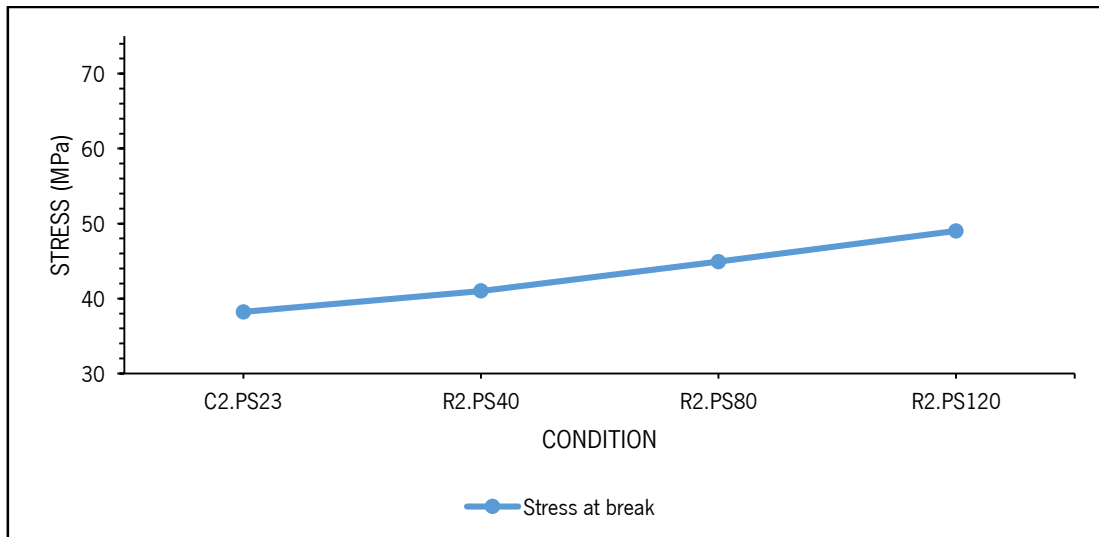


Figure 52 – Stress results obtained for the two gates polystyrene specimens

As seen in figures 51 and 52, as the surface temperature is increased, stress at break is also increased for the polystyrene specimens. Performing the exact same comparison as previously, i.e comparing the conventional with the best tensile test, the stress at break results are increased by 8.9 and 10.8 MPa for one and two gates respectively. The increase of stress at break for the polystyrene specimens is higher than the polypropylene since the fluidity of the amorphous polymer melt becomes much better with the increase of the surface temperature, improving in that way the orientation.

As expected too, the results achieved for one gate are superior than the two gates, especially on the polystyrene specimens

As a note, if the heat was uniform on both zone AA and BB, the results obtained would most likely be better than the ones presented.

5.3. Thermal Properties

The thermal properties evaluate the behaviour of a material when heat is provided or removed, i.e. thermal energy. Due to their low density, the polymers present low thermal diffusivity, which associated with high dependency in the temperature molecular mobility, makes their behaviour highly dependent of the respective thermal level. One of the thermal tests which can be performed is the differential scanning calorimetry (DSC). This test monitors the heat flux difference between one sample and one reference, i.e. measures the absorbed or produced energy by a material in function of time and temperature. [56]

The objective of these tests is to measure and compare the crystallinity degree of the polypropylene specimens at different mold surface temperatures. Therefore, a DSC 7 produced by Perkin Elmer was used, figure 53. The average weight of the samples is about 2 mg and those samples were heated at a rate of 10°C/min from 30°C to 200°C under nitrogen atmosphere. All the tests followed the standard ASTM D3418. The zones studied are the same as the optical properties ones, i.e. figure 41 mainly due to the results obtained. Therefore, in each condition, two zones were investigated: the zone with more oriented molecules (Zone AA) and the other zone (Zone BB). The exception made is for the conventional system since there is no heating and so, zone AA and BB are expected to have similar results.



Figure 53 – DSC 7 produced by Perkin Elmer.

5.3.1. Results

According to the measured curves of the heat flow during the whole heating process, the melting heat of the sample, ΔH_m , can be determined from the peak area. The percent degree of crystallinity, χ_c , can be calculated with the following equation:

$$\chi_c = \frac{\Delta H_m - \Delta H_c}{\Delta H_m^0} \times 100\% \quad (6)$$

Where ΔH_c is the cold temperature that is observed during the heating of the sample and ΔH_m^0 the reference heat of melting a hypothetical 100% crystalline sample. The heat of melting for a 100% polypropylene was determined as 177 J/g. With this in mind, the results obtained for each condition can be verified in the figures 54 and 55

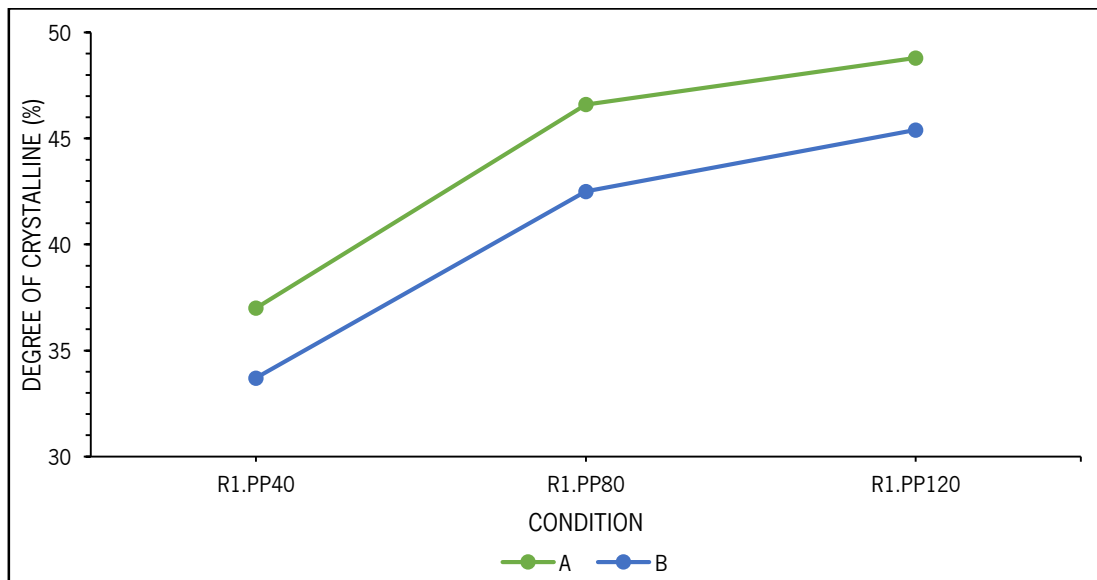


Figure 54 – Degree of crystalline results obtained for the one gate polypropylene specimens.

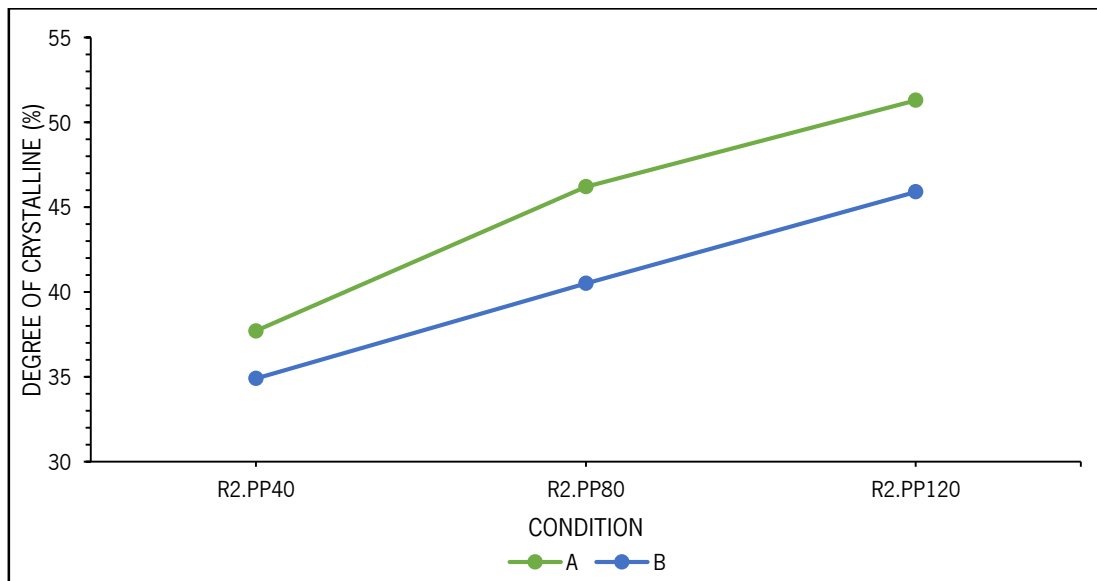


Figure 55 – Degree of crystalline results obtained for the two gates polypropylene specimens.

As the mold surface temperature increases, the crystalline degree of the PP specimen increases because the cooling rate of the polymer melt is decreased and therefore, the polymer melt has more than enough time to crystallize. This can be observed particularly in zone AA (in figures as A) since it is closer from the heating source and therefore, the crystalline polymer melt will flow easier and wrap more the amorphous phase. And recalling the light polarized results, the different which was observed in the crystalline orientation and structure between the two zones can be confirmed by the DSC results.

Since the objective is the comparison between the conventional system and the rapid heating surface temperature system, the crystalline degree difference for the best result achieved in the two figures is 19.2% and 15.8% (R1.PP120) and 20.2% and 14.8% (R2.PP120), for zones AA and BB respectively.

It is also noticed that having the same conditions but different number of gate (R1 and R2), the maximum difference of results is 5.7% (R2.PP80) and so, by this result it is verified that the temperature is the parameter with the biggest impact in the crystalline degree results.

CHAPTER 6

CONCLUSION

6.1. Conclusion

A system for heating the cavity surface was thought and tested. On the thought stage, it was concluded that polyethersulfone is a very efficient insulator, which can support relatively high service temperatures and, can be easily transformed to a film with the desired thickness and free of defects by controlling the pressure, temperature and time. Moreover, also strain gages can heat up the cavity surface even knowing that their main use is not meant for heating and plus, have interesting characteristics for an application on micro-injection molding process. Furthermore, the steel remains a good choice for giving mechanical stability, durability and strength needed to the cavity and mold. On the test stage, a theoretical study made by FlexPDE software allowed to check that with determined characteristics, the system can reach 106°C after 1 second of heating generation and, concluded also that there is a huge difference for surface temperature between having and not having an insulator, namely 63°C. Plus, it was observed that the strain gages must be as close as possible from each other to maximize the heating efficiency and, the thermal conductivity and the insulation and protective coating layers are factors that impact greatly the achievement of higher surface temperatures. Nevertheless, the most important conclusion from this stage is that, when comparing all the theoretical assumptions with a practical study, the results displayed were similar and so, all the theoretical conclusions formed are valid.

Concerning the optical characterization, it can be concluded that the surface temperature of 120°C is the best result according to the definition and orientation of the crystalline structure. It was observed a difference in the core of the specimens (zone AA and BB) originated by the generation of heat provided by the strain gages and, the zone AA presented spherulites with bigger dimensions. Moreover, as the surface temperatures increased, the skin-core decreased especially when comparing the results for a conventional system with the system created for this work. Unfortunately, the weld lines were only possible to locate by bright-field microscopy and therefore, no significant conclusions can be made from this issue.

Considering the mechanical characterization, as the surface temperature is increased, the stress of the both polypropylene and polystyrene conditions are also increased. However, the results and the increase is higher on the polystyrene conditions when comparing the break point for the conventional system with the best surface temperature result (120°C). On both polypropylene and polysterene conditions, the results are superior when comparing having one

gate instead of two gates, especially on the polystyrene conditions (difference of 21.5 MPa between a surface temperature of 120°C)

Regarding the thermal properties, the conclusion made was that increasing the surface temperature, an increase of the degree of crystalline of all polypropylene conditions was also observed and the zone AA has more crystalline regions than the zone BB. The best degree of crystalline achieved was a surface temperature of 120°C which compared to the conventional system, had a difference of 19.2% and 15.8% (R1.PP120) and 20.2% and 14.8% (R2.PP120), for zones AA and BB respectively.

6.2. Future Works

As future works, it is highly recommended the continuity of the study around the system developed in this work. Accordingly, it is proposed:

- Possibility on placing the surface heating created on both moveable and core parts in order to standardize the temperature along all the specimen;
- Study of variation on the processing conditions (injection pressure, injection speed, ...);
- Influence and effect of using a circling coolant as the cooling method;
- Injection of materials with difficult processability;
- Study of the system influence on roughness and brightness;
- Application of the surface heating system on injection molding process;
- Improve the system created on various levels such as heating efficiency, easier assembly of all components, integration of different materials, automation of the process, among others;

BIBLIOGRAPHY

- [1] G. Wang, G. Zhao, G. Li and Y. Guan, "Analysis of thermal cycling efficiency and optimal design of heating/cooling systems for rapid heat cycle injection molding process," *Materials and Design*, vol. 31, pp. 3426-3444, 2010.
- [2] A. Iannaccone, F. Santis, R. Pantani and R. Sora, "Development of a rapid surface temperature heating system and its application to a micro-injected part," in *International Conference on Polymers and Moulds Innovations - PMI 2014*, 2014.
- [3] G. Wang, G. Zhao, H. Li and Y. Guan, "Research on optimization design of the heating/cooling channels for rapid heat cycle molding based on response surface methodology and constrained particle swarm optimization," *Expert Systems with Applications*, vol. 38, pp. 6705-6719, 2011.
- [4] U. Attia, S. Marson and J. Alcock, "Micro-Injection Moulding of Polymer Microfluidic Devices," *Microfluidics and Nanofluidics*, vol. 7, pp. 1-28, 2009.
- [5] Y. Qin, *Micro-Manufacturing Engineering and Technology*, William Andrew, 2010.
- [6] S. Meister and D. Drummer, "Influence of manufacturing conditions on measurement of mechanical material properties on thermoplastic micro tensile bars," *Polymer Testing*, vol. 32, pp. 432-437, 2013.
- [7] P.-C. Chang, S.-J. Hwang, H.-H. Lee and D.-Y. Huang, "Development of an external-type microinjection molding module for thermoplastic polymer," *Journal of Materials Processing Technology*, vol. 184, pp. 163-172, 2007.
- [8] B. Murray and S. Hinstead, "Micromoulding Developments Alternative Technology," *Polymer Process Engineering*, pp. 28-32.
- [9] B. Whiteside, K. Howell, M. Martyn and R. Spares, "Micromoulding: extreme process monitoring and in-line product assessment," *Plastics Rubber And Composites*, vol. 34, pp. 380-386, 2009.
- [10] Y. Ono, B. Whiteside, E. Brown, M. Kobayashi, C. Cheng, C. Jen and P. Coates, "Real-time process monitoring of micromoulding using integrated ultrasonic sensors," *Transactions of the Institute of Measurement and Control*, vol. 29, pp. 383-401, 2007.

- [11] J. O. C. V. Vasco, "A Micro-Fabricação aplicada ao processo de Micro-Injecção," Universidade do Minho, 2006.
- [12] M. Hecke and W. Schomburg, "Review on micro molding of thermoplastic polymers," *Journal of Micromechanics and Microengineering*, vol. 14, pp. R1-R14, 2004.
- [13] [Online]. Available: <http://www.bayern-innovativ.de/ib/site/documents/image/media/Thumb/55c67ad5-387a-1635-eeab-88f37b104ba0.jpg%3FWidth%3D540%26Height%3D540%26Quality%3D90%26NoUpscale%3D1%26ForceRGB%3D1%26Confirm%3D1>. [Accessed 25th February 2014].
- [14] B. Whiteside, M. Martyn, P. Coates, P. Allan, P. Hornsby and G. Greenway, "Micromoulding process characteristic and product properties," *Plastics Rubber And Composites*, vol. 32, pp. 231-239, 2003.
- [15] C. Kukla, "Micro Injection Moulding," *International Journal of Forming Processes*, vol. 4, pp. 253-267, 2001.
- [16] J. Giboz, T. Copponnex and P. Mélé, "Microinjection molding of thermoplastic polymers: a review," *Journal of Micromechanics and Microengineering*, vol. 17, pp. 96-109, 2007.
- [17] A. Cunha, Micro-Injecção de NanoCompósitos, Universidade do Minho, 2009.
- [18] M. Ganz, "Micro Injection Moulding and Compression Moulding," in *Polymer Technology toward Nano, future technology for Europe*, Karlsruhe, Germany, 2005.
- [19] V. Piötter, T. Hanemann, R. Ruprecht and J. Haubelt, "Injection molding and related techniques for fabrication of microstructures," *Springer-Verlag*, vol. 3, pp. 129-133, 1997.
- [20] L. Xie, T. Niesel, M. Leester-Schädel, G. Ziegmann and S. Büttgenbach, "A novel approach to realize the local precise variotherm process in micro injection molding," *Microsystem Technologies*, vol. 19, pp. 1017-1023, 2013.
- [21] Battenfeld, Perfect business performanc for small and micro parts technology working for you, 2011.
- [22] C. Gornik, "Injection moulding of parts with microstrutred surfaces for medical applications," *Macromolecular Symposia*, vol. 217, pp. 365-374, 2004.
- [23] D. Yao and B. Kim, "Development of a rapid heating and cooling systems for injection molding applications," *Polymer Engineering Science*, vol. 42, pp. 2471-2481, 2002.

- [24] M. Huang, J. Yu and Y. Lin, "Effects of Rapid Mold Surface Inducting Heating on the Replication Ability of Microinjection Molding Light-Guided Plates with V-grooved Microfeatures," *Journal of Applied Polymer Science*, vol. 118, pp. 3058-3065, 2010.
- [25] G. Wang, Z. Guoqun, L. Huiping and G. Yanjin, "Analysis of thermal cycling efficiency and optimal design of heating/cooling systems for rapid heat cycle injection molding process," *Materials and Design*, vol. 31, pp. 3426-3441, 2010.
- [26] M. Yu, W. Young and P. Hsu, "Micro-injection molding with the infrared assisted mold heating system," *Materials Science and Engineering*, Vols. 460-461, pp. 288-295, 2007.
- [27] G. Wang, G. Zhao and X. Wang, "Experimental rearch on the effects of cavity surface temperature on surface appearance properties of the moulded part in rapid heat cycle moulding process," *International Journal of Advanced Manufacturing Technology*, vol. 68, pp. 1293-1310, 2013.
- [28] G. Wang, G. Zhao and Y. Guan, "Thermal response of an electric heating rapid heat cycle molding mold and its effect on surface appearance and tensile strength of the molded part," *Journal of Applied Polymer Science* , vol. 128, pp. 1339-1352, 2012.
- [29] G. Wang, G. Zhao and G. Yanjin, "Research on Optimum Heating System Design for Rapi Thermal Response Mold with Electric Heating Based on Response Surfce Methodology and Particle Swarm Optimization," *Journal of Applied Polymer Science*, vol. 119, pp. 902-921, 2011.
- [30] G. Wang, G. Zhao, H. Li and Y. Guan, "Research of thermal response simulation and mold structure optimization for rapid heat cycle moding processes, respectively, with steam heating and electric heating," *Materials and Design*, vol. 31, pp. 382-395, 2010.
- [31] D. Yao, S. Chen and B. Kim, "Rapid Thermal Cycling of Injection Molds: An Overview on Technical Approaches and Applications," *Advances in Polymer Technology*, vol. 27, pp. 233-255, 2008.
- [32] H. Lin, S. Chen, M. Jeng, P. Minh, J. Chang and J. Hwang, "Induction heating with the ring effect for injection molding plates," *International Communications in Heat and Mass Transfer*, vol. 39, pp. 514-522, 2012 .
- [33] S. Chen, W. Jong, Y. Chang, J. Chang and J. Cin, "Rapid mold temperature variation for assisting the micrro injection of high aspect micro-feature parts using induction heating

- technology," *Journal of micromechanics and microengineering*, vol. 16, pp. 1783-1791, 2006.
- [34] R. Rocha, Aproveitamento do Calor dos Gases de Escape para Geração de Energia Eléctrica, Universidade do Minho, 2011.
- [35] D. Kim, M. Kang and Y. Chun, "Development of a new injection molding technology: momentary mold surface heating process," *Journal of Injection Molding Technology*, vol. 5, pp. 229-232, 2001.
- [36] S. Chen, W. Jong, Y. Chang, J. Chang and J. Cin, "Rapid mold temperature variation for assisting the micro injection of high aspect ratio micro-feature parts using induction heating technology," *Journal of Micromechanics and Microengineering*, vol. 16, pp. 1783-1791, 2006.
- [37] P. Chang and S. Hwang, "Experimental investigation of infrared rapid surface heating for injection molding," *Journal of Applied Polymer Science*, vol. 102, pp. 3704-3713, 2006.
- [38] S. Chen, R. Chien, S. Lin, M. Lin and J. Chang, "Feasibility evaluation of gas-assisted heating for mold surface temperature control during injection molding process," *International Communications in Heat and Mass Transfer*, vol. 36, pp. 806-812, 2009.
- [39] K. Jansen and A. Flaman, *Polym Eng Sci*, vol. 34, pp. 894-897, 1994.
- [40] D. Yao and B. Kim, "Increasing flow length in thin wall injection molding using a rapidly heated mold," *Polymer-Plastics Technology and Engineering*, vol. 41, pp. 819-832, 2002.
- [41] Y. Kim, Y. Choi and S. Kang, "Replication of high density optical disc using injection mold with MEMS heater," *Microsystem Technologies*, vol. 11, pp. 464-469, 2005.
- [42] Y. Kim, J. Bae, H. Kim and S. Kang, "Modelling of passive heating for replication of sub-micron patterns in optical disk substrates," *Journal of Physics and Applications*, vol. 36, pp. 1030-1035, 2004.
- [43] H. M. and T. N., "Experimental rapid surface heating by induction for micro-injection molding of light-guided plates," *Journal of Applied Polymer Science*, vol. 113, pp. 1345-1354, 2009.

- [44] J. Yoon, S. Hong, J. Kim and S. Sha, "A mold surface treatment for improving surface finish of injection molded microcellular parts," *Cellular Polymers Journal*, vol. 23, pp. 39-47, 2004.
- [45] L. Chen, R. Chien and S. Chen, "Using thermally insulated polymer film for mold temperature control to improve surface quality of microcellular injection molded parts," *International Communications in Heat and Mass Transfer*, vol. 35, pp. 991-994, 2008.
- [46] G. Wang, G. Zhao, H. Li and Y. Guan, "Research on a new variotherm injection molding technology and its application on the molding of a large LCD panel," *Polymer-Plastic Technologies and Engineering*, vol. 48, pp. 671-681, 2009.
- [47] S. Chen, W. Jong and J. Chang, "Dynamic mold surface temperature using induction heating and its effects on the surface appearance of weld line," *Journal of Applied Polymer Science*, vol. 101, pp. 1174-1180, 2006.
- [48] M. Costa, Estudo do comportamento do fluxo em microcavidade na microinjeção, Guimarães: Universidade do Minho, 2013.
- [49] [Online]. Available: http://www.goodfellow.com/catalogue/GFCat2C.php?ewd_token=g9mZvVuA0h4mF1kG MbRhbkeEJIT7HD&n=ocpRZIVmIWFOyge27Q7k1bE6LboTIQ&ewd_urlNo=GFCat26&type=30&prop=6. [Accessed 8th April 2014].
- [50] [Online]. Available: <http://www.omnexus.com/tc/polymerselector/polymerprofiles.aspx>. [Accessed 11th April 2014].
- [51] R. Hannah and S. Reed, Strain Gage Users' Handbook, Chapman & Hall, 1992.
- [52] [Online]. Available: http://sts.bwk.tue.nl/7s533/readers/FPDE_User_Guide.pdf. [Accessed 20th April 2014].
- [53] D. Hemsley, The Light Microscopy of Synthetic Polymers, RMS, 1984.
- [54] K. Menard, Dynamic Mechanical Analysis-A Practical Introduction, Taylor & Francis Group, 1999.
- [55] F. Beer, E. Johnston and J. DeWolf, Mechanics of Materials, McGraw Hill, 2004.
- [56] M. Sepe, "Thermal Analysis of Polymers," *Rapra Technology Limited*, vol. 8, pp. 3-13, 1997.

ATTACHMENTS

Attachment 1


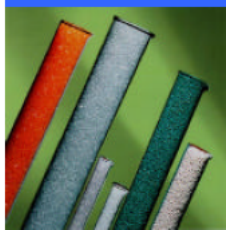
 POLIMERI EUROPA	
	Edistir[®] Polystyrene
N 1910	
<u>TECHNICAL DATA SHEET</u>	
<i>Product description</i>	
<p>Very easy flow general purpose polystyrene.</p> <p>Used for injection of thin-wall, multi-cavity, very fast-cycle mouldings and for sheet extrusion in glossy capping of HIPS and in blend with HIPS or clear SBS.</p> <p>Designation: Thermoplastics ISO 1622-PS,G,085-20</p>	
<i>Applications</i>	
<p>Typical uses include cups, packaging containers for foods and cosmetics, toys, medical articles.</p> <p>Thanks to its high flow it is particularly suitable as carrier for master batches.</p>	
<i>Typical processing data</i>	
<p>Injection moulding: • predrying normally not required • melt temperature 200-250°C • mould temperature 10-50°C</p> <p>Extrusion: • melt temperature 210-240°C</p>	
<i>General information</i>	
<p>N 1910 is certified UL94 HB "all colors" at 1.5 mm (UL file E83071).</p> <p>This grade in its natural version complies by composition with the requirements set by the main Regulations for plastic materials intended for food contact (including the EEC Directive 90/128 and subsequent amendments).</p>	
<small>Issue 01/02</small>	

Figure 56 – Datasheet of Edistir N1910 (part 1).

Properties	Test conditions	Test methods	Units	Values
General				
Density		ISO 1183	g/cm ³	1.05
Bulk density		ISO 60	g/cm ³	0.65
Water absorption	24 h - 23°C	ISO 62	%	<0.1
Rheological				
Melt flow rate	200°C - 5 kg	ISO 1133	g/10 min	27
Mechanical				
Tensile stress at yield	5 mm/min	ISO 527	MPa	-
Tensile stress at break	5 mm/min	ISO 527	MPa	37
Tensile strain at break	5 mm/min	ISO 527	%	1.3
Tensile modulus	1 mm/min	ISO 527	MPa	3200
Flexural strength	2 mm/min	ISO 178	MPa	67
Izod impact strength, notched	+23°C - thickness 3.2 mm	ISO 180/4A	J/m	-
	+23°C - thickness 4 mm	ISO 180/1A	kJ/m ²	1.7
	-30°C - thickness 4 mm	ISO 180/1A	kJ/m ²	1.5
Rockwell hardness	L/M scale	ISO 2039/2	-	M80
Thermal				
Vicat softening temperature	10 N - 50°C/h	ISO 306/A	°C	89
	50 N - 50°C/h	ISO 306/B	°C	83
Deflection temperature under load (annealed)	1.8 MPa - 120°C/h	ASTM D 648	°C	82
Coefficient of linear thermal expansion		ASTM D 696	10 ⁻⁵ /°C	7
Thermal conductivity		ISO 8302	W/(K·m)	0.17
Moulding shrinkage		internal method	%	0.3 - 0.6
Flammability				
Flame behaviour	thickness 1.5 mm	UL 94	class	HB
Glow wire test (GWT)	thickness 1.6 mm	IEC 60695-2-1	°C	650
Electrical				
Surface resistivity		IEC 60093	ohm	>1.5·10E+15
Volume resistivity		IEC 60093	ohm·cm	>7·10E+15
Comparative tracking index (CTI)	solution A	IEC 60112	-	375
Dielectric strength		IEC 60243	kV/mm	70
Dielectric constant (relative permittivity)	50 Hz	IEC 60250	-	2.5
Dissipation factor	50 Hz	IEC 60250	-	2·10E-4

Issue 01/02

All indicated data refer to natural grades.

The data, information and suggestions are provided for guidance purposes only.

The Company accepts no responsibility for the results obtained therefrom, as neither for their utilization in infringement of possible patent rights.

However the Company will provide the guaranteed values for each product on demand.

Polimeri Europa S.p.A.
Divisione Elastomeri e Stirenici
Piazza Boldrini, 1
I-20097 San Donato Milanese - Milano
e-mail: stir.pst@polimerieuropa.com
www.polimerieuropa.com

Figure 57 – Datasheet of Edistir N1910 (part 2).

lyondellbasell			
Moplen HP548R			
Polypropylene, Homopolymer			
Product Description			
<p><i>Moplen</i> HP548R is a nucleated homopolymer with antistatic additivation used for injection moulding applications.</p> <p><i>Moplen</i> HP548R exhibits a good stiffness combined with a good flowability.</p> <p>The main applications of <i>Moplen</i> HP548R are caps, closures, furniture and housewares.</p> <p><i>Moplen</i> HP548R is suitable for food contact.</p>			
Product Characteristics			
Status	Commercial: Active		
Test Method used	ISO		
Availability	Europe, Africa-Middle East		
Processing Methods	Injection Molding		
Features	Antistatic, Good Flow, Nucleated, Good Stiffness		
Typical Customer Applications	Caps & Closures, Furniture, Housewares, Opaque Containers		
Typical Properties	Method	Value	Unit
Physical			
Density	ISO 1183	0.9	g/cm ³
Melt flow rate (MFR) (230°C/2.16kg)	ISO 1133	23	g/10 min
Melt volume flow rate (230°C/2.16kg)	ISO 1133	31	cm ³ /10min
Mechanical			
Tensile Modulus	ISO 527-1, -2	1650	MPa
Tensile Stress at Yield	ISO 527-1, -2	35	MPa
Tensile Strain at Break	ISO 527-1, -2	>50	%
Tensile Strain at Yield	ISO 527-1, -2	8	%
Impact			
Charpy unnotched impact strength (23 °C, Type 1, Edgewise)	ISO 179	110	kJ/m ²
Charpy notched impact strength (23 °C, Type 1, Edgewise, Notch A)	ISO 179	2.5	kJ/m ²
Hardness			
Ball indentation hardness (H 358/30)	ISO 2039-1	78	MPa
Thermal			
Heat deflection temperature B (0.45 MPa) Unannealed	ISO 75B-1, -2	95	°C
Vicat softening temperature (A50 (50°C/h 10N))	ISO 306	154	°C
(B50 (50°C/h 50N))		94	°C
Notes			
Typical properties; not to be construed as specifications.			

Figure 58 – Datasheet of Moplen HP548R


Product Information		Ultrason® E 3010 PESU (Polyethersulfone)	 BASF The Chemical Company
Sep 2014			
Product Description			
Ultrason E 3010 is an unfilled, higher viscosity injection molding and extrusion PESU grade, tougher and with improved chemical resistance.			
PHYSICAL	ISO Test Method	Property Value	
Density, g/cm	1183	1.37	
Mold Shrinkage, parallel, %	294.4	0.85	
Mold Shrinkage, normal, %	294.4	0.9	
Moisture, %	62		
(50% RH)		0.8	
(Saturation)		2.2	
RHEOLOGICAL	ISO Test Method	Property Value	
Melt Volume Rate (360 C/10 Kg), cc/10min.	1133	35	
MECHANICAL	ISO Test Method	Property Value	
Tensile Modulus, MPa	527		
23C		2,650	
Tensile stress at yield, MPa	527		
23C		85	
Tensile strain at yield, %	527		
23C		6.9	
Ball Indentation, MPa	2039-1	154	
IMPACT	ISO Test Method	Property Value	
Izod Notched Impact, kJ/m ²	180		
23C		8	
-30C		8	
Charpy Notched, kJ/m ²	179		
23C		8	
-30C		8	
Charpy Unnotched, kJ/m ²	179		
23C		N	
-30C		N	
THERMAL	ISO Test Method	Property Value	
HDT A, C	75	207	
Coef. of Linear Thermal Expansion, Parallel, mm/mm C		0.52 X10 ⁻⁴	
ELECTRICAL	ISO Test Method	Property Value	
Comparative Tracking Index	IEC 60112	125	
Volume Resistivity	IEC 60093	>1E13	
Surface Resistivity	IEC 60093	>1E15	
Dielectric Constant (100 Hz)	IEC 60250	3.9	
Dielectric Constant (1 MHz)	IEC 60250	3.8	
Dissipation Factor (100 Hz)	IEC 60250	17	
Dissipation Factor (1 MHz)	IEC 60250	140	
BASF Corporation Engineering Plastics 1609 Biddle Avenue Wyandotte, MI 48192		General Information: 800-BC-RESIN Technical Assistance: 800-527-TECH (734-324-5150) Web address: http://www.plasticsportal.com/usa	
		Page 1 of 2	

Figure 59 – Datasheet of BASF Ultrason E 3010 (part 1).

Dielectric Strength, KV/mm		IEC 60243-1	34
UL RATINGS			
		UL Test Method	Property Value
Flammability Rating, 1.6mm		UL94	V-0
Relative Temperature Index, 1.6mm		UL748B	
Mechanical w/o Impact, C			190
Mechanical w/ Impact, C			180
Electrical, C			180
Flammability Rating, 3.0mm		UL94	V-0
Relative Temperature Index, 3.0mm		UL748B	
Mechanical w/o Impact, C			190
Mechanical w/ Impact, C			180
Electrical, C			180
Processing Guidelines			
<p>Material Handling Max. Water content: 0.02% Ultrason pellets can absorb moisture very rapidly and must be dried before processing. A vacuum or dry air oven operating at 130-150 degC (266-302 degF) is recommended. Circulating air ovens are unsuitable. Drying time is dependent on moisture level, but the materials must be dried at least 4 hours. Further information concerning safe handling procedures can be obtained from the Material Safety Data Sheet. Alternatively, please contact your BASF representative.</p>			
<p>Typical Profile Melt Temperature 340-390 degC (644-734 degF) Mold Temperature 140-180 degC (284-356 degF) Injection and Packing Pressure 35-125 bar (500-1500 psi)</p>			
<p>Mold Temperatures Injection pressure controls the filling of the part and should be applied for 90% of ram travel. Packing pressure affects the final part and can be used effectively in controlling sink marks and shrinkage. It should be applied and maintained until the gate area is completely frozen off.</p> <p>Back pressure can be utilized to provide uniform melt consistency and reduce trapped air and gas. Minimal back pressure should be utilized to prevent glass breakage.</p>			
<p>Pressures Fast fill rates are recommended to ensure uniform melt delivery to the cavity and prevent premature freezing. Surface appearance is directly affected by injection rate.</p>			
Note			
<p>Although all statements and information in this publication are believed to be accurate and reliable, they are presented gratis and for guidance only, and risks and liability for results obtained by use of the products or application of the suggestions described are assumed by the user. NO WARRANTIES OF ANY KIND, EITHER EXPRESS OR IMPLIED, INCLUDING WARRANTIES OF MERCHANTABILITY OR FITNESS FOR A PARTICULAR PURPOSE, ARE MADE REGARDING PRODUCTS DESCRIBED OR DESIGNS, DATA OR INFORMATION SET FORTH. Statements or suggestions concerning possible use of the products are made without representation or warranty that any such use is free of patent infringement and are not recommendations to infringe any patent. The user should not assume that toxicity data and safety measures are indicated or that other measures may not be required.</p>			
BASF Corporation Engineering Plastics 1609 Biddle Avenue Wyandotte, MI 48192		General Information: 800-BC-RESIN Technical Assistance: 800-527-TECH (734-324-5150) Web address: http://www.plasticsportal.com/usa	
			Page 2 of 2

Figure 60 – Datasheet of BASF Ultrason E 3010 (part 2).

Attachment 4





Physical Properties	Metric	English	Comments
Density	1.33 g/cc	0.0480 lb/in ³	ASTM D792
Water Absorption	0.34 %	0.34 %	24 hours; ASTM D570
Moisture Absorption at Equilibrium	0.24 %	0.24 %	24 hours, 23°C, 60% RH
Linear Mold Shrinkage	0.0083 cm/cm	0.0083 in/in	ASTM D955
Mechanical Properties	Metric	English	Comments
Hardness, Rockwell M	95	95	ASTM D785
Hardness, Rockwell R	129	129	ASTM D785
Tensile Strength at Break	92.2 MPa	13400 psi	ASTM D638
Tensile Strength, Ultimate	57.9 MPa @Temperature 150 °C	8400 psi @Temperature 302 °F	ASTM D638
Elongation at Break	90 %	90 %	ASTM D638
 Elongation at Break	90 % @Temperature 150 °C	90 % @Temperature 302 °F	ASTM D638
Flexural Strength	137 MPa	19900 psi	ASTM D790
	88.3 MPa @Temperature 150 °C	12800 psi @Temperature 302 °F	ASTM D790
Flexural Modulus	2.94 GPa	426 ksi	ASTM D790
 Flexural Modulus	2.55 GPa @Temperature 150 °C	370 ksi @Temperature 302 °F	ASTM D790
Compressive Strength 	76.5 MPa @Temperature 150 °C	11100 psi @Temperature 302 °F	JIS K7208
	120 MPa @Temperature 23.0 °C	17400 psi @Temperature 73.4 °F	JIS K7208
Compressive Modulus	1.57 GPa	228 ksi	At 150°C; JIS K7208
	2.16 GPa	313 ksi	At 23°C; JIS K7208
Shear Strength 	78.5 MPa @Temperature 150 °C	11400 psi @Temperature 302 °F	JIS K7214
	81.4 MPa @Temperature 23.0 °C	11800 psi @Temperature 73.4 °F	JIS K7214
Izod Impact, Notched	0.883 J/cm	1.65 ft-lb/in	ASTM D256

Figure 61 – Datasheet of Mitsui AURUM 450 (part 1).





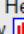

Electrical Properties	Metric	English	Comments
Volume Resistivity	1.00e+17 - 1.00e+18 ohm-cm	1.00e+17 - 1.00e+18 ohm-cm	ASTM D257
Surface Resistance	1.00e+17 - 1.00e+18 ohm	1.00e+17 - 1.00e+18 ohm	ASTM D257
Dielectric Constant 	3.1 @Frequency 1e+6 Hz	3.1 @Frequency 1e+6 Hz	ASTM D150
	3.2 @Frequency 1000 Hz	3.2 @Frequency 1000 Hz	ASTM D150
Dissipation Factor 	0.00090 @Frequency 1000 Hz	0.00090 @Frequency 1000 Hz	ASTM D150
	0.0034 @Frequency 1e+6 Hz	0.0034 @Frequency 1e+6 Hz	ASTM D150
Thermal Properties	Metric	English	Comments
CTE, linear 	55.0 µm/m-°C @Temperature 23.0 °C	30.6 µin/in-°F @Temperature 73.4 °F	MD; ASTM D696
	55.0 µm/m-°C @Temperature 200 °C	30.6 µin/in-°F @Temperature 392 °F	MD; ASTM D696
CTE, linear, Transverse to Flow 	55.0 µm/m-°C @Temperature 23.0 °C	30.6 µin/in-°F @Temperature 73.4 °F	ASTM D696
	55.0 µm/m-°C @Temperature 200 °C	30.6 µin/in-°F @Temperature 392 °F	ASTM D696
Specific Heat Capacity 	1.00 J/g-°C @Temperature 23.0 °C	0.239 BTU/lb-°F @Temperature 73.4 °F	By DSC
	1.00 J/g-°C @Temperature 100 °C	0.239 BTU/lb-°F @Temperature 212 °F	By DSC
	1.42 J/g-°C @Temperature 300 °C	0.339 BTU/lb-°F @Temperature 572 °F	By DSC
Thermal Conductivity	0.174 W/m-K	1.21 BTU-in/hr-ft²-°F	
Melting Point	388 °C	730 °F	
Maximum Service Temperature, Air	238 °C	460 °F	Heat distortion temperature, load unknown; ASTM D648
Glass Transition Temp, Tg	250 °C	482 °F	By DSC
Decomposition Temperature	570 °C	1060 °F	5% weight reduction temperature, by DTG
Flammability, UL94 	V-0 @Thickness 0.400 mm	V-0 @Thickness 0.0157 in	all color
	5VA @Thickness 2.00 mm	5VA @Thickness 0.0787 in	all color
Oxygen Index	47 % @Thickness 3.20 mm	47 % @Thickness 0.126 in	ASTM D256
Processing Properties	Metric	English	Comments
Processing Temperature	390 - 420 °C	734 - 788 °F	Injection molding, extrusion

Figure 62 – Datasheet of Mitsui AURUM 450 (part 2).

Attachment 5

Table 16 – Datasheet of OMEGA SGD-4/120-LY13

SGD Specifications		
Foil Measuring Grid	-	Constantan foil 5 μm thick
Carrier	-	Polyimide
Substrate Thickness	μm	20
Cover Thickness	μm	25
Connection Dimensions	mm	30 L x 0.1 D x 0.3 W
Nominal Resistance	Ω	120
Resistance Tolerance	%	± 0.15 to ± 0.5
Gage Factor	%	2.0 ± 5
Gage Factor Tolerance	%	1
Thermal Properties		
Reference Temperature	$^{\circ}\text{C}$	23
Service Temperature		
Static Measurements	$^{\circ}\text{C}$	-75 to 200
Dynamic Measurements	$^{\circ}\text{C}$	-75 to 200
Temperature Characteristics		
Steel (and certain Stainless Steels)	ppm/ $^{\circ}\text{C}$	11
Aluminium	ppm/ $^{\circ}\text{C}$	23
Uncompensated	ppm/ $^{\circ}\text{C}$	± 20
Temperature Compensated Range	$^{\circ}\text{C}$	-5 to 120
Tolerance of Temperature Compensation	ppm/ $^{\circ}\text{C}$	2
Mechanical Properties		
Maximum Strain	%	3

Hysteresis	-	Negligible
Fatigue (at ± 1500 microstrain)	cycles	>10000000
Smallest Bending Radius	mm	3
Transverse Sensivity	-	-

Attachment 6

```
TITLE 'Surface heating by strain gages' {SolidiAContatto.pde}

COORDINATES cartesian2 { il problema e' bi-dimensionale }

VARIABLES          temp      {temperatura}

SELECT             erlim=1e-3

DEFINITIONS { parameter definitions }

kappa alfa gen Tinf { proprieta' rilevanti dei solidi (da definire) }
```

Figure 63 – Variables of the FlexPDE script.

```
'solido 1: stampo'

Tinf1=300

xmold=28e-3 { spessore della lastra di materiale "1" }

ymold=54.4e-3

kappa1=15 { conducibilita' del solido "1" }

alfa1=8.01e-6 { diffusivita' del solido "1" }
```

Figure 64 – Example of the material properties input on FlexPDE software.


```

'strain gage'

xsg=120e-6 { spessore della lastra di materiale "2" }

kappasg=0.37

alfasg=1.90e-7

{ calcolo della generazione nello strain gage }

volt=32

ohm=120

watt=volt^2/ohm

ampere=volt/ohm

ysg=3.7e-3

sup_sg=5.5e-3*ysg

vol_sg=sup_sg*xsg

gen_sg=watt/vol_sg

tgen=1 { tempo di alimentazione}

```

Figure 65 – Example of the strain gage input on FlexPDE software.

EQUATIONS

$$\text{kappa}/\text{alfa}*\text{dt}(\text{temp})=\text{div}(\text{kappa}*\text{grad}(\text{temp}))+\text{gen} \{ \text{diffusione calore con generazione} \}$$

Figure 66 – Equation implanted for the generation of heat.

```

REGION 1 { in tutto il dominio }

Tinf=Tinf1

kappa=kappa1 { propriet? del solido "1" }

alfa=alfa1

gen=0

START(0,-ymold/2)

Natural(temp)=0 { parete adiabatica sotto }

LINE TO (xmax,-ymold/2)

Natural(temp)=h*(temp-Ta) { parete adiabatica a destra }

LINE TO (xmax, ymold/2)

Natural(temp)=0 { parete adiabatica sopra}

LINE TO (0,ymold/2)

Natural(temp)=0 { parete adiabatica a sinistra }

LINE TO CLOSE

```

Figure 67 – Implementation of region 1 (all components) on FlexPDE.

<pre> REGION 2 { nell'isolante} Tinf=Tinf1 kappa=kappaiso { propriet? del solido "2"} alfa=alfaiso gen=0 START(xmold,-ymold/2) LINE TO (xmold+xiso,-ymold/2) LINE TO (xmold+xiso,ymold/2) LINE TO (xmold,ymold/2) LINE TO CLOSE </pre>	<pre> REGION 3 { attorno allo strain gage} Tinf=Tinf1 kappa=kappasg { propriet? del solido "2"} alfa=alfasg gen=0 START(xmold+xiso,-ymold/2) LINE TO (xmold+xiso+xsg,-ymold/2) LINE TO (xmold+xiso+xsg, ymold/2) LINE TO (xmold+xiso, ymold/2) LINE TO CLOSE </pre>
---	--

Figure 68 – On left, implementation of region 2 (insulation layer). On right, implementation of region 3 (heating generation layer).

<pre> REGION 4 { nello strain gage 1} Tinf=Tinf1 kappa=kappasg { proprieta' del solido "2"} alfa=alfasg gen=if t<tgen then gen_sg else 0 START(xmold+xiso,-ysg-dist/2) LINE TO (xmold+xiso+xsg,-ysg-dist/2) LINE TO (xmold+xiso+xsg,-dist/2) LINE TO (xmold+xiso,-dist/2) LINE TO CLOSE </pre>	<pre> REGION 5 { nello strain gage 2} Tinf=Tinf1 kappa=kappasg { proprieta' del solido "2"} alfa=alfasg gen=if t<tgen then gen_sg else 0 START(xmold+xiso,ysg+dist/2) LINE TO (xmold+xiso+xsg,ysg+dist/2) LINE TO (xmold+xiso+xsg,dist/2) LINE TO (xmold+xiso,dist/2) LINE TO CLOSE </pre>
---	---

Figure 69 – On left, implementation of region 4 (in the strain gage). On right, implementation of region 5 (in the strain gage, if used more than 1).

<pre> REGION 6 { nella lastrina} Tinf=Tinf1 kappa=kappa2 { proprieta' del solido "2"} alfa=alfa2 gen=0 START(xmold+xiso+xsg,-ymold/2) LINE TO (xmold+xiso+xsg+xslab,-ymold/2) LINE TO (xmold+xiso+xsg+xslab,ymold/2) LINE TO (xmold+xiso+xsg,ymold/2) LINE TO CLOSE </pre>	<pre> REGION 7 { nel polimero} Tinf=Tinf2 kappa=kappapol { proprieta' del solido "2"} alfa=alfapol gen=0 START(xmax-xpol,-ymold/2) LINE TO (xmax,-ymold/2) LINE TO (xmax,ymold/2) LINE TO (xmax-xpol,ymold/2) LINE TO CLOSE </pre>
--	--

Figure 70 – Implementation of regions 6 and 7 (in the polymer layer).

```

T1=val(temp,xmold+xiso,0)
T2=val(temp,xmold+xiso+xsg,0)
T3=val(temp,xmold+xiso+xsg+xslab,0)
Tpol=val(temp,xmax,0)

```

Figure 71 – Code related to the temperatures reached between each layer.

```
MONITORS    { progresso }

for cycle=25

elevation(temp, strain_gage) from (xmax-xpol,-ymold/2) to (xmax-xpol,ymold/2)

elevation(temp) from (0,0) to (xmax,0) as "Temp"

elevation(f) from (0,0) to (xmax,0) as "Flux"

for t=0

SUMMARY

REPORT(gen_sg) as "generazione"

REPORT(ampere) as "ampere"

PLOTS      { save result displays }

HISTORIES  { grafici nel tempo }

History(T1,T2,T3,Tpol) as "Surface Temperatures" export format "#t#b#1#b#2#b#3#b#4" file="Temp.txt" { Esporta i profili di temperatura}

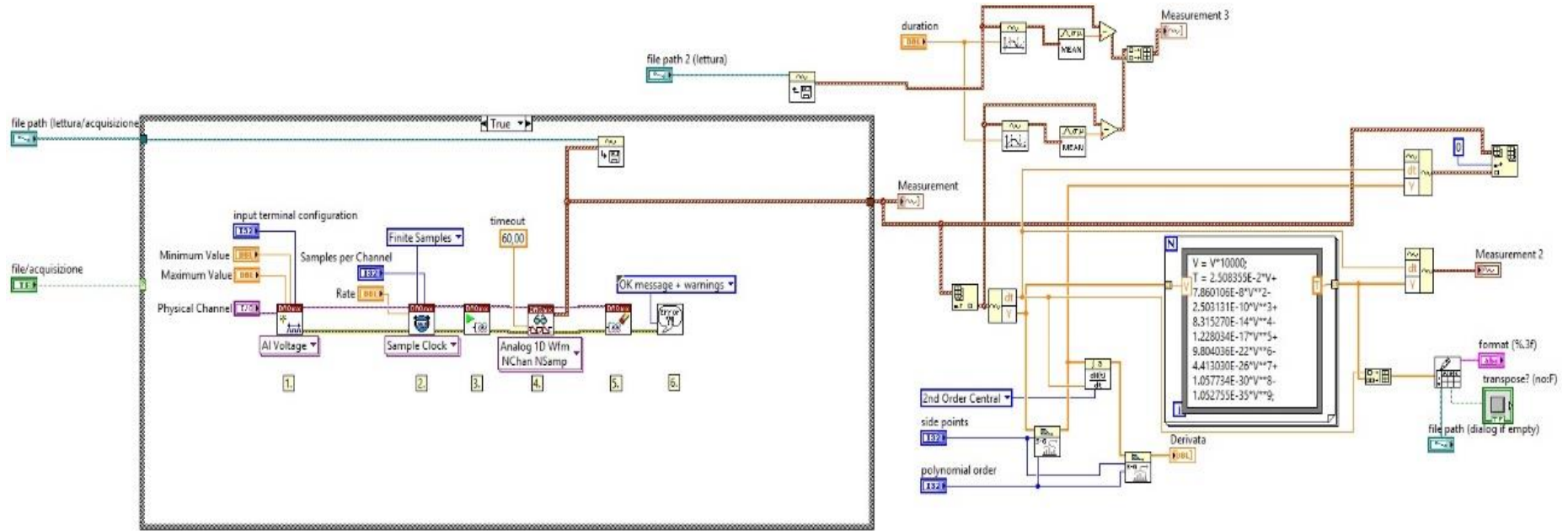
History(-f1,f2) as "flusso"

History((-f1+f2)*sup_sg/watt) as "flusso normalizzato"

END
```

Figure 72 – Code related to the visualization and data save.

Attachment 7



Attachment 8

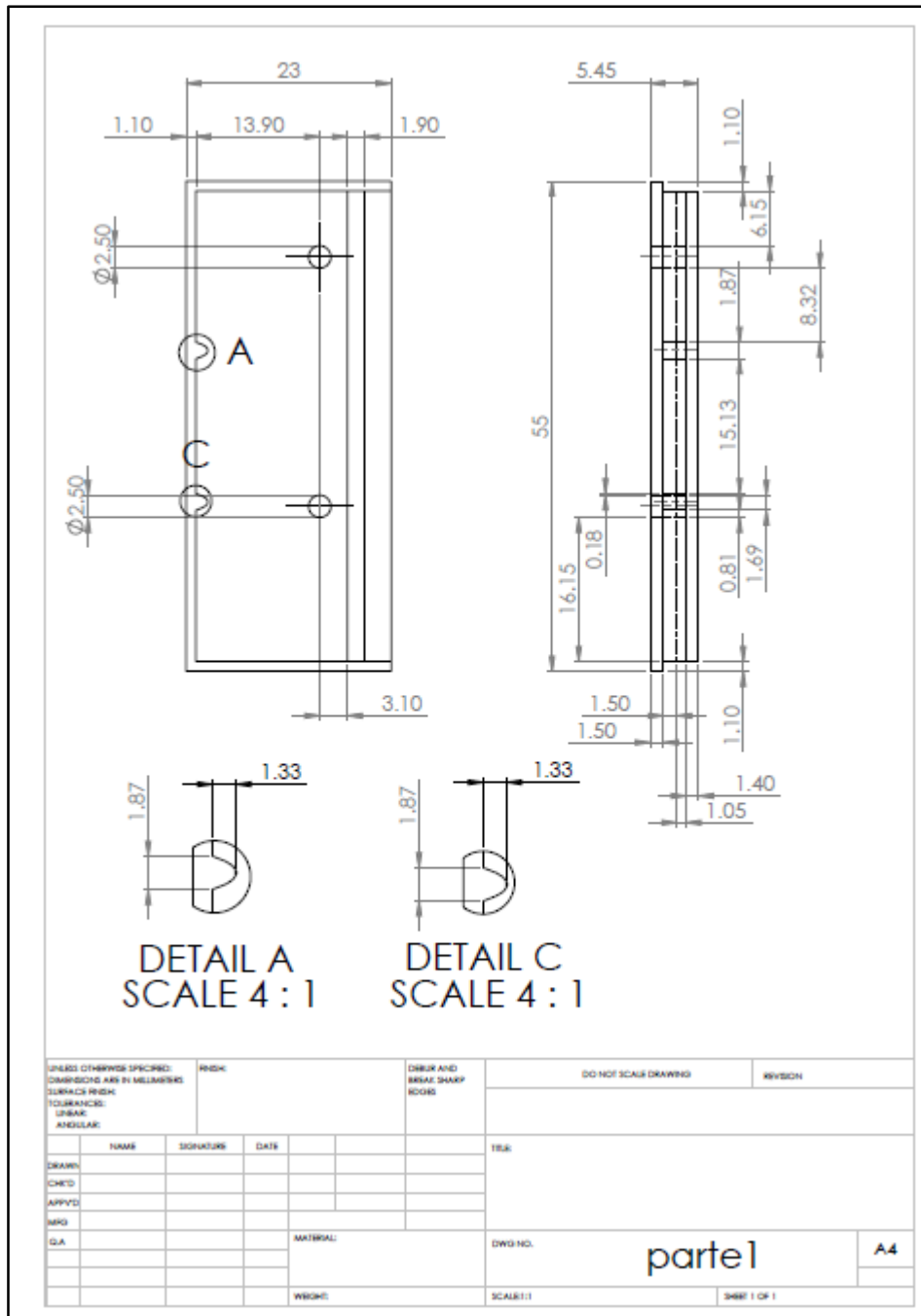


Figure 73 – Technical drawing of one open-close compartment.

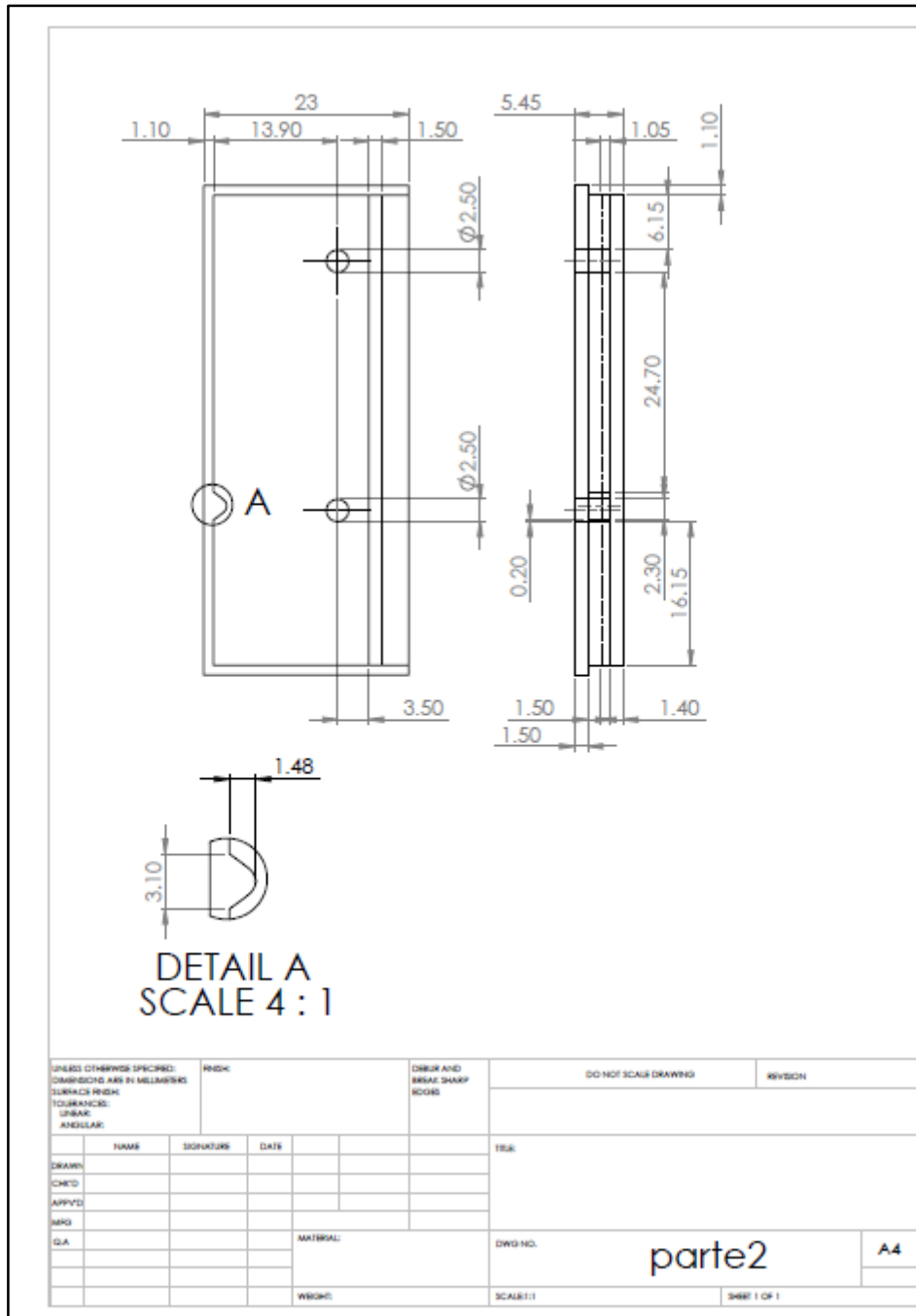


Figure 74 – Technical drawing of the other open-close compartment.

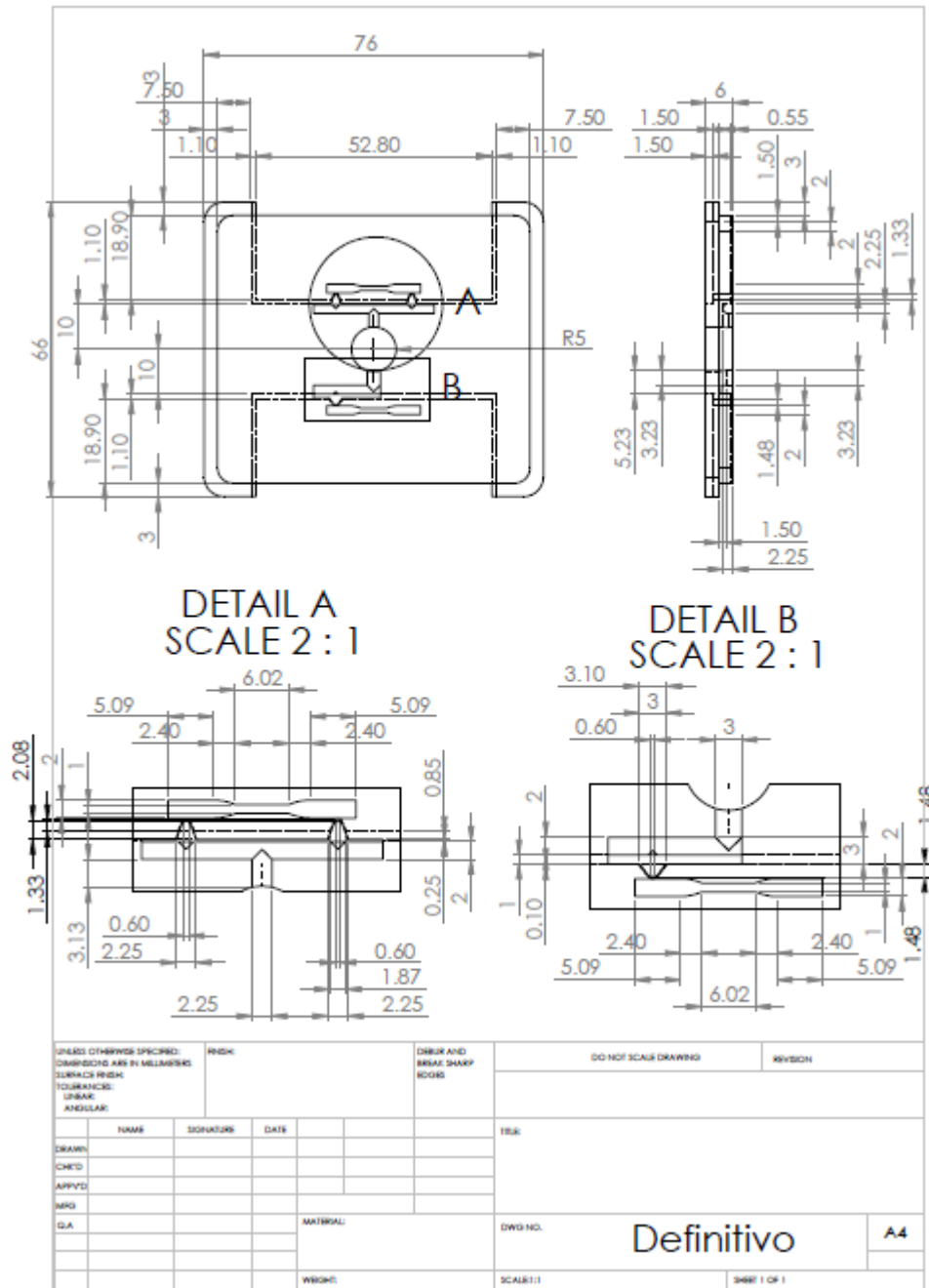


Figure 75 – Technical drawing of the cavity insert without the open-close compartments.

Attachment 9


		BOY 12		
Euromap Size		129-11	129-15	129-18
				
Injection unit for processing thermoplastics				
Screw diameter	mm	12	14	18
Screw- L/D-ratio		18	18	20
Max. stroke volume (theoretical)	cm ³	4,5	6,1	10,1
Max. shot weight in PS	g	4,45	5,6	9,6
Injection force	kN	27,7	37,1	45,7
Injection flow	g/s	18,5	30,6	45,1
Max. spec. injection pressure	bar	2450	2413	1795
Max. screw stroke	mm	40	40	40
Nozzle force / contact pressure	kN	36 (120 bar)	36 (120 bar)	36 (120 bar)
Nozzle retraction stroke	mm	180	180	180
Screw torque	Nm	50 (40 bar)	75 (68 bar)	130 (120 bar)
Screw speed (infinitely variable)	U / min, standard alternatively	max. 500	max. 500	max. 500
Screw pullback force	kN	34,3	34,3	34,3
Heating power (Nozzle + Cylinder)	W	235+465+2x450+850	235+465+2x450+850	235+465+650+700+1200
Hopper capacity	litre	7,5	7,5	7,5
Clamping unit				
Clamping force	kN	129	129	129
Tie bar clearance	mm (h x v)	259	259	259
Max. platen daylight	mm	300	300	300
Max. opening stroke (adjustable)	mm	200	200	200
Min. mould height	mm	100	100	100
Mould opening force	kN	23	23	23
Mould closing force	kN	15	15	15
Ejector stroke (max.)	mm	80	80	80
Ejector force pushing / pulling	kN	13,5 / 9	13,5 / 9	13,5 / 9
General				
Installed driving power	kW	5,5	5,5	5,5
Installed total power	kW	7,95 / 400 V	7,95 / 400 V	8,70 / 400 V
Hydraulic system pressure	bar	160	160	160
Oil tank capacity	litre	115	115	115
Dimensions and weights				
Dimensions (LxWxH) / Footprint	mm / m ²	2280 x 810 x 1648 / 1,85		
Total weight net (without oil)	kg	760		

Figure 76 – Characteristics of Boy 12A micro-injection machine.

Attachment 10

Table 17 – Data related to the tensile tests.

Condition	Yield Stress		Break Point	
	Modulus	Standard Deviation	Modulus	Standard Deviation
C1.PP23	34.1	1.02	38.1	4.20
R1.PP40	37.2	1.80	42.3	2.35
R1.PP80	41.6	2.62	42.9	2.96
R1.PP120	41.9	1.85	43.9	5.64
C2.PP23	30.7	2.31	33	3.32
R2.PP40	31.9	1.15	33.9	6.54
R2.PP80	32.4	1.67	36	2.87
R2.PP120	35	1.40	40.1	1.80
C1.PS23	-	-	61.6	9.20
R1.PS40	-	-	63.6	7.35
R1.PS80	-	-	64.5	10.97
R1.PS120	-	-	70.5	2.16
C2.PS23	-	-	38.2	4.21
R2.PS40	-	-	41	1.88
R2.PS80	-	-	44.9	2.18
R2.PS120	-	-	49	1.19

Attachment 11

Table 18 – Data related to the DSC tests.

Condition	Zone	Degree of crystalline (%)	Temperature Peak (°C)	Weight (mg)
C1.PP23	-	29.6	163.3	2.203
R1.PP40	A	37	164.2	2.134
	B	33.7	164.3	2.078
R1.PP80	A	46.6	164.4	1.608
	B	42.5	166.2	2.209
R1.PP120	A	48.8	165.0	1.814
	B	45.4	165.3	1.817
C2.PP23	-	31.1	165.9	2.226
R2.PP40	A	37.7	166.0	1.909
	B	34.9	164.1	1.958
R2.PP80	A	46.2	164.4	2.335
	A	40.5	164.4	2.245
R2.PP120	B	51.3	165.6	1.677
	A	45.9	164.2	2.269